Investigation of Diversity of Unusual Pigments and Novel Photosynthetic Apparatus in Aerobic Anoxygenic Phototrophic Bacteria

By

Elizabeth Hughes

A Thesis Submitted to the Faculty of Graduate Studies in Partial Fulfillment of the Requirements for the Degree of

Doctor of Philosophy

Department of Microbiology
University of Manitoba
Winnipeg, Manitoba
Canada

Copyright © 2017 by Elizabeth Hughes

Abstract

Photosynthetic complexes produced by aerobic anoxygenic phototrophs (AAP) *Roseicyclus mahoneyensis*, strain ML6, *Chromocurvus halotolerans*, EG19 and *Charonomicrobium ambiphototrophicum*, EG17 were studied to examine unusual pigments, proteins and photosynthetic function. We found ML6 spontaneously mutates to lose its light harvesting (LH) complex 2, or reaction centre (RC) and LH1, resulting in mutants ML6(BN9O), ML6(B) and ML6(DB). EG19 and EG17 contain a red-shifted LH1 complex, and EG17 is the first AAP known to photosynthesize both aerobically and anaerobically. From all organisms, membranes and complexes were purified. Flash induced difference spectra revealed ML6, ML6(BN9O), EG19 and EG17 were photosynthetically active aerobically, though only EG17 was capable of rapid electron transport without oxygen. ML6(B) and ML6(DB) were not capable of photosynthesis. Action spectra universally showed that bacteriochlorophyll and bacteriopheophytin were the primary LH pigments and carotenoids were not involved in photosynthesis. Redox midpoint potentials of the Q_A, P^+ and RC-bound cytochrome were typical of AAP, except for the Q_A of EG17 (+5mV, between what is expected for AAP and anaerobic purple non-sulfur bacteria). RC, LH1 and LH2 subunits were of typical sizes. The exception was the LH1 of EG19 and EG17, which was slightly larger than previously published.

Strain EG19 excretes an orange-brown compound into the growth medium, previously hypothesized to be a siderophore. We identified it as a catechol siderophore, measuring approximately 800Da. It is hydrophilic and may contain the amino acids valine, proline, aspartate, 2-aminobutenoic acid, and N-acetyl-L-glutamate.

Lastly, a sampling trip to Central Gold Mine, Nopiming Provincial Park, Canada was undertaken to study the presence of AAP in this extreme environment. Abundant AAP were found and five were chosen for study: strains NM4.16, NM4.18, C4, C9, and C11. All are mesophiles, grow on complex media, and tolerate a wide range of pH, temperature and salinity. Isolates were highly resistant to the toxic metalloid oxides tellurite, tellurate, selenite, selenate, metavanadate and orthometavanadate and reduced tellurite to tellurium. All are *α-Proteobacteria*, with C4 and NM4.16 closely related to *Porphyrobacter colymbi* (99.4% and 99.7% sequence similarity, respectively), C9 to *Brevundimonas variabilis* (99.1%), C11 to *Brevundimonas bacteroides* (98.6%), and NM4.18 to *Erythromonas ursincola* (98.5%).

Acknowledgements

I wish to express my gratitude to my advisor Dr. Vladimir Yurkov for guiding me in my graduate studies of microbiology, and for his support and patience as I honed my skills in experimental design, techniques and writing.

I also wish to thank my advisory committee, Dr. Michele Piercey-Normore and Dr. Teri DeKievit for their invaluable guidance, advice and suggestions. Also, to my external examiner Dr. Paul de Giorgio for his insightful comments and questions.

I would like to express my gratitude to all the past and present members of our lab for their constructive feedback and help with experiments, particularly Dr. Chris Maltman, Steven Kuzyk, Dr. Julius Csotonyi, Mike Bilyj and Xiao Ma. To my collaborators Dr. Michele Piercey-Normore (for her aid with DNA sequencing) Dr. Lynda Donald (for her help with mass spectroscopy) and Dr. Jean Alric (for his guidance with the biophysical work performed in France) thank you for making these aspects of my project possible.

Most importantly I would like to thank my family and especially my husband Kiprian Warren for their support through so many years of schooling, I could never have made it to this point without them.

This work was funded by an NSERC Discovery Grant held by Dr. V. Yurkov and a University of Manitoba GETS grant also held by Dr. V. Yurkov.

Table of Contents

List of Tables

List of Figures

Publications

Hughes, E., Head, B., Maltman, C., Piercey-Normore, M., and Yurkov, V. (2017) Aerobic anoxygenic phototrophs in gold mine tailings in Nopiming Provincial Park, Manitoba, Canada. Canadian Journal of Microbiology. 63: 212–218.

Hughes, E., Alric, J., and Yurkov, V. (In Prep) Photosynthetic complexes and light dependant electron transport chain in the aerobic anoxygenic phototroph Roseicyclus mahoneyensis and its spontaneous mutants. Photosynthesis Research.

Hughes, E., Alric, J., and Yurkov, V. (In Prep) Photosynthetic function of reaction center and light harvesting complexes in the aerobic anoxygenic phototrophs Chromocurvus halotolerans and Charonomicrobium ambiphototrophicum. Archives of Microbiology.

Hughes, E., and Yurkov, V. (In Prep) Novel Siderophore Identified for First Time in the Aerobic Anoxygenic Phototroph *Chromocurvus halotolerans*. Applied and Environmental Microbiology.

List of Abbreviations

AAP	Aerobic anoxygenic phototroph
ATP	Adenosine triphosphate
BChl	Bacteriochlorophyll
BLAST	Basic Local Alignment Search Tool
BPheo	Bacteriopheophytin
CAS	Chromeazurol S
CFU	Colony forming unit
Crt	Carotenoids
Cyt	Cytochrome
EDTA	Ethylenediaminetetraacetic acid
e^-	electron
ES	Electrospray
ETC	Electron transport chain
FA	Fatty acid
GC	Gas chromatography
HDTMA	Hexadecyltrimethylammonium
HiPiP	High potential iron-sulfur protein
ICP	Inductively coupled plasma
LDAO	Lauryldimethylamine N-oxide
LH	Light harvesting
MA	Medium A
MB	Medium B
MS	Mass spectrometry
NMR	Nuclear magnetic resonance spectroscopy
P^+	Excited bacteriochlorophyll
PGC	Photosynthetic gene cluster

PITC	Phenylisothiocyanate
PMSF	Phenylmethanesulfonyl fluoride
PNSB	Purple non-sulfur bacteria
Q	Quinone
RC	Reaction centre
RO	Rich organic
RUBISCO	Ribulose bisphosphate carboxylase/oxygenase
SDS-PAGE	Sodium dodecyl sulfate – polyacrylamide gel electrophoresis
TCA	Tricarboxylic acid

Chapter 1.

Introduction

1.1. Aerobic Anoxygenic Phototrophs

1.1.1. Distribution, Morphology and Ecological Role in the Environment

The aerobic anoxygenic phototrophs (AAP) are an interesting group of bacteria for study. They first became known to the scientific community with the discovery of strains OCh101 and OCh114 from a marine sampling trip in 1978 (Shiba, Simidu and Taga, 1979). Both are obligately aerobic bacteria containing bacteriochlorophyll (BChl) *a* that were later named *Erythrobacter longus* and *Roseobacter denitrificans*, respectively (Shiba and Simidu, 1982; Shiba, 1991). Before this time, it was thought that the only organisms capable of anoxygenic photosynthesis were the green and purple sulfur and non-sulfur bacteria as well as the heliobacteria (Yurkov and Beatty, 1998). Soon after, the search was moved to freshwater habitats, where *Erythrobacter sibiricus* (later re-classified as *Erythromicrobium sibiricum* (Yurkov, Lysenko and Gorlenko, 1991) and again as *Sandaracinobacter sibiricus* (Yurkov *et al*., 1997)), *Erythromicrobium ursincola* (re-classified as *Erythromonas ursincola* (Yurkov *et al*., 1997)), *Erythromicrobium ezovicum*, *Erythromicrobium ramosum*, *Erythromicrobium hydrolyticum* and *Roseococcus thiosulfatophilus* were found in the early 1990's (Yurkov and Gorlenko, 1990, 1992a, 1992b; Yurkov, Gorlenko and Kompantseva, 1993). With the discovery of AAP in both marine and freshwater systems (Fig. 1A), the search for them exploded. Since that time, they have been found in every habitat tested, all over the globe, including extreme habitats such as deep sea hydrothermal vents (Fig. 1D), hypersaline springs (Fig. 1B), hot springs (Fig. 1C), mine tailings (Fig. 1E), soil crusts (Fig. 1F) and the phyllosphere (Yurkov and Csotonyi, 2009; Csotonyi *et al*., 2010; Steifel, Zambelli and Vorholt, 2013; Bilyj *et al*., 2014; Yurkov and Hughes, 2017).

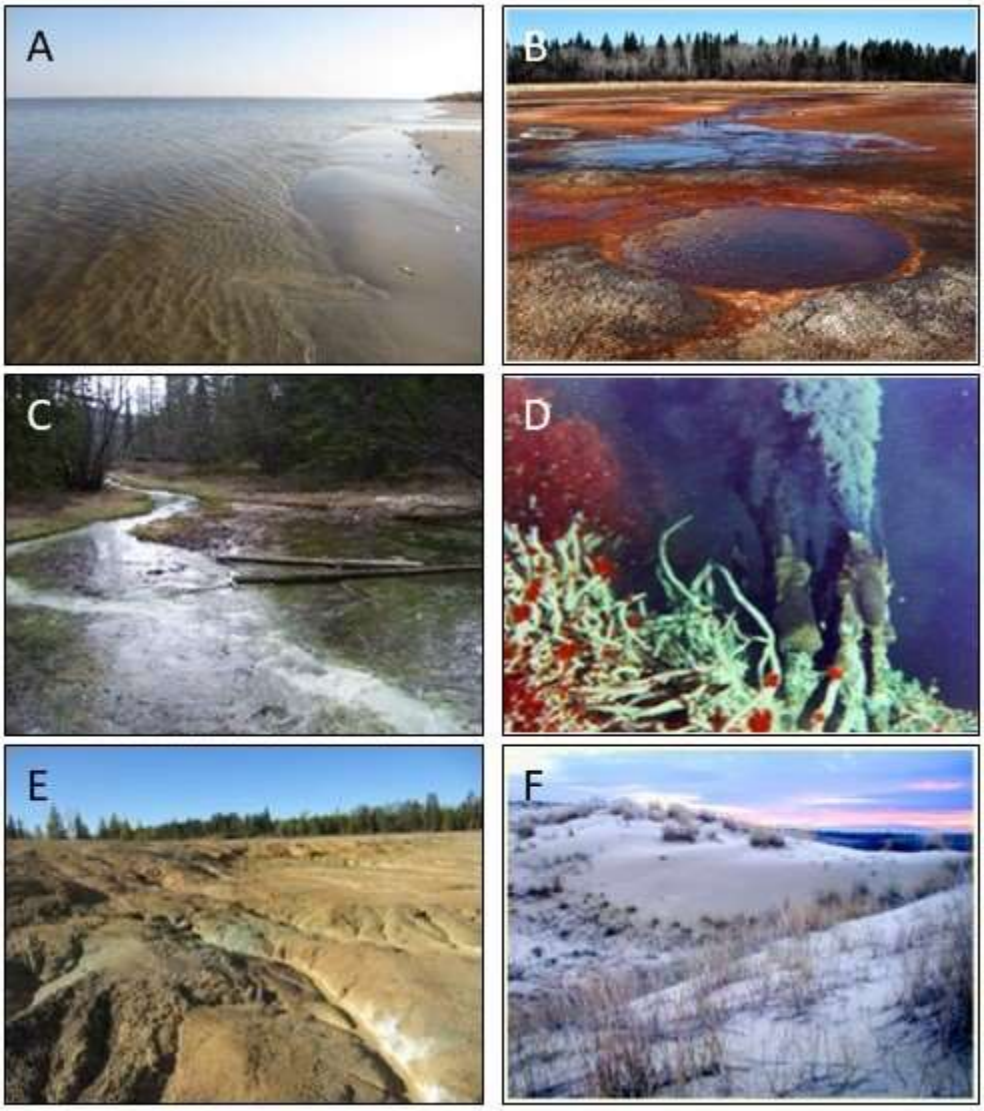

Fig. 1. Diversity of AAP habitats: (A) Lake Winnipeg, Manitoba, Canada; (B)East German Creek System, Northern Manitoba, Canada; (C) Sulfur Mountain hot springs, Banff, Alberta, Canada; (D) Hydrothermal vent, Juan de Fuca Ridge, Pacific Ocean; (E) Central Mine, Nopiming Provincial Park, Canada; (F) Soil crusts, Manitoba, Canada. All photographs are from the archives of the Yurkov laboratory, Department of Microbiology, University of Manitoba.

In the ocean, the AAP have been found to consistently make up approximately 10% of the total microbial biomass (Rathgeber, Beatty and Yurkov, 2004; Yurkov and Csotonyi, 2009; Yurkov and Hughes, 2013; Yurkov and Hughes, 2017), though there is some variability. In the Japanese Uwa Sea, 3.5-7.9% of total bacteria were found to be AAP (Sato-Takabe *et al.*, 2015), with levels rising up to 24% in the areas of aquaculture (Sato-Takabe *et al*., 2016). That number was 10-14% in the Northeast Pacific and Arctic Oceans (Boeuf *et al*., 2013), and up to 23.8% in a coastal bay in Arraial do Cabo, Brazil (Cuadrat *et al*., 2016). These organisms have even been suggested to make up as much as 80% of the bacteria in the Mediterranean Sea (Eiler *et al*., 2009). Freshwater systems are no different, with AAP enumerated at as high as 2-12% in lakes throughout Germany, Finland and Poland (Masin *et al*., 2012), 21.4% in lakes on James Ross Island on the Antarctic Peninsula (Medova *et al*., 2016), 29% in Austrian alpine lakes (Cuperova *et al*., 2013), and up to 30% of total prokaryotes in highly eutrophic habitats such as freshwater hot spring mats (Yurkov and Beatty, 1998). Other notable environments include peat bogs where the microbial community consisted of up to 18.3% AAP (Lew, Lew and Koblížek, 2016) and soil crusts showed 6% AAP among culturable bacteria (Csotonyi *et al*., 2010). The evolution of AAP to thrive in high numbers in such a wide range of locales could be linked to their ability to partially supplement energy production photosynthetically. This extra boost of ATP could give them a competitive advantage over other heterotrophs allowing for faster growth.

It is important to note that the enumeration of AAP in some studies can be deceptive. Culture based techniques, while allowing for definite identification of AAP based on spectrophotometry and inability to grow anaerobically, has some shortcomings. For instance,

relatively few microbes can be cultured in a laboratory setting, opening up the possibility that bacterial counts are actually much higher than is being observed on plates. This causes scientists to instead use culture-independent techniques. Shotgun-sequencing of *pufLM* genes from environmental samples is a common method (Jiang *et al*., 2009; Zeng, Shen and Jiao, 2009; Salka *et al*., 2011; Cuadrat *et al*., 2016; Zeng *et al*., 2016); however, the genes, which are responsible for production of the L and M subunits of the photosynthetic reaction centre (RC), are present and virtually identical in both AAP and purple non-sulfur bacteria (PNSB), making it impossible to differentiate between the two. This causes overestimations in the number of AAP present in the environment. Recently, another method was proposed, infrared epifluorescence microscopy to view BChl *a* in whole cells (Garcia-Chaves *et al*., 2016). It was thought that if sample collection was limited to the aerated portion of the water column, any PNSB present would be incapable of producing BChl *a* and would instead be growing exclusively heterotrophically (Masin *et al*., 2012; Garcia-Chaves *et al*., 2016). This, while better than shotgun sequencing, may also be insufficient as there are some PNSB, such as *Rhodobacter capsulatus*, *Rhodocista centenria* and *Rhodovulum sulfidophilum*, that are capable of producing small amounts of BChl *a* in oxygenated environments (Hebermehl and Klug, 1998; Yildiz *et al*., 1991; Masuda *et al*., 2008; Csotonyi *et al*., 2011b). Until a way is found to definitively select for AAP and exclude all other bacteria without a doubt, culture-independent and culture-dependent methods will have to be used in conjunction to produce unbiased reports of distribution and quantity.

Despite these possible enumeration biases, the presence of AAP in high amounts in such a wide range of habitats suggests they may play an important ecological role. For instance, AAP are invaluable in nutrient and energy cycling (Kolber *et al*., 2001; Koblížek *et al*., 2007; Yurkov and Csotonyi, 2009; Yurkov and Hughes, 2017). Recent studies have shown that in both marine and freshwater environments, on average, AAP have a faster growth rate (1.5-3 times higher) than that of the total microbial community (Liu, Zhang and Jiao, 2010; Ferrera *et al*., 2011; Stegman *et al*., 2014; Garcia-Chaves, 2015; Cepakova *et al*., 2016). Photosynthetic ability could contribute to their rapid proliferation, as they are able to produce some energy from light in addition to using cellular respiration. This allows AAP to also achieve a greater size than the typical heterotrophs, as seen in various aquatic studies (Stegman *et al*., 2014; Fauteaux *et al*., 2015; Garcia-Chaves *et al*., 2015; Sato-Takabe *et al*., 2015; Garcia-Chaves *et al*., 2016). For instance, in samples from the Uwa Sea, AAP cells were approximately 2.23 times larger than the average total bacterial size (Sato-Takabe *et al*., 2016). The large cell size makes them contribute a disproportionately high amount to total microbial biomass and also may cause them to be preferentially grazed upon by zooplankton and other protists (Masin *et al*., 2012; Stegman *et al*., 2014; Garcia-Chaves *at al*., 2015; Sato-Takabe *et al*., 2015; Cepakova *et al*., 2016). This puts the AAP at the bottom of the food chain. Their fast growth rate and rapid demise due to grazing allows them to swiftly pass nutrients and energy up the food chain to higher trophic levels and, therefore, contribute significantly to carbon cycling in the euphotic zone (Cepakova *et al*., 2016; Yurkov and Hughes, 2017).

1.1.2. Phylogenetic Position, Evolution and Taxonomy

Most AAP belong to the α-*Proteobacteria* and are ubiquitous all over the world in many environments (Yurkov and Csotonyi, 2009; Yurkov and Hughes, 2017). There is also one taxonomically described β-Proteobacterium, *Roseatales depolymerans* (Suyama *et al*., 1999), and two in the γ-*Proteobacteria*, *Chromocurvus halotolerans* (Csotonyi *et al*., 2011) and *Congregibacter litoralis* (Spring *et al*., 2009). Genomic studies have, however, revealed the presence of many more β- and γ-*Proteobacteria* that have been neither cultured nor taxonomically described (Jiang *et al*., 2009; Zeng *et al*., 2009; Cottrell, Ras and kirchman, 2010; Lehours *et al*., 2010; Feng *et al*., 2011; Ritchie and Johnson, 2012; Lehours and Jeanthon, 2015; Zheng *et al*., 2015). In general, it has been found that the β-*Proteobacteria* are prominent in freshwater habitats and the γ-*Proteobacteria* dominate saline environments (Yurkov and Hughes, 2017; Ferrera *et al*., 2017). A notable exception to this rule is the high numbers of β-*Proteobacteria* observed in the Northeast Pacific and Arctic Ocean (Boeuf *et al*., 2013).

While they are definitely distinct, the AAP are phylogenetically tangled among other groups. Some AAP species are most closely related to other AAP, some to the PNSB, and still others to non-phototrophic heterotrophs. This has created problems in classification of AAP as, in some cases, they have been placed in genera that do not represent photosynthetic organisms such as the classifications of the AAP *Hoeflea phototrophica* and *Stappia marina* (Biebl *et al*., 2006; Kim *et al*., 2006). In others, non-phototrophs are placed in genera that were originally described with phototrophy as an important feature. This is the situation, for example, with the genus *Erythrobacter* (Table 1). In this genus, the type species, *E. longus*, is an

Table 1. Taxonomic confusion in the genus *Erythrobacter*.

Organisms described as	Metabolic category	Presence of BChl	Presence of PGC
Erythrobacter longus[a] (Shiba and Simidu, 1982)	Ph[b]	+	+
Erythrobacter litoralis T4 (Yurkov *et al*., 1994)	Ph	+	ND[d]
Erythrobacter sp. NAP1 (Koblížek *et al*., 2011)	Ph	+	+
Erythrobacter sp. JL-475 (Feng *et al*., 2011)	Ph	+	ND
Erythrobacter litoralis HTCC2594 (Oh *et al*., 2009)	NPh[c]	-	-
Erythrobacter sp. SD-21 (Denner *et al*., 2002)	NPh	-	ND
Erythrobacter citreus (Denner *et al*., 2002)	NPh	-	ND
Erythrobacter flavus (Yoon *et al*., 2003)	NPh	-	ND
Erythrobacter vulgaris (Ivanova *et al*., 2005)	NPh	-	ND
Erythrobacter aquimaris (Yoon *et al*., 2004)	NPh	-	ND
Erythrobacter seohaensis (Yoon *et al*., 2005b)	NPh	-	ND
Erythrobacter gaetbuli (Yoon *et al*., 2005b)	NPh	-	ND
Erythrobacter luteolus (Yoon *et al*., 2005a)	NPh	-	ND
Erythrobacter gangjinensis (Lee *et al*., 2010)	NPh	-	ND
Erythrobacter nanhaisediminis (Xu *et al*., 2010)	NPh	-	ND
Erythrobacter pelagi (Wu *et al*., 2012)	NPh	-	ND
Erythrobacter marinus (Jung *et al*., 2011)	NPh	-	ND
Erythrobacter jejuensis (Yoon *et al*., 2012)	NPh	-	ND

[a]name in bold indicates the type species of the genus; [b]Ph, indicates phototrophic; [c]NPh, indicates Non-phototrophic; [d]ND, indicates not determined

obligately aerobic BChl *a*- containing bacterium (Shiba and Simidu, 1982) as are three other isolates; however, 14 other organisms have been classified alongside the AAP, but have shown no sign of photosynthetic ability or pigment production (Table 1). These tangles are the result of using 16S rRNA gene sequencing as the sole method of taxonomic classification of novel strains, without taking into account defining phenotypic physiological traits.

Everything mentioned above allows the formulation of questions about how the AAP originally evolved to end up in so many phylogenetic branches. One school of thought is that upon oxygenation of the atmosphere 2.5 GYa ago due to the activity of oxygenic phototrophic cyanobacteria (Beatty, 2005), the AAP evolved directly from the PNSB. As aeration occurred, a new niche for life emerged. Competition for space in anoxic habitats would have been fierce as toxic O_2 filled the air, causing selection pressure for anoxygenic phototrophs to develop an aerobic counterpart and move into these new environments. Most likely, PNSB candidates developed aerobic metabolic pathways, such as oxidative phosphorylation for energy generation so that photosynthetic pathways could be lost, therefore allowing for their descendants to be non-phototrophic heterotrophs. From there, the aerobic bacteria would have re-gained the photosynthetic gene cluster (PGC) through horizontal gene transfer (Jiao, Zhang and Zheng, 2010; Yurkov and Hughes, 2013; Cuadrat *et al*., 2016). This theory has support through genomic studies, which show the presence of phage DNA directly associated with the PGC. In *Citromicrobium bathyomarinum*, strain JL354, sequencing actually revealed the presence of two copies of the PGC, both associated with phage DNA. This included one complete α-proteobacterial copy and an incomplete γ-proteobacterial copy, suggesting only a

partial transfer occurred (Jiao *et al*., 2010). This hypothesis could explain why so many AAP are most closely related to the aerobic non-phototrophs and also why AAP may have emerged from many different lineages (Yurkov and Csotonyi, 2009; Yurkov and Hughes, 2013). The second school of thought is that the AAP evolved directly from a single PNSB ancestor, having never lost photosynthetic ability (Woese, 1987; Beatty, 2005), though this currently has less support. In reality, it is probably a combination of the two hypotheses, possibly with some AAP that are most closely related to non-phototrophs having arisen through the first strategy and those more closely related to PNSB being derived from the second option (Yurkov and Csotonyi, 2009).

1.1.3. Physiological Properties and Carbon Fixation

Without exception, the AAP are all aerobic, Gram negative, BChl *a*-producing, highly pigmented bacteria. There is no growth medium or condition to select for them exclusively, as they perform best on rich medium using complex carbon sources, which also supports growth of most other culturable heterotrophs. Hence, the only way to putatively identify them is by recognizing their bright colony colours (from yellow to orange to pink to red), which all stand out amongst the other more mundanely coloured bacteria. From there, the isolates are tested spectrophotometrically for BChl *a* production and for the inability to photosynthesize anaerobically, to ensure their identity as phototrophic organisms (Yurkov and Csotonyi, 2009; Yurkov and Hughes, 2013).

It was discovered that AAP are incapable of autotrophic growth as they lack the Calvin Cycle, the primary pathway for CO_2 fixation. This is due to the lack of the key enzyme ribulose bisphosphate carboxylase/oxygenase (RUBISCO) as determined first in *E. longus* and *S. sibiricus* (Yurkov, 1990; Yurkov and Beatty, 1998) and later confirmed through genome sequencing of *R. denitrificans*, *Sandarakinorhabus* sp. AAP62, *Blastomonas* sp. AAP53, *Porphyrobacter* sp. AAP82 and *Sphingomonas* sp. FukuSWIS1 (Swingley *et al*., 2007; Tang *et al*., 2009; Sato-Takabe *et al*., 2011; Li *et al*., 2013; Zeng *et al*., 2013a; Zeng *et al*., 2013b; Salka *et al*., 2014). Despite the absence of autotrophic genes, AAP are capable of basal levels of CO_2 fixation through anapleurotic reactions (Fig. 2). *S. sibiricus* indicated incorporation of only 0.4% carbon from radiolabelled CO_2 (Yurkov, 1990); however, species from the *Roseobacter* clade, including *R. denitrificans* fixed up to 15% of their carbon anapleurotically (Tang *et al*., 2009). Interestingly, when grown on defined medium, the carbon source can have an impact on levels of photosynthesis and anapleurotic reactions in *Erythrobacter* sp. NAP1 (Hauruseu and Koblížek, 2012). When provided with glutamate, growth was inhibited by high light intensities, though greater amounts of biomass were produced with a moderate amount of light. Additionally, almost none of the incorporated carbon came from anapleurotic reactions (1%). Conversely, light intensity made no difference when medium contained pyruvate instead of glutamate, and 4% (dark) and up to 11% (light) of incorporated carbon originated from anapleurotic reactions (Hauruseu and Koblížek, 2012). These values are, however, lower than the 10-15% anapleurotic CO_2 fixation carried out by *R. denitrificans*, suggesting species specificity (Hauruseu and Koblížek, 2012). It was discovered long ago that photosynthetic activity allows AAP to increase

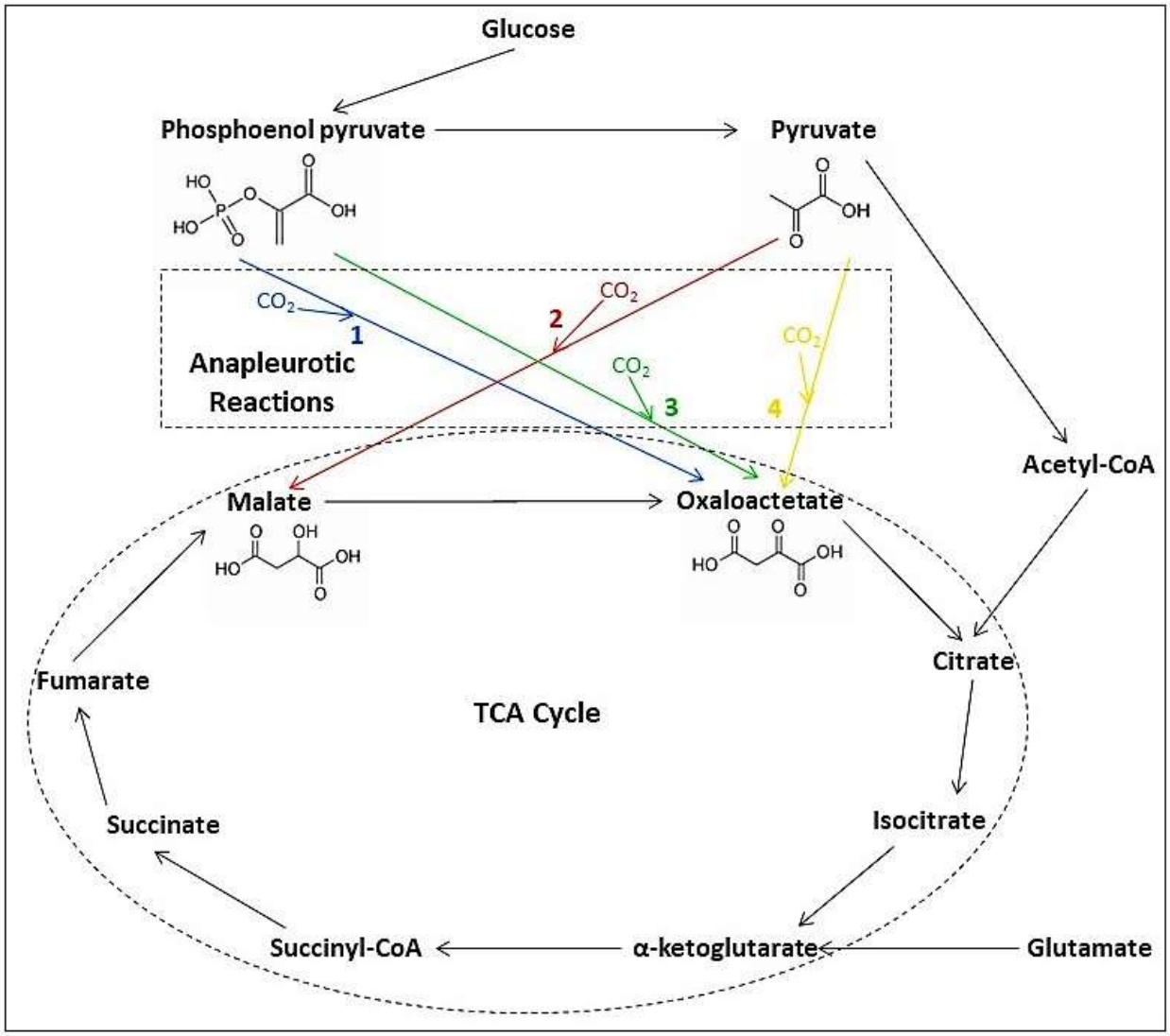

Fig. 2. Fixation of CO_2 through anapleurotic reactions catalyzed by the enzymes: (1, blue) Phosphoenol pyruvate carboxykinase; (2, red) Malic enzyme; (3, green) Phosphoenol pyruvate carboxylase; and (4, yellow) Pyruvate carboxylase replenishes the TCA cycle. Glucose feeds into the TCA cycle through pyruvate, and therefore anapleurotic reactions or acetyl-CoA. Glutamate replenishes the TCA cycle through α-ketoglutarate.

their protein production (Yurkov and Van Gemerden, 1993) and now it is confirmed that the organic carbon source also makes a difference. For instance, light exposure allowed a 30% biomass increase, when grown in media containing pyruvate; however, photosynthesis in the presence of glucose resulted in 49.1% increase (Hauruseu and Koblížek, 2012). It is likely that anapleurotic reactions are used by AAP simply to replenish the TCA cycle. Anapleurotic reactions use pyruvate or phosophoenol pyruvate as a substrate (Fig. 2), hence more carbon fixation occurs in pyruvate and glucose grown cultures. Glutamate, however, can be easily converted to α-ketoglutarate to feed into the TCA cycle (Fig. 2) (Hauruseu and Koblížek, 2012). It is also conceivable that this explanation ties into why light intensity makes a difference with glutamate and not with pyruvate. With glutamate, higher light intensities provide more energy than is required by the cell, which in the end causes downregulation of metabolism. However, anapleurotic reactions using pyruvate as a substrate require a large amount of energy, so the possibility of excess is avoided, and metabolism is not down-regulated (Hauruseu and Koblížek, 2012). Additionally, some species of AAP, such as *Dinoroseobacter shibae*, use the ethylmalonyl-CoA pathway for minimal CO_2 fixation (Tang *et al*., 2011; Bill *et al*., 2017). Three molecules of acetyl-CoA and one molecule of CO_2 form malate and propionyl-CoA. Once again, however, this pathway does not allow for true autotrophy.

Morphologically, AAP fall into a broad range of categories such as rods, cocci, vibroid, cyclic (such as in *Roseicyclus mahoneyensis* (Fig. 3A; Rathgeber *et al*., 2005)), and pleomorphic (*E. ramosum* (Fig. 3C), *C. bathyomarinum* (Fig. 3F), *Porphyrobacter meromictius* (Fig. 3D)) (Yurkov *et al*., 1999; Rathgeber *et al*., 2007; Yurkov and Csotonyi, 2009). The only shape yet to

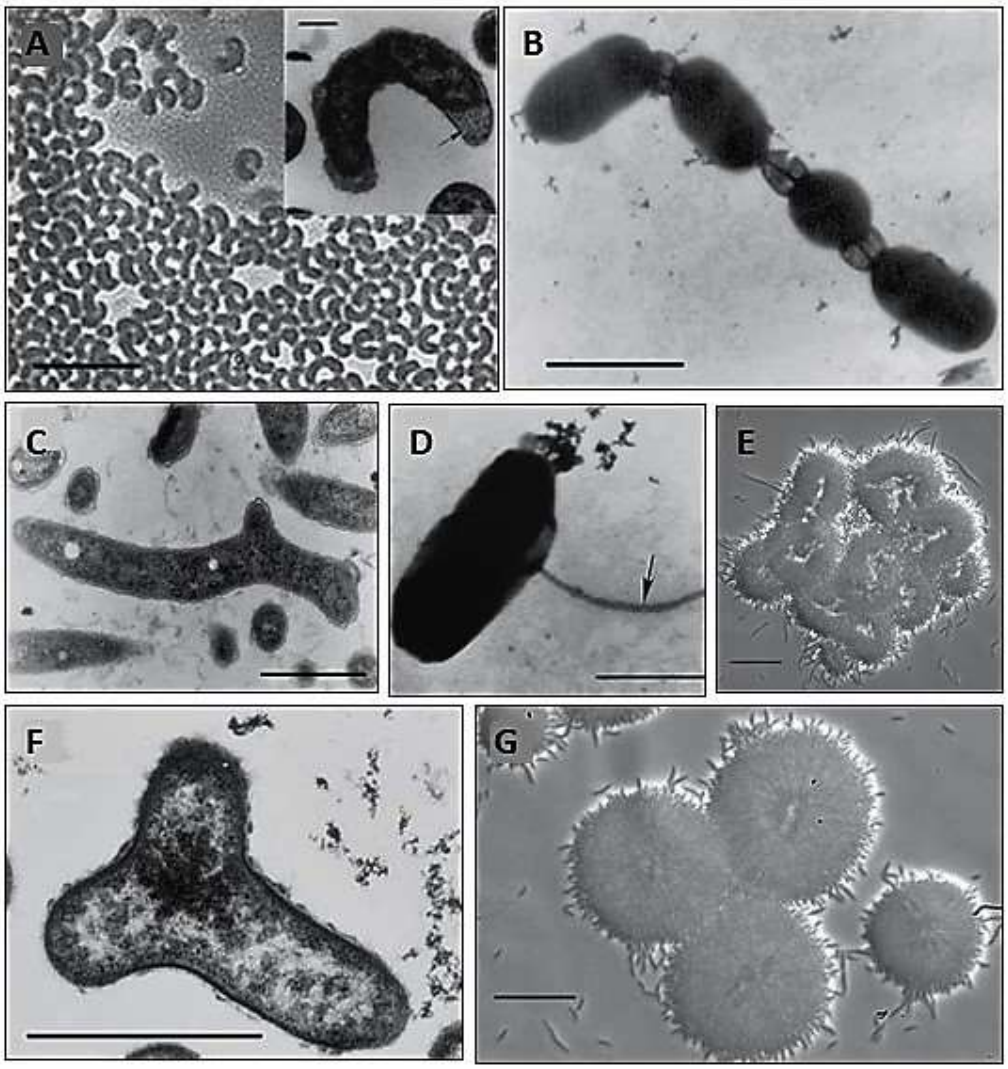

Fig. 3. Morphological diversity of AAP: (A) *Roseicyclus mahoneyensis* almost cyclic cells (bar 5µm, inset bar 0.25µm); (B) *Porphyrobacter meromictius* chains of cells connected by bubble-like structures (bar 1µm); (C) *Erythromicrobium ramosum* branched cells (bar 1µm); (D) *Porphyrobacter meromictius* appendaged cells (bar 0.5µm); (E) Strain BL14 brain coral-like formations (bar 2.5µm); (F) *Citromicrobium bathyomarinum* Y-shaped cells (bar 1µm); (G) Strain BL7 dandelion-like aggregations (bar 2.5µm). All micrographs are from the archives of the Yurkov laboratory, Department of Microbiology, University of Manitoba.

be described is true spirilloid, though uncultured examples attributed to AAP with such morphology have been hypothesized in the Sargasso Sea (Sieracki *et al*., 2006). In addition to their morphological diversity, certain strains isolated from meromictic lakes and oceans appear to form complex rosettes, possibly to aid in buoyancy or quorum sensing in cell populations. These include organisms such as *S. marina*, *Roseovarius mucosus*, ocean strain C8 and meromictic lake strains BL7 (Fig. 3G) and BL14 (Fig. 3E) (Yurkov and Csotonyi, 2009), which produce the most complex configurations resembling dandelion heads or corals. Some, including *C. bathyomarinum* and *P. meromictius* (Fig. 3B) have also been shown to form chains with bubble like formations connecting the cells, which could aid in the exchange of cellular materials and nutrients in oligotrophic environments, though it has yet to be proven (Yurkov *et al*., 1999; Rathgeber *et al*., 2007).

Having been discovered in so many habitats, it is not surprising that the AAP grow under a very wide range of conditions and have varied physiological abilities depending on the habitat. They are typically mesophilic, but tolerate wide ranges of temperatures and pH (Yurkova *et al*., 2002; Csotonyi *et al*., 2008; Csotonyi *et al*., 2010). This makes sense, as in nature, the sun will heat up the soil or water quite drastically at the surface and in shallow zones, particularly in the summer months, and the temperature will cool quite severely in winter or even simply at night. In terms of pH, changes in precipitation will cause salts and minerals to be either concentrated or diluted changing the acidity of the environment.

AAP also have a tendency to be extremely resistant to toxic heavy metal(loid) oxides, such as tellurite, tellurate, selenite, selenate, metavanadate and orthovanadate (Yurkov and Csotonyi, 2003), and to reduce them to their less toxic elemental forms. For example, many known bacterial species are killed by only 1.0 μg/ml of tellurite, but AAP can resist upwards of 2000 μg/ml or higher (Maltman and Yurkov, 2015). This resistance may contribute to their ability to grow in such a wide range of extreme environments. One strategy of resistance by AAP includes mechanisms allowing them to use toxic compounds in metabolic processes. Strains EG13 and EG8 are vanadiphilic, meaning vanadium oxides actually enhance the bacterial growth (Csotonyi *et al*., 2015). Similarily, *E. ursincola* and *E. ramosum* increase biomass and ATP production when grown in the presence of tellurite (Maltman and Yurkov, 2014; Maltman and Yurkov, 2015). Alternately, instead of benefitting from the oxides, some species can simply tolerate them as is seen in *C. bathyomarinum*, which needs to adapt to the shock of the addition of tellurite by experiencing a lag phase before resuming normal biomass production (Maltman and Yurkov, 2014). *R. thiosulfatophilus*, *E. ezovicum*, *S. sibiricus*, *E. hydrolyticum*, and *Erythrobacter litoralis*, all have decreased biomass and ATP levels in the presence of high concentrations of tellurite, suggesting it has a toxic effect on the cells (Maltman and Yurkov, 2015). When a search for a tellurite specific reductase was carried out in strains *E. ursincola*, *E. ramosum*, *R. thiosulfatophilus*, *E. ezovicum*, *S. sibiricus*, *E. hydrolyticum*, *E. litoralis* and *C. bathyomarinum*, multiple mechanisms of dealing with TeO_4^{2-} were determined. *E. ramosum* requires fully intact cells and *de novo* protein synthesis reduce TeO_4^{2-}. *C. bathyomarinum* and *E. litoralis*, while still requiring *de novo* synthesis, only needed an intact cytoplasmic membrane for reductase production as shown by activity in spheroplast lysates (Maltman and Yurkov,

2014). In the other tested strains, a constitutively expressed membrane-bound tellurite reductase was present, suggesting the function of a different enzyme (Maltman and Yurkov, 2015). Future research will provide answers on how other AAP resist such high levels of toxic compounds and, in some cases, how they have evolved to benefit from them. Reduction of oxides is easy to see due to colour change in the culture from accumulation of the elemental metalloids inside the cells. Reduction of tellurite and tellurate to tellurium results in a black appearance, selenite and selenate conversion to selenium brings a red colour, and vanadate being reduced to vanadium appears as blueish colouration (Yurkov and Csotonyi 2003; Maltman and Yurkov, 2015). In the future, this ability of AAP has the potential to be used in bioremediation of toxic oxides and biometallurgy of rare elements by collecting concentrated pure tellurium or other accumulated metals as they are quite rare in the biosphere.

Because AAP are so highly resistant to tellurite, the question was asked whether that feature is tied to photosynthesis. BChl *a* and carotenoids (crt) were monitored in *E. ramosum*, *E. ursincola*, *C. bathyomarinum*, *E. litoralis*, and *Erythrobacter* relative strain EG15 in the presence and absence of tellurite (Csotonyi *et al*., 2014). Levels of BChl *a* increased when cultures were grown with tellurite in *E. ursincola*, *C. bathyomarinum*, *E. litoralis* and strain EG15, indicating the pigment may play the role of an antioxidant. Contrarily, concentrations decreased in *E. ramosum*, showing that oxidative stress due to tellurite toxicity could be exceeding the cell's ability to cope causing the production of photosynthetic pigments to be down-regulated. However, when carbon availability was decreased, BChl *a* levels increased in *E. ramosum* despite the presence of tellurite (Csotonyi *et al*., 2014). The same pattern holds true for cellular

crt except for in *C. bathyomarinum*, as its crt decreased (Csotonyi *et al*., 2014). Speculations into the above results proposed three hypotheses. First, tellurite may act on the promoters to induce transcription of the entire PGC, even if crt are the only pigments involved in oxidative defense. Second, BChl *a* may act in conjunction with crt as antioxidants. Third, resistance to tellurite may be energetically quite costly, causing the upregulation of the photosynthetic apparatus to supply the cells with as much additional energy as possible (Csotonyi *et al*., 2014).

1.1.4. Carotenoids and Bacteriochlorophyll

All anoxygenic phototrophs incorporate BChl into their RC and light harvesting (LH) complexes to act as the primary LH pigment. The process of BChl *a* synthesis in the presence of both light and oxygen results in the formation of triplet BChl and singlet oxygen, both of which exert high levels of oxidative stress on the cells (Yurkov and Csotonyi, 2009). This results in a barrier that all anoxygenic phototrophs have to overcome. PNSB resolve this issue by producing its photosynthetic pigments only under anaerobic conditions. While this is a good strategy, the AAP require O_2 for both growth and photosynthetic function. Therefore, they synthesize BChl *a* only in the dark and then expend it during periods of illumination (Yurkov and Van Germeden, 1993; Yurkov and Beatty, 1998). One exception to this rule is strain EG13, which can produce BChl *a* regardless of light. This could be tied to its high resistance to vanadium oxides, because the cells may have developed a strong method to deal with oxidative stress (Csotonyi *et al*., 2015). Additionally, the AAP keep the concentration of photosynthetic complexes in their membranes low and produce high levels of crt, which may protect the cells from damage (Yurkov and Hughes, 2017).

Though the BChl *a* molecule is the same in both AAP and PNSB, there are a couple of possible differences in biosynthesis. The step in the pathway converting Mg-protoporphyrin IX monomethylester to Mg-divinyl protochlorophyllide uses the enzyme Mg-protoporphyrin IX monomethylester cyclase, which can be encoded by two different genes. The first is the *acsF* gene that uses an O_2 molecule to catalyze the reaction and the second, the *bchE* gene instead takes an oxygen atom from H_2O (Fig. 4) (Raymond and Blankenship, 2004; Zheng *et al*., 2011; Boldareva-Nuianzina *et al*., 2013; Yurkov and Hughes, 2017). It was hypothesized that anaerobic bacteria would all use the oxygen independent form of the enzyme and that aerobic bacteria (AAP) would utilize the oxygen dependent type, however, this did not end up being the case. All purple sulfur bacteria have only the *bchE* gene, all PNSB tested contain both genes and AAP all contain *acsF*, though there are exceptions, with AAP that also have *bchE* (Boldareva-Nuianzina *et al*., 2013; Yurkov and Hughes, 2017). Possibly, *acsF* was gained very early in evolution as its position in the PGC is highly conserved and a phylogenetic tree based on its sequence grouped all tested organisms in the same way as 16S rRNA gene sequences (Boldareva-Nuianzina *et al*., 2013; Yurkov and Hughes, 2017). It is probable that the gene was acquired when cyanobacteria passed it to PNSB through horizontal gene transfer, allowing them to proliferate into oxygenated environments. Conversely, the *bchE* gene may have been gained by each individual organism at different times, as it is highly variable in both position and sequence as compared to 16S rRNA gene sequence (Boldareva-Nuianzina *et al*., 2013; Yurkov and Hughes, 2017). While the procurement of the O_2-dependent *acsF* gene may help to explain how the PNSB were able

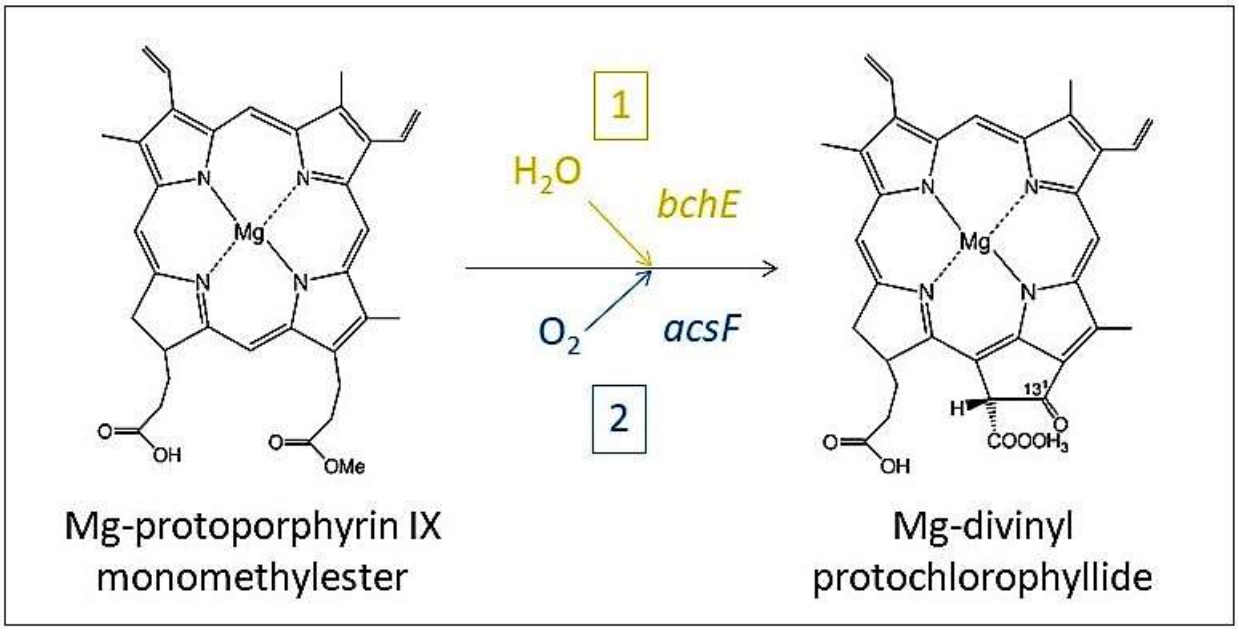

Fig. 4. Conversion of Mg-protoporphyrin IX monomethylester to Mg-divinyl protochlorophyllide, using two different forms of the enzyme Mg-protoporphyrin IX monomethylester cyclase. The first form (1, yellow) is encoded by the gene *bchE* to use an oxygen atom from H_2O. The second (2, blue) is encoded by the gene *acsF* to use atmospheric O_2.

to evolve into AAP, requiring atmospheric oxygen for photosynthetic function, there are still questions about the enigma that is BChl *a* synthesis in aerobic habitats.

As was already eluded to, the AAP are vibrantly coloured due to the high levels of crt incorporated into their membranes. The AAP are divided into three groups based on crt content. The first is the *Roseobacter* clade which contains spheroidenone as its main crt closely associated with the photosynthetic apparatus. The second is the order *Shingomonadales*, primarily producing the non-photosynthetic erythroxanthin sulfate in high amounts. Instead, this group uses the less abundant bacteriorubixanthinal, zeaxanthin and β-carotene for light harvesting (Yurkov and Beatty, 1998, Sato-Takabe *et al*., 2011). Finally, the third group is the NOR5/OM60 clade producing spirilloxanthin associated with the photosynthetic complexes (Sato-Takabe *et al*., 2011; Yurkov and Hughes, 2013).

The roles of crt in AAP are poorly investigated and still debated, but two have been proposed. The first role for crt involves their use as accessory LH pigments, allowing cells to collect a broader range of wavelengths than BChl *a* alone allows. This is speculated in *Roseobacter* strain OBYS0001, which produces spheroidenone as its primary crt. Under substrate-deficient conditions spheroidenone production was increased, suggesting that it may provide some benefit to nutrient starved cells by absorbing green light to increase photosynthetic energy production (Sato-Takabe, Hamasaki and Suzuki, 2012). Further supporting this idea, energy transfer from spheroidenone to BChl *a* was also confirmed in *R. denitrificans* (Slouf *et al*., 2013). The second theory is that crt are involved in photoprotection of

the cells against oxidative stress caused by triplet BChl and singlet oxygen by neutralizing these reactive agents (Yurkov and Beatty, 1998; Klassen, 2009; Zheng *et al*., 2011). For example, zeaxanthin, largely produced in *Erythrobacter* sp. NAP1, is not being used in energy transfer, indicating it has an alternative role (Slouf *et al*., 2013). One AAP species can have numerous different crt, in some cases up to 20 or more (Yurkov, Gad'on and Drews, 1993), with each one presumably playing a different role. It is still unresolved whether all species have crt that aid in light harvesting, or if the majority are used for protection. It is even possible that there are other metabolic functions crt carry out. The only way to answer this question is to continue culture-dependant studies of crt in AAP.

1.1.5. Photosynthetic Complexes and the Electron Transport Chain

The membrane bound photosynthetic complexes of the AAP are structurally almost identical to those of the PNSB. The RC can be observed spectrophotometrically at 800 nm and 860-870 nm due to the bound BChl *a* as well as 750-760 nm from bacteriopheophytin (BPheo), a BChl precursor, also incorporated in the RC. The RC is a complex composed of three subunits (L, H and M) with 4 BChl *a* molecules, two BPheo, two ubiquinones, a non-heme iron and various crt (Yurkov and Beatty, 1998; Yurkov and Csotonyi, 2009). There can be anywhere between 140 and 1800 RC per cell, a full order of magnitude less than is produced by PNSB (Selyanin *et al*., 2016). This small number is presumably to keep oxidative stress to a minimum, while still taking advantage of the benefits of photophosphorylation.

Spectrophotometrically the typical LH1 shows a single peak at 870 nm, though this can be somewhat shifted. Red-shifting is observed in *C. halotolerans* (Fig. 5B) and *Charonomicrobium ambiphototrophicum* (Csotonyi *et al*., 2011a, 2011b) and blue-shifting as far as 855 nm in *R. thiosulfatophilus* (Fig. 5A) (Yurkov and Csotonyi, 2009; Yurkov and Hughes, 2013). These shifts are likely caused by alterations in the proteins. Structurally, the LH1 is a ring of 16 heterodimeric alpha and beta subunits with approximately 30 BChl *a* molecules and various bound crt (Yurkov and Beatty, 1998; Tang *et al*., 2010). Some strains of AAP can also employ an accessory LH2 with dual BChl *a* peaks at 805 and 850 nm. As is seen in the LH1, the LH2 can also have different protein environments causing shifts in the absorption peaks. For instance, *E. ramosum* has a peak at 832 nm and *Porphyrobacter dokdonensis* at 835 nm (Yurkov and Csotontyi, 2009). Additionally, in some rare cases, such as in *R. mahoneyensis* and species of *Roseobacter* and *Rubrimonas*, there is a monomodal peak instead of the more typical dual peaks (Fig. 5C) (Shiba, 1991; Suzuki *et al*., 1999; Rathgeber *et al*., 2005). Structurally, the LH2 is similar to the LH1, however it has only 8-9 heterodimeric alpha/beta subunits (Tang *et al*., 2010; Yurkov and Hughes, 2017).

Exposure to light has been shown to decrease cellular respiration by about 25%, suggesting that AAP can partially replace oxidative phosphorylation with photophosphorylation (Hauruseu and Koblížek, 2012). Also, light intensity can have an effect on the size of the RC-LH1 complex. *Roseobacter litoralis*, under high light intensity had more RC-LH1 complexes than under low light. The complexes were smaller in cells grown in the light (39±3 BChl *a* molecules) compared to grown in the dark (115±30 BChl *a* molecules) (Selyanin *et al*., 2016). It is likely that

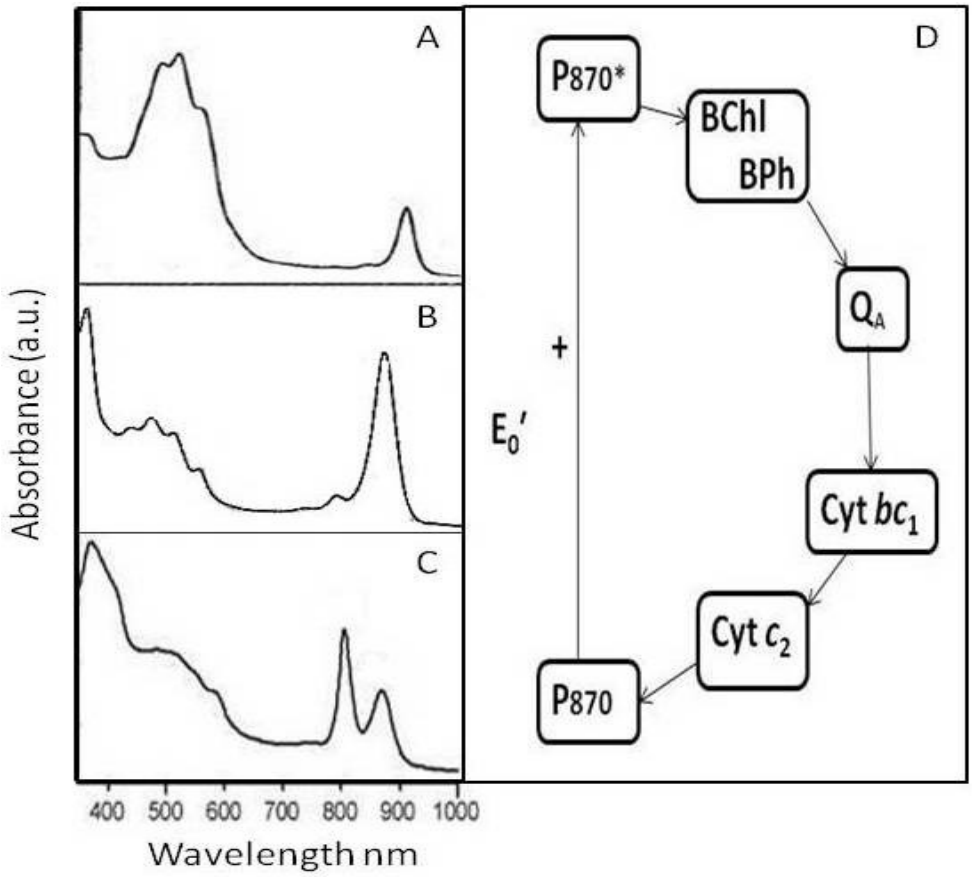

Fig. 5. Variation in LH and RC complexes based on spectrophotometric characteristics: (A) *Roseococcus thiosulfatophilus* blue shifted LH1 (855 nm); (B) *Chromocurvus halotolerans* red-shifted LH1 (877 nm); (C) *Roseicyclus mahoneyensis* rare monomodal LH2 (805 nm) and typical LH1 (870 nm); (D) suggested AAP electron transport chain.

the cultures grown under very low illumination had larger antennae to maximize light harvesting and when grown under intensive light, they are smaller to reduce damage to the RC and cells from oxidative stress (Selyanin *et al*., 2016). It would be interesting to study if this pattern holds true for other AAP species, both marine and freshwater.

Recent studies on the PGC of *Erythrobacter* species have shown that it is between 37 and 38.9kb in length, making up approximately 1.08-1.36% of the total genome (Zheng *et al*., 2016). The genes encoding the LH1 complex are located alongside those for the L and M subunits of the RC in the *puf* operon, while the RC H subunit is in the *puh* operon. Alpha and beta portions of the LH2 complex are placed in the separate *puc* operon (Zheng *et al*., 2011; Yurkov and Hughes, 2013). Encoding the LH2 on a separate operon from the RC-LH1 complex permits independent gene regulation. This means that cells may turn on or off the genes for the LH2 without entirely eliminating photosynthetic activity as has been observed in *C. litoralis* (Spring *et al*., 2009). Additionally, while genes for crt synthesis can be found in the PGC, they can also be dispersed throughout the remainder of the bacterial genome, allowing for autonomous regulation supporting the idea that they are not all involved in photosynthesis (Zheng *et al*., 2011; Yurkov and Hughes, 2013; Zheng *et al*., 2016).

The AAP employ a cyclic electron (e^-) transport chain (ETC) similar to that of the PNSB. Once light energy has been harvested by BChl *a* and accessory pigments, it has to be funneled into the LH complexes and then to the RC to be converted to chemical energy. Photons trigger e^- transfer within the RC from an excited BChl *a* (P^+) to the primary e^- acceptor, a Q_A (quinone)

and then to a Q_B. Reduced Q_B is oxidized in the membrane-bound cytochrome (cyt) *bc₁* complex and cyt*c* in the periplasmic space transfer e^- back to the RC (Fig. 5D) (Yurkov and Beatty, 1998; Yurkov and Csotonyi, 2009). The cyt*c* used for photosynthesis divides the AAP into two major groups. The first, seen in *E. ramosum*, *E. hydrolyticum*, *E. ezovicum*, *E. litoralis* and *E. longus* contains a soluble cyt*c* in the periplasmic space, that passes the e^- directly from the cyt*bc₁* complex to the RC. The second has a tetraheme cyt*c* bound tightly to the RC to accept an e^- from another cyt before passing them to the RC. This is the case for *E. ursincola*, *S. sibiricus*, *R. thiosulfatophilus*, *R. mahoneyensis* and *R. denitrificans* (Yurkov and Beatty, 1998; Yurkov and Csotonyi, 2009; Yurkov and Hughes, 2013).

There are a few possible reasons why the photosynthetic ETC in AAP works under aerobic conditions but can't function anaerobically despite its similarities to the ETC in anaerobic PNSB. First is the redox midpoint potential of the primary e^- acceptor Q_A. In AAP, this typically falls between +5 and +150 mV though, as with everything, there are exceptions. For example, that of *P. meromictius* is -25 mV and *R. denitrificans* has a Q_A midpoint potential of -50 mV (Schwarze *et al.*, 2000; Rathgeber *et al.*, 2012). Contrarily, the Q_A in PNSB has a redox midpoint potential that is generally much lower, in the significantly negative numbers (typically below -20 mV) (Prince and Dutton, 1978; Yurkov and Csotonyi, 2009). High redox midpoint potentials under reduced (anoxic) conditions can cause the Q_A in AAP membranes to become over-reduced, so it cannot accept e^- (Rathgeber *et al*., 2004; Yurkov and Csotonyi, 2009; Yurkov and Hughes, 2013). Second, PNSB may use an alternative quinol oxidase pathway to keep the Q_A in the correct redox state for efficient photosynthetic function. This pathway may be absent

in AAP, forcing them to rely on environmental conditions for control of redox state. For example, the Calvin cycle, which is missing in AAP, requires NADH. The PNSB could use excess e^- from the Q_A to reduce NAD^+, which in turn oxidizes the Q_A. Third, in *R. denitrificans* O_2 is required for soluble cyt to transfer e^- from cyt_{bc1} complex to the RC-bound cyt*c*. This may be true of other AAP species and could cause anaerobic e^- transfer to come to an abrupt halt (Yurkov and Beatty, 1998; Yurkov and Csotonyi, 2009). While there are several theories based on available data for the lack of anaerobic photosynthesis in AAP, none have been solidly confirmed and this remains one of the great unanswered questions related to the AAP.

1.1.6. Bacterial Mutations

A mutation is defined as a permanent alteration in DNA sequence, and may affect phenotype of an organism (Najafi and Pezeshki, 2013). This can occur spontaneously or can be induced by environmental factors. Common forms are: point mutations, where a single nucleotide is replaced by another nucleotide; and either the deletion or addition of a nucleotide (Najafi and Pezeshki, 2013). The changes in nucleotide sequence can result in many different types of mutations. They include: missense mutation, where a single amino acid is changed; nonsense mutation, when a stop codon is formed, causing protein synthesis to be interrupted; silent mutation, which does not cause a change in amino acid sequence; and frameshift mutation, where the reading frame of the DNA is shifted due to the addition or deletion of a nucleotide, causing all amino acids to be changed (Najafi and Pezeshki, 2013). In some cases, a mutation will occur in a vital gene, and therefore be lethal to the cell. In other cases, a simple

phenotypic change will be seen in the organism (Najafi and Pezeshki, 2013). Mutations in bacteria are of great interest, as they may hint at the evolution of microorganisms as they adapt to new conditions.

1.1.7. Description of *Roseicyclus mahoneyensis*

R. mahoneyensis, type strain ML6 was isolated in 1997 from Mahoney Lake in British Columbia, Canada (Yurkova *et al*., 2002). This is a meromictic lake, meaning it remains stratified at all times with an aerated top layer (mixolimnion), a sharp chemocline and a fully anoxic bottom layer (monimolimnion). The lake is highly saline, having been classified as a sodium sulfate lake (Yurkova *et al*., 2002; Hall and Northcote, 1986). As would be expected for an obligately aerobic bacterium, the strain was collected from the oxygenated mixolimnion at a depth of 3m (Yurkova *et al*., 2002). It is a non-motile, Gram-negative α-proteobacterium that forms pink-purple coloured colonies and morphologically, the cells are either rods or are so sharply vibroid that they are almost cyclic, as has previously been observed in the PNSB *Rhodocyclus purpureus* (Pfennig, 1978; Yurkova *et al*., 2002; Rathgeber *et al*., 2005). Based on 16S rRNA gene sequence similarity, the closest relatives of ML6 are only distantly related with the non-phototrophic bacteria from the genera *Octadecabacter* and *Ketogulonicigenium* sharing 92.0-92.9% and 92.2-92.6% sequence similarity, respectively and the AAP species *Roseivivax halodurans* and *Roseovarius tolerans* showing only 92.2-92.9% and 91.7-92.6% similarity, respectively (Rathgeber *et al*., 2005).

Photosynthetically, ML6 is quite unusual. While it contains a very typical LH1-RC with BChl *a* peak at 870 nm, its LH2 is quite odd, as it is a monomodal complex with a single peak at approximately 805 nm, a feature that has only ever been seen twice before (Yurkova *et al*., 2002), as described in section 1.1.5. This species utilizes a RC-bound cyt*c* for photosynthetic e^- transfer and, oddly, it performs photosynthesis most efficiently under microaerophilic conditions (Rathgeber *et al*., 2012), making it a possible evolutionary link between the AAP and the PNSB. This could indicate that ML6 primarily uses photosynthesis for energy production during periods of O_2 depletion, which could arise when other heterotrophs within the community rapidly respire the available O_2 (Rathgeber *et al*., 2012). These unconventional photosynthetic features make ML6 an ideal organism for continued study as they could reveal new information about photosynthetic function of unusual complexes.

1.1.8. Novel Proteins and Pigments in *Chromocurvus halotolerans*

C. halotolerans, strain EG19 is one of only two taxonomically described γ-proteobacterial AAP (Csotonyi *et al*., 2008). It is most closely related to non-phototrophs from the genus *Haliea* (95.1-96.1% 16S rRNA gene sequence similarity) and to the only other γ-*Proteobacteria* AAP, *C. litoralis* (95.6% similarity) (Csotonyi *et al*., 2011a). It was isolated from floating microbial mats from a sampling trip to the East German Creek System, Manitoba, Canada in the spring of 2002. This is a landlocked hypersaline spring system, making it likely to contain highly endemic communities of microorganisms that have not been mixed with or affected by outside populations (Csotonyi *et al*., 2008).

Strain EG19 forms motile, short rod or longer curved rod-shaped, orange-pink bacteria. Photosynthetically, BChl *a* peaks incorporated into the LH1 and RC complexes appear at approximately 802 and 877 nm (Csotonyi *et al*., 2011a), making the LH1 somewhat red-shifted from the norm. Interestingly, when grown with complex carbon sources, EG19 produces an orange-brown pigmented hydrophilic compound, which it excretes into the growth medium. This phenomenon has never been reported in AAP. Spectrophotometric analysis showed peaks at 230, 280, and 325 nm, suggesting it may be a siderophore (Csotonyi *et al*., 2011a). The classification of EG19 in the γ-*Proteobacteria* as well as the red-shifted LH1 and the mystery compound excreted into the growth medium make it an intriguing AAP for study. These could reveal novel protein environments for BChl *a* and therefore differences in photosynthetic ability. Additionally, the compound could reveal new roles and strategies for AAP in their natural habitats.

1.1.9. The Enigma of Dual Aerobic/Anaerobic Photosynthesis Apparatus Production in *Charonomicrobium ambiphototrophicum*

C. ambiphototrophicum, strain EG17 is potentially the most compelling of the species of AAP being studied in this thesis. Like strain EG19, it was isolated from the East German Creek System, Manitoba, Canada in May 2002 (Csotonyi *et al*., 2008). It forms deep orange-brown colonies on agar media and cells are coccoid to rod shaped (Csotonyi *et al*., 2011b). It is most closely related to AAP species *Roseibacterium elongatum* (98.3% 16S rRNA gene sequence similarity), *D. shibae* (95.2% similarity) and *R. mahoneyensis* (94.7%).

What is most interesting about EG17 is that it produces photosynthetic pigments and proteins under both aerobic and anaerobic conditions. Aerobically, when grown in the dark, BChl *a* peaks are observed at 802 and 879 nm, indicating a typical RC and a red-shifted LH1, similar to what is seen in *C. halotolerans*, strain EG19. However, when grown in anoxic circumstances with illumination, in addition to those same peaks, we observe an LH2 peak at 850 nm (Csotonyi *et al*., 2011b). This was highly unexpected as it blurs the line between its identification as either AAP, which are obligately aerobic photosynthesizers or PNSB, which should not be able to produce photosynthetic pigments in oxygen rich environments. There are, of course, exceptions such as the PNSB *R. centenaria* and *R. sulfidophilum*, in which their PGC are only partially repressed aerobically. These both, however, retain photosynthetic functions only anaerobically (Yildiz *et al*. 1991; Masuda *et al*. 2008; Csotonyi *et al*., 2011b). Contrarily, EG17 was capable of anaerobic photosynthesis, displaying growth curves similar to those of the PNSB, as well as aerobic photosynthesis with greater biomass production when grown aerobically in a light/dark cycle than when grown solely in the dark (Csotonyi *et al*., 2011b). Typically, PNSB would also be capable of autotrophy, however, EG17 showed no sign of autotrophic growth anaerobically, suggesting the Calvin Cycle is not present, though only genome sequencing will be able to confirm this. Absence of photoautotrophy along with the dual photosynthetic ability (aerobic and anaerobic) suggests that EG17 could be a true evolutionary intermediate between the PNSB and the AAP. This makes it an important bacterium to investigate as it could lead to some answers about bacterial evolution upon oxygenation of the atmosphere.

1.2. Siderophores and Bacterial Iron Acquisition

Iron is one of the essential elements for all forms of life. In microorganisms, it is used as a co-factor for enzymatic processes, such as in e^- transfer in both aerobic and anaerobic respiration and photosynthesis, nucleic acid synthesis, chlorophyll synthesis, nitrate reduction, nitrogen fixation and even in detoxification of oxygen radicals (Granger and Price, 1999; Challis, 2005; Schalk, Hannauer and Braud, 2011). The use of iron in chlorophyll production and in photophosphorylation makes it particularly important to phototrophic organisms and may be especially crucial to AAP to protect the cells from oxidative stress due to singlet oxygen. Unfortunately, despite being abundant in the Earth's crust, iron can be very difficult for cells to collect from their natural environments, especially for aerobic bacteria as the bioavailability of soluble Fe is very low at the surface of soil and water. This is because at neutral or alkaline pH, iron reacts with O_2 to produce oxyhydroxide complexes, which cannot be used by microbes (Challis, 2005). Therefore, to be able to compete for the available Fe in the environment, bacteria and fungi have developed siderophores (Faraldo-Gomez and Sansom, 2003).

Siderophores are low molecular weight molecules (no more than 1500-2000 Da and generally lower than 1000 Da) with a high-affinity for iron (Reid *et al*., 1993; Wandersman and Delepelaire, 2004; Challis, 2005; Schalk, Hannauer and Braud, 2011; Grobelak and Hiller, 2017). These molecules are often short polypeptide backbones with modified or D-amino acids incorporated (Crosa and Walsh, 2002; Wandersman and Delepelaire, 2004; Challis, 2005). Others, such as aerobactin, rhizobactin, achromobactin, vibrioferrin, alcalignin and desferrioxamine are not polypeptides (Challis, 2005). These are instead made from dicarboxylic

acids and diamine or amino alcohols, linked by amide and ester bonds. These building blocks are derived from amino acids and retain some of their characteristics (Challis, 2005). Based on the functional groups that are used to bind iron, the siderophores can be classified into two main groups. The first is the hydroxamate group, which uses hydroxamic acid and is produced by both fungi and bacteria. Second is the catechol group, which contains catechol rings and is only produced by bacteria (Faraldo-Gomez and Sansom, 2003; Wandersman and Delepelaire, 2004; Grobelak and Hiller, 2017). Additionally, there are smaller groups such as the hydroxyacids and the α-hydroxy carboxylates, which are used by far fewer bacteria (Wandersman and Delepelaire, 2004; Grobelak and Hiller, 2017).

Siderophores are constructed and then secreted by cells in energetically costly processes under iron-deplete growth conditions, therefore when iron concentrations are high, siderophore biosynthesis is down-regulated (Reid *et al*., 1993). Once bound to iron, the complex is taken up again by the cells in a highly substrate specific ATP consuming process (Challis, 2005). Once inside the cell, there are two proposed mechanisms for release of the iron. The first takes into account that the molecules have a much lower affinity for ferrous iron than for ferric iron. In this case, intracellular e^- donors will reduce the iron causing the siderophore to release it and then the iron-chelator can be re-used by being secreted back out into the environment (Wandersman and Delepelaire, 2004; Schalk, Hannauer and Braud, 2011). This theory may be accurate for siderophores with relatively low chelating affinity, however it is not very well supported at this time. The second, more likely argument is that upon entry, the siderophore is degraded as there is no way for the cell to force the release of iron. In this case,

each molecule can only be used once (Wandersman and Delepelaire, 2004; Schalk, Hannauer and Braud, 2011) and is likely what occurs in siderophores with very high iron-affinity.

As siderophore production is such an energetically costly process, a phenomenon called "social cheating" can come into effect (Hibbing *et al*., 2010). This means that some species will only develop the ability to take up siderophore-iron complexes, but will not actually construct the siderophore molecule themselves. It will instead use the secreted siderophores from other organisms as common property, giving them a competitive advantage over the microbes that have synthesized the compound (Hibbing *et al*., 2010) and can even cause dependence on the siderophore-producing bacterium, with the social cheater unable to grow in laboratory conditions without the presence of the other organism (D'Onofrio *et al*., 2010). Another form of siderophore competition arises when many organisms in a single community all produce iron-chelators. In this instance, the bacterium that has the siderophore with the highest affinity for iron wins (Hibbing *et al*., 2010).

While the main purpose of siderophores is iron acquisition, they may play additional roles. In *Pseudomonas aeruginosa*, pyoverdine controls virulence factor production (Lamont *et al*., 2002). *Escherichia coli* can be protected from oxidative stress by the catechol type siderophore enterobactin due to its ability to reduce reactive oxygen species (Adler *et al*., 2012). Pyochelin in *P. aeruginosa* has a toxic effect on eukaryotic cells by producing reactive oxygen species, possibly aiding in the bacterium's virulence (Adler *et al*., 2012). Watasemycins, sideromycins, oxachelin and fusigen have antibacterial activity, which may aid their producers

in competition against other bacteria in the community (Adler *et al*., 2012). Additionally, many siderophores can actually bind metals other than iron (Schalk, Hannauer and Braud, 2011). This has implicated them in some toxic heavy metal tolerances. In extreme environments in particular, necessary metals such as copper, chromium and cobalt can be in high enough concentrations to become toxic to bacteria, thereby requiring a mechanism to keep them from overwhelming the cells (Schalk, Hannauer and Braud, 2011). Most metal ions can diffuse freely through porins in the cellular membrane. This is not however possible if the metal is bound to a siderophore making it too large to pass through unimpeded. Additionally, the receptors on the membrane that recognize siderophores are very specific to siderophore-iron complexes and therefore cannot identify a complex involving an alternate ion, causing the cell to not absorb the molecule. This reduces the free metals in proximity to the bacterium, lowering their toxic effect (Schalk, Hannauer and Braud, 2011). Confirmation was afforded when it was shown that *P. aeruginosa*, which produced pyochelin and pyoverdine, had increased toxic metal resistance compared to cultures of the same bacterium that could not produce siderophores (Schalk, Hannauer and Braud, 2011). This is a very interesting concept, as it has been noted above, the AAP tend to have very high resistance to toxic heavy metalloid oxides. Perhaps a similar mechanism can be found in them. Additionally, the siderophores' ability to reduce reactive oxygen species could come in to play in AAP as they need so much protection against oxidative stress due to the aerobic production of BChl *a*. Only more study will provide the answer as siderophores have not yet been positively identified in AAP.

1.3. Gold Mine Tailings at Nopiming Provincial Park

Nopiming Provincial Park is located in Manitoba, Canada in the Rice Lake Greenstone Belt (Tycholiz *et al*., 2016). This area was full of gold mines in the early to mid 1900's. The Central Gold Mine was the largest and the first one to come into operation in 1927. It was in operation for 10 years before closing for good in 1937 (Tycholiz *et al*., 2016). In the mining process, ore was crushed, followed by the addition of sodium cyanide, which acted to dissolve the gold. Zinc powder was added to this slurry to precipitate the gold, allowing for its collection (Fig. 6A) (Tycholiz *et al*., 2016). The processing of over 500 kilotons of ore created large amounts of contaminated waste called tailings, which were simply disposed of directly in the surrounding terrain (Londry and Sherriff, 2007; Tycholiz *et al*., 2016). Once production ended, the tailings were abandoned without any attempt at remediation of the site. The tailings are so high in toxic compounds that they turned the forest into a barren wasteland, which remains unchanged to this day, 80 years later (Fig. 6B).

Chemical analysis of the tailings revealed that it consists of mostly quartz, pyrite, chalcopyrite, and calcite with very high concentrations of copper, potentially enough to cause toxicity to microorganisms. Gold atoms were below detectable limits, confirming the efficacy of the mining process (Londry and Sherriff, 2007; Sherriff, Sidenko and Salzsauler, 2006). When sulfides in the tailings are exposed to the air, oxidation occurs causing acid production, which can then be mobilized through water flow and further erosion (Sherriff, Sidenko and Salzsauler, 2006; Tycholiz *et al*., 2016). This is the main way acid mine drainage occurs and is a vicious

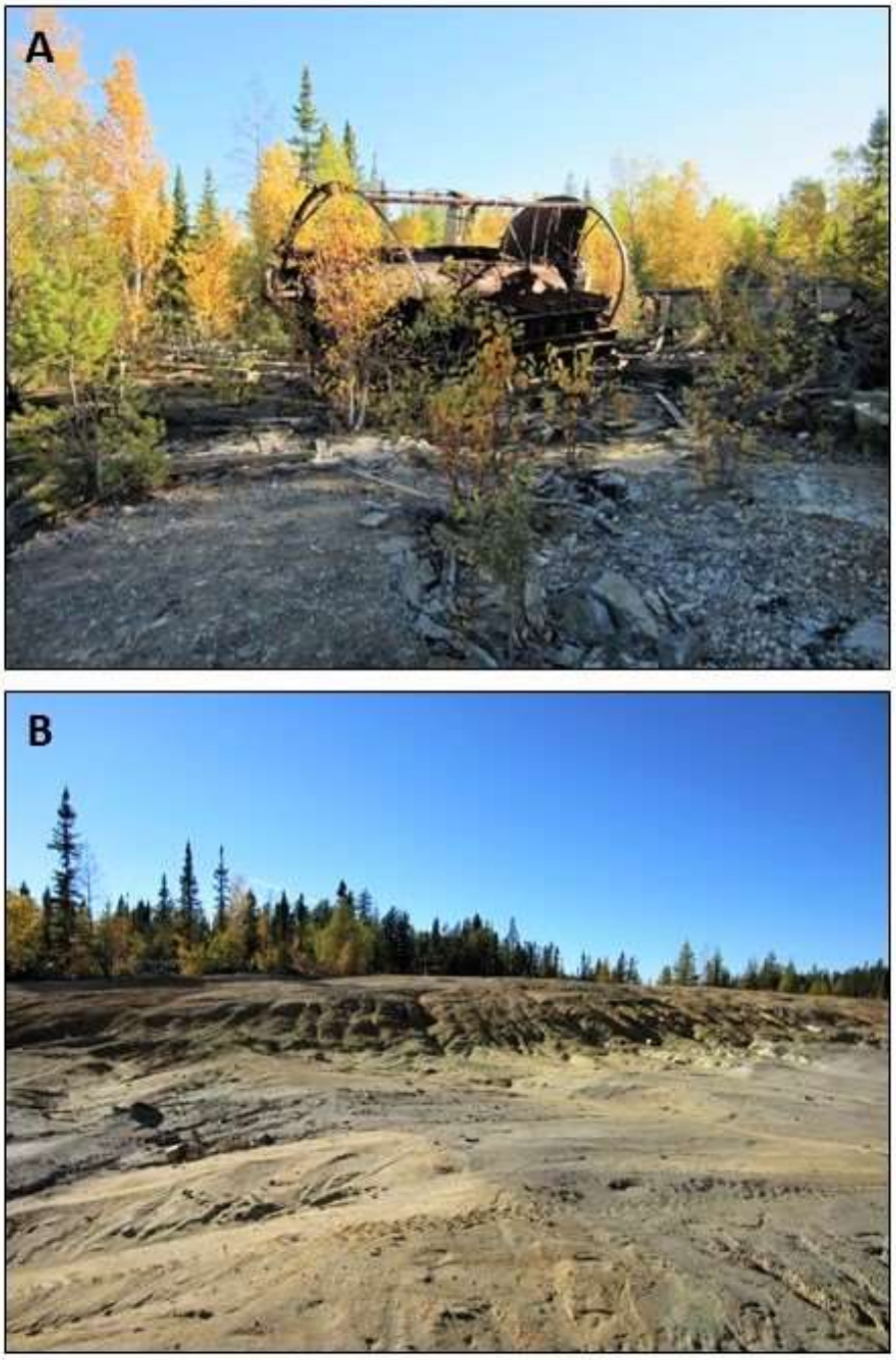

Fig. 6. Central Gold Mine, Nopiming Provincial Park, Manitoba, Canada: (A) Abandoned mining equipment; (B) Mine tailings appear as a barren wasteland surrounded by forest. Photographs are from the archives of the Yurkov laboratory, Department of Microbiology, University of Manitoba.

cycle, as erosion transports the acid revealing more sulfides underneath, which are then also oxidized creating even more acid. The acid mine drainage can have a negative impact on the forest, waterbodies, wildlife, and human health (Tycholiz *et al*., 2016). This is apparent by the lack of vegetation at the tailings site and the pH was shown to be lower at the surface than in lower layers (Londry and Sherriff, 2007). Microbiological studies done at the Central Gold Mine showed that the high levels of minerals and ions supported an abundant and diverse biomass, with few bacteria at the surface and much more in middle layers of the sediment, suggesting the majority of cells are anaerobic (Londry and Sherriff, 2007). Biological processes observed include anaerobic respiration using iron reduction, sulfate reduction, and methanogenesis. Further study into this extreme environment is required to determine more about the microbial community and how it may interact with the toxic compounds present in the tailings.

1.4. Thesis Objectives

As presented in previous sections of this literature review, there is much to learn about the diversity, distribution and ecology of AAP, and their photosynthetic physiology. I therefore set out to study the unusual photosynthetic apparatuses of *R. mahoneyensis*, strain ML6, *C. halotolerans*, EG19 and *C. ambiphototrophicum*, EG17. My aim was three-fold. First, to isolate and purify the red-shifted LH1-RC complex of both EG19 and EG17 as well as the monomodal LH2 and LH1-RC complexes of ML6 and its spontaneous mutants. From there, I performed a biokinetic analysis of the pure complexes, isolated membranes and whole cells of all strains with the purpose of determining photosynthetic function, redox midpoint potentials of e^- carriers and finally the light harvesting role of crt in the studied AAP. Second, the unknown

pigmented compound secreted into the growth medium by strain EG19 warranted investigation. I identified it as a siderophore, purified it and attempted to characterize its structure. Finally, I endeavored to isolate novel species of AAP from the extreme environment of Central Gold Mine, Nopiming Provincial Park, Manitoba, Canada. The specific goals were as follows:

(1) To investigate photosynthetic activity of AAP with unusual pigment-protein complexes. Strains chosen for study were: ML6 due to its odd monomodal LH2 and its rapid mutations; EG19 for its red-shifted LH1; and EG17 for two reasons, its red-shifted LH1 and, more importantly, its ability to produce the photosynthetic complexes under both aerobic and anaerobic conditions.

(2) To identify the brown-orange pigmented compound secreted by cells of EG19 into the growth medium. It is hypothesized to be a siderophore, which could make it an important discovery, as it would be the first one to be determined in AAP.

(3) With so many unanswered questions about the distribution of AAP and their ecological role, especially in extreme environments, and in keeping with the interests of the Yurkov laboratory, it is important to continually search for novel AAP. I therefore set out to isolate novel strains from gold mine tailings at Nopiming Provincial Park, Canada.

Chapter 2.

Materials and Methods

2.1. Analysis of Photosynthetic Pigment-Protein Complexes

2.1.1. Microorganisms and Growth Conditions

Species used for study are *Roseicyclus mahoneyensis*, strain ML6, (Rathgeber *et al*., 2005), *Chromocurvus halotolerans*, strain EG19 (Csotonyi *et al*., 2011a), and *Charonomicrobium ambiphototrophicum*, strain EG17 (Csotonyi *et al*., 2011b).

Unless otherwise stated *R. mahoneyensis*, ML6 and all of its spontaneous mutants were grown aerobically in the dark at 28°C on N1 medium containing (g/l): $MgSO_4$, 2.0; NH_4Cl, 0.3; KCl, 0.3; Na_2SO_4, 15.0; Na-acetate, 1.0; malic acid, 1.0; yeast extract, 1.0; and bactopeptone (0.5), as well as vitamins and trace elements solutions, 2.0 ml each. After autoclaving at pH 5.9, 3.0 ml of 10% KH_2PO_4, 0.5 ml of 10% $CaCl_2$ and 5.0 ml of 10% $NaHCO_3$ are added to the medium before it is adjusted to pH 7.8 with sterile 0.5N NaOH. *C. halotolerans*, EG19 and *C. ambiphototrophicum*, EG17 were also grown in the presence of oxygen at 28°C on Medium A (MA) containing (g/l): $MgSO_4$, 3.0; Na_2SO_4, 1.8; KH_2PO_4, 0.3; NH_4Cl, 0.3; KCl, 0.7; $CaCl_2$, 0.05; NaCl, 40.0; Na-acetate, 1.0; yeast extract, 1.0; bactopeptone, 0.5; and casamino acids, 0.5; as well as vitamins and trace elements solutions, 2.0 ml each. After autoclaving at pH5.9, medium is adjusted to pH 7.8 with sterile 0.5N NaOH. For anaerobic growth, strain EG17 is cultured in an illuminated incubator in liquid medium in either degassed bulch tubes or screw cap tubes filled to the top, or on agar plates in an anaerobic chamber, at 28°C on Medium B (MB) containing (g/l): $MgCl_2$, 2.5; Na_2SO_4, 3.5; KH_2PO_4, 0.3; NH_4Cl, 0.5; KCl, 0.7; $CaCl_2$, 0.05; NaCl, 40.0; Na-acetate, 1.0; and yeast extract, 0.5; as well as vitamins and trace elements solutions, 2.0 ml and 10.0 ml, respectively. After autoclaving at pH 5.9, 30.0 ml of 5% $NaHCO_3$, 0.029 ml of 1% $FeCl_3$

and 3.0 ml of 10% $Na_2S_2O_3$ were added to the medium, which was then adjusted to pH 7.8 with sterile 0.5N NaOH. Vitamins solution contains (mg/200 ml): nicotinic acid, 80.0; biotin, 16.0; thiamine, 80.0; and vitamin B_{12}, 4.0. Trace elements solution contains (mg/500 ml): $FeSO_4$, 150.0; $CoCl_2$, 2.5; $MnCl_2$, 1.5; $CuCl_2$, 0.5; $NiCl_2$, 1.0; Na_2MoO_4, 1.5; $ZnSO_4$, 2.5; and H_3BO_3, 1.0.

2.1.2. Study of Spontaneous Mutants in ML6

Single colonies of strain ML6 were serially diluted and spread plated for single colonies on N1 medium plates (2% agar) to observe spontaneous mutations based on colony characteristics. Frequency of mutation was subsequently calculated as number of mutated colonies divided by total number of colonies on a plate. This was then expressed as a percentage by multiplying by 100. Mutated colonies were picked and purified through further serial dilutions and sub-cultured at least 10 times to ensure stability.

Stable spontaneous mutant strains designated ML6(B), ML6(DB), ML6(N1), ML6(N5), ML6(N9O), ML6(N9P) and ML6(BN9O) were then grown under a range of environmental conditions in an attempt to force reversion to the wild type or to induce further mutations. N1 medium was altered to be pH 7.0 or pH 10.0. In addition to 28°C, N1 agar plates were also grown at room temperature. Cultures were subjected to growth under a light/dark regimen matching the night/day. Finally, cells were cultured on N1 medium containing decreased (1%) Na_2SO_4 to change the salinity of the medium. Mutant colonies were initially identified by differences in colony colour and were then all tested spectrophotometrically for the presence of BChl *a* and, therefore photosynthetic complex production using spectrophotometry. They

were later observed microscopically for cell morphology. Three mutants, ML6(B), ML6(DB) and ML6(BN9O), with unusual photosynthetic pigment-protein complexes were selected for further study.

Strains ML6, ML6(B), ML6(DB) and ML6(BN9O), as well as strains EG19 and EG17 were grown in liquid culture for 7 days on a shaking incubator at 200 rpm. At 24 h intervals, cultures were tested for levels of BChl *a* to determine optimal incubation time for maximal photosynthetic protein complex production for isolation and purification.

2.1.3. Spectrophotometry and Microscopy

Absorption spectra were recorded by full wavelength scans through the entire visible light spectrum from 380 nm to 1100 nm on a Hitachi U-2010 spectrophotometer using the computer program UV Solutions. A loopful of bacteria was collected from agar plates, or 1.0 ml liquid culture was centrifuged to pellet cells. Whole cells were then suspended in 300µl of 20mM Tris HCl buffer, pH 7.8 and 700µl of 30% bovine serum albumin was then added to reduce light scattering and the sample was mixed well. The machine was calibrated with 300µl 20mM Tris-HCl buffer, pH 7.8 mixed with 700µl BSA. Absorption spectra of isolated membranes and pure pigment-protein complexes were obtained by mixing 100µl of a thick sample suspension in 900µl of 20mM Tris HCl, pH 7.8. The spectrophotometer was calibrated with 20mM Tris HCl, pH 7.8.

Microscopy was performed on a Zeiss Axioskop2 phase contrast microscope by placing 15µl of liquid culture on a glass slide or by suspending cells from an agar plate in 15µl of sterile tap water on a glass slide.

2.1.4. Isolation of Membrane and Soluble Fractions

Strains ML6, ML6(B), ML6(DB), ML6(BN9O) and EG19 were grown for 3 days in liquid medium in a shaking incubator at 200 rpm. Aerobic cultures of EG17 were grown for 24 hours in liquid medium in a shaking incubator at 200 rpm and anaerobic cultures of EG17 were grown for 7 days on 2% agar plates in anaerobic jars in an illuminated incubator. All steps from here on were done with samples kept in the dark and on ice to prevent degradation of BChl *a* and denaturation of protein complexes. Cells from liquid culture were collected using centrifugation at 10K rpm for 20 min at 4°C on a Beckmann J2HS centrifuge with a JA-10 rotor and agar plates of anaerobically grown EG17 were scraped to collect cells. Cells from all cultures were washed with 20mM Tris-HCl, pH 7.8 buffer and pelleted using centrifugation under the same conditions as above. Washing was repeated two more times, and finally pellets were mixed in 20mM Tris-HCl, pH 7.8 buffer to form a thick homogeneous suspension. For every 100 ml of cell suspension 1.0 ml 10% EDTA in 20mM Tris-HCl pH 7.8, 1.0 ml of 1mM PMSF in 95% ethanol and 0.05g DNAse were added. The suspension was then subjected to pressure using a French press cell at 20K psi three consecutive times to break cells open. This cell homogenate was centrifuged one hour at 15K rpm at 4°C in a Beckman JH2S centrifuge in a JA-20 rotor to pellet cell debris and unbroken cells. The supernatant was collected and centrifuged 15 h at 60K rpm at 4°C using a Beckman Optima LE-80K ultracentrifuge and a 70-Ti rotor to pellet the membranes. The

membrane pellet was homogenized in 20mM Tris-HCl pH 7.8 buffer to make a very thick suspension and the soluble fraction (supernatant) was collected to test for the presence of soluble cyt*c* based on absorption spectra.

2.1.5. Purification of Photosynthetic Complexes

All steps in purification of photosynthetic complexes were performed in the dark to prevent degradation of pigment-protein complexes. All strains were tested with multiple treatment conditions to determine the most effective method for complex purification. Membranes were treated when they were ice cold, at room temperature, or warmed to 30°C (in the case of EG19). Concentrations of detergents tested included 0.6% LDAO, 1.2% LDAO, 1.5% LDAO, 8% Triton X-100, and 4% Triton X-100. Samples were also subjected to vigorous, moderate or slow mixing for either 20 or 30min. Optimal treatment for strains ML6, ML6(B), ML6(DB) and ML6(BN9O), was when thick suspensions of ice cold membranes were treated for 30 min with 8% Triton X-100 with slow mixing. Samples were then loaded onto sucrose density gradients (0.6M, 0.9M, 1.2M, and 1.5M sucrose in 20mM Tris-HCl, pH 7.8, with 0.05% Triton X-100). Ice cold membranes from aerobically grown EG17 were also treated with 8% Triton X-100, but for only 20 min with a moderate mixing speed and loaded onto sucrose density gradients (0.6M, 0.9M, 1.2M, and 1.5M sucrose in 20mM Tris-HCl, pH 7.8, with 0.05% Triton X-100). Room temperature membranes from EG19 were treated for 20 min in 1.2% LDAO with fast mixing and loaded on sucrose density gradients (0.6M, 0.9M, 1.2M and 1.5M sucrose in 20mM Tris-HCl pH 7.8, with 0.05% LDAO). Gradients were all spun in a Beckman Optima LE-80K ultracentrifuge with a 70-Ti rotor for 15 h at 38K rpm to separate photosynthetic complexes.

Individual bands were carefully removed from the gradient using a pipette and full wavelength scans were performed to spectrophotometrically test for the presence of photosynthetic complexes. Relevant samples were dialyzed with 12 KDa molecular weight cut-off dialysis tubing three times for 8 h each in 20mM Tris-HCl, pH 7.8 to remove sucrose and detergents. Tubing was packed in PEG6000 to concentrate the complexes.

Further purification was carried out by loading concentrated samples on a DEAE-Sephacel anion exchange column equilibrated with 20mM Tris-HCl, pH 7.8 with either 0.05% Triton X-100 (for ML6, ML6(B), ML6(DB), ML6(BN9O) and EG17 samples) or 0.05% LDAO (for EG19 samples). Fractions were collected, and again tested for presence of intact photosynthetic complexes through spectrophotometry, dialyzed and concentrated, as described above.

2.1.6. Biophysical Analysis

Flash induced difference spectra were carried out on whole cells of ML6, ML6(B), ML6(DB), ML6(BN9O), EG19 and aerobic EG17, as well as membrane fractions from the same aerobically grown strains and membranes from anaerobically grown EG17, and finally, pure pigment-protein complexes from all aerobically grown cultures using a Joliot type spectrophotometer (Joliot, Béal and Frilley, 1980) with excitation by a xenon flash bulb with absorbance detected 5, 30 and 60ms after the flash. Whole cells were put in a closed cuvette and allowed to deplete the O_2 through respiration for a period of 2h before flash induced difference spectra were performed again for analysis on anaerobic photosynthesis.

Action spectra were performed on membrane fractions and pure complexes. Monochromatic continuous illumination (10 nm bandwidth) was provided by a SPEX Fluorolog-2 illuminator (a xenon arc-lamp fitted to a 1681 Minimate f/4 monochromator with 2.5 mm slits). The photochemical rate was determined as the rate of accumulation of P^+ (measured at 605 nm) after illumination was switched on by a computer-controlled mechanical shutter opening faster than 6ms. Action spectra represent the photochemical rate corrected by the irradiance of the illuminator, measured with a Macam photometer.

Membrane fractions were used for redox titrations of the Q_A, RC-bound cyt*c* and P^+ using the redox mediators ferrocenecarboxylic acid, 1',1'-dimethylferrocene, 1,2-naphthoquinone, menadione, p-benzoquinone and 2,5-dimethyl-p-benzoquinone in 100% ethanol at a concentration of 10mM as well as potassium ferricyanide, 2-hydroxy-1,4-naphthoquinone, anthraquinone-2-sulfonic acid, benzyl viologen dichloride, methyl viologen dichloride and phenazine methylsulfate in water, also at 10mM concentration. 100mM KCl was added for conductivity.

2.1.7. Polyacrylamide Gel Electrophoresis

SDS-PAGE was performed with 10% acrylamide/bisacrylamide for separation of RC complex subunits and 14% acrylamide/bisacrylamide for LH complex subunits.

2.2. Characterization of the Pigmented Compound Secreted by *Chromocurvus halotolerans*

2.2.1. Chromeazurol S Assay

Strain EG19 was grown on altered MA plates containing the dye chromeazurol S (CAS), which is blue when bound to iron and turns yellow/orange when released (Schwyn and Neilands, 1987). To make media, 60.5mg CAS was dissolved in 50 ml distilled water. This was mixed with 10 ml of an iron solution containing 1mM $FeCl_3$ and 10mM HCl. 72.9 mg HDTMA was dissolved in 40 ml distilled water and the CAS/iron solution was added to the HDTMA, bringing the volume to 100 ml. 900 ml modified MA containing no iron was made with the correct amount of solutes for 1000 ml of media as that would be the final volume of medium after addition of the CAS solution. Medium was then autoclaved at pH 5.9, separate from the CAS mixture. After autoclaving, the medium was adjusted to pH 6.8 with 0.5N NaOH and the CAS solution was added. Agar plates were poured and were blue when solidified. If measurements of ingredients are not exact or are added in the incorrect order, CAS precipitates out of solution and if plates are at higher than pH 6.8, they appear green instead of blue. Therefore, accuracy was very important in this assay! This allowed us to colorimetrically determine the presence of a siderophore (Schwyn and Neilands, 1987).

This same test was also performed on 101 strains of AAP from our collections: From the Central Gold Mine, Nopiming Provincial Park, Canada (strains C4, C9, C11, NM4.16, NM4.18) on rich organic (RO) medium containing (g/l): $MgSO_4$, 1.0; KH_2PO_4, 0.3; NH_4Cl, 0.3; $CaCl_2$, 0.1; Na-acetate, 1.0; yeast extract, 1.0; bactopeptone, 0.5; and casamino acids, 0.5; with vitamins and trace elements solutions, 2.0 ml each; Mahoney Lake, Canada (ML1, ML3, ML4, ML6, ML6(B),

ML6(DB), ML6(N1), ML6(N5), ML6(N9P), ML6(N9O), ML6(BN9O), ML10, ML14, ML15, ML16, ML17, ML18, ML19, ML20, ML21, ML22, ML23, ML29, ML30, ML31, ML32, ML33, ML34, ML35, ML36, ML37, ML38, ML39, ML40, ML42, ML43, ML44, ML45, and ML47) on N1 medium as described in section 2.1.1.; Blue Lake, Canada (BL1, BL4, BL5, BL7, BL8, BL9, BL11, BL14, BL17, and BL22) with medium containing (g/l): $MgSO_4$, 0.5; NH_4Cl, 0.3; KCl, 0.3; NaCl, 12.0; Na-acetate, 1.0; Malic acid, 1.0; yeast extract, 1.0; bactopeptone, 0.5; with vitamins and trace elements solutions, 2.0 ml each; autoclaved at pH 5.9 and then the addition of 10% KH_2PO_4, 3.0 ml; 10% $CaCl_2$, 0.5 ml; and $NaHCO_3$, 5.0 ml; East German Creek System, Canada (EG1, EG2, EG3, EG4, EG5, EG6, EG7, EG8, EG9, EG10, EG11, EG12, EG13, and EG17) using MA as described in section 2.1.1.; marine environments as well as microbial mats near underwater hydrothermal springs of the Bol'shoi River, Russia (JF1, T4, C6, C7, C8, C12, C14, C23, C26, C46, N25, N34, N48, N56, and N78, Se-1-2-red, ER-Te-40B, ER-Te-65, Te-2-2, CB-10, Se-6-2-red, 23-SB, 15-SB, SS56, SS63, SS335, and P-13, KR99, E1, E4(1), E5, RB3, RB16-17) with either RO medium or RO medium with 20.0 g/l NaCl added, to determine distribution of siderophores amongst AAP.

2.2.2. Siderophore Isolation and Purification

Filtration with a 5000 Da molecular weight cut off membrane was attempted to capture the siderophore on the filter paper. When that proved unsuccessful, extraction with organic solvents was attempted. Siderophore-containing medium was mixed with equal volume of either ether, petroleum ether or chloroform and was mixed well and allowed to separate into water and organic layers. This was, once again ineffective. Finally, methanol was added in equal

volume to change the polarity of the unknown molecule and extraction with organic solvents was repeated again to no avail.

Cultures were grown for 5 days in MA followed by centrifugation for 20 min at 10K rpm on a Beckman J2HS centrifuge using a JA-10 rotor to pellet the cells. The supernatant containing the excreted siderophore in solution was frozen in a flask, allowing the siderophore to be pushed to the top to concentrate it. This highly concentrated layer of sample in medium could then be collected and thawed for siderophore purification. Yamamoto, Okujo and Sakakibara (1994) described a batch type method of siderophore purification, which was used in this study. The sample was adjusted to pH 6.0 and XAD 7-HP resin was added. This slurry was shaken 1 h on a rotary shaker at 200 rpm and then filtered with a glass filter funnel. Resin on the filter paper was thoroughly washed with distilled water to remove all residual salts and contaminants. The clean resin was soaked in methanol for 30min to release the siderophore. This was filtered and soaked once more in methanol and filtered one last time. Methanol extracts were combined and were evaporated to dryness. The resulting powder was the isolated protein.

A number of methods were attempted on the sample to remove iron from the siderophore-iron complex as this metal can interfere with both NMR and MS analysis. One method used methanol and hydroxyquiniline mixed with the sample for 3 days, followed by drying the sample and extracting in chloroform 5 times and repeating the full siderophore purification process (Budde and Leong, 1989). Another involved a similar method, but using

EDTA to bind the iron instead of hydroxyquiniline, as EDTA bind metals very strongly. Unfortunately, none were successful. When it was determined to be near impossible to remove iron from the siderophore after purification, an alternate method was used, where the siderophore was never exposed to iron, to which it could bind. MA with a modified trace elements solution containing no iron was used to grow strain EG19 for protein isolation. Chelex resin was then added to the medium in a batch method to remove trace levels of iron introduced through the complex nutrient sources such as yeast extract, bactopeptone and casamino acids (Barker *et al*., 1978). The solution was filtered to remove the chelex resin bound to iron and the medium was autoclaved and adjusted to pH 7.8 using 0.5N NaOH. From there, cells were grown for 5 days and purification using XAD 7-HP resin was repeated as described above.

Further purification was carried out using SDS-PAGE (6% acrylamide/bisacrylamide), which removed residual contaminants from the sample and the pure protein band was extracted from the gel using extraction buffer containing 1:2 vol/vol 5% formic acid/acetonitrile. 100µl of extraction buffer was added to the gel band, which was then vortexed at room temperature every 2 min for 30 min total. Supernatant was collected and dried in a speed vacuum and dry sample was re-suspended in sterile distilled water.

2.2.3. Structural Analysis of Siderophore

Inductively coupled plasma (ICP) mass spectrometry (MS) was performed by the Manitoba Chemical Analysis Laboratory using a Varian 725-E5 spectrophotometer by running

200 ppm of the purified protein sample dissolved in 2% nitric acid against a standard control, where all tested elements were at a concentration of 5 mg/l. Tested elements were Au, B, Ba, Be, Bi, Ca, Cd, Ce, Co, Cr, Cs, Cu, Dy, Er, Eu, Fe, Ga, Gd, Ge, Hf, Hg, Ho, In, Ir, K, La, Li, Lu, Mg, Mn, Mo, Na, Nb, Nd, Ni, P, Pb, Pd, Pr, Pt, Rb, Re, Rh, Ru, S, Sb, Sc, Se, Si, Sm, Sn, Sr, Ta, Tb, Te, Th, Ti, Tl, Tm, U, V, W, Y, Yb, Zn and Zr.

ES-MS was carried out on purified siderophore samples with the help of our collaborator Dr. Lynda Donald.

Amino acid analysis was performed at the Hospital for Sick Children, Peter Gilgan Centre for Research & Learning, SPARC BioCentre, Toronto. Analysis was derived by PITC against a standard containing 50.0 picomoles of each amino acid.

2.3. Field Studies at Central Gold Mine, Nopiming Provincial Park

2.3.1. Sampling and Growth Conditions

Four locations within the mine tailings at the Central Gold Mine, Nopiming Provincial Park, Manitoba, Canada were chosen for sampling in September 2011 (Maltman, Piercey-Normore and Yurkov, 2015; Hughes, *et al.*, 2017). Soil samples (1.0 cm^3) from each site were suspended in 10 ml of dilution medium, containing (g/l): $MgCl_2$, 0.5; KH_2PO_4, 0.3; NH_4Cl, 0.3; and $CaCl_2$ (0.1). Medium was adjusted to pH 7.0 after autoclaving using 0.5N NaOH. Samples were tested for pH and then serially diluted and plated on various media types. First, RO

medium, containing (g/l): $MgSO_4$, 1.0; KH_2PO_4, 0.3; NH_4Cl, 0.3; $CaCl_2$, 0.1; Na-acetate, 1.0; yeast extract, 1.0; bactopeptone, 0.5; casamino acids, 0.5; and vitamins and trace elements solutions, 2 ml each, adjusted to pH 5.0, 7.0, or 9.0 after autoclaving (Yurkov *et al*., 1994); second, RO medium + Na_2SO_4 (0.5 g/l), pH 5.0, 7.0, and 9.0, as previous work has shown this mine site to be high in sulfates (Sherriff *et al*., 2006); and finally, RO pH 7.0 + 100 µg/l of either K_2TeO_3, Na_2SeO_3, or $NaVO_3$.

2.3.2. Isolation and Enumeration of AAP

After sampling, plates were incubated at 28°C in the dark for 7 days before colonies were counted. Pigmented colonies were then picked and grown on fresh medium before being screened for presence of BChl *a* to determine their identity as AAP. Those containing BChl *a* were purified further for additional study.

2.3.3. Spectroscopy and Microscopy

Spectroscopy and microscopy were performed as described in section 2.1.2.

2.3.4. Taxonomic Tests

All taxonomic tests were performed in triplicate in liquid RO medium, pH 7.0 and incubated on a rotary incubator at 28°C in the dark for 7 days, with growth monitored visually unless otherwise indicated. Morphology, Gram stain and motility were determined using a Zeiss Axioskop2 phase contrast microscope. Cultures from liquid medium as well as RO pH 7.0, agar (2.0%) plates were checked for motility after 2 and 7 days using a hanging drop slide method.

Carbon source utilization was tested in liquid minimal salts medium containing (g/l): $MgSO_4$, 1.0; KH_2PO_4, 0.3; NH_4Cl, 0.3; $CaCl_2$, 0.1; adjusted to pH 7.0 and with the addition of one of the following (1.0 g/l): acetate, butyrate, citrate, formate, glutamate, glycolate, lactate, malate, propionate, pyruvate, succinate, fructose, glucose, sucrose, ethanol, methanol, glycerol, casamino acids, bactopeptone, or yeast extract. Growth at pH 5.0 to 12.0 was investigated at one point increments. Temperature optimals were determined on RO plates, pH 7.0 at 2, 7, 12, 28, 37 and 45^oC over a 14 day incubation period. NaCl tolerance was defined using concentrations of 0, 0.5, 1, 2, 3, 3.5, 4, 4.5 and 5%.

Antibiotic disk diffusion assay on RO, pH 7.0 agar (2.0%) plates was used to examine sensitivity to ampicillin (2.0 μg), chloramphenicol (30.0 μg), kanamycin (30.0 μg), penicillin (10.0 IU), polymyxin B (300.0 IU), nalidixic acid (30.0 μg), streptomycin (10.0 μg), and imipenem (10.0 μg).

Requirement for vitamins B_{12}, biotin, nicotinic acid and thiamine were investigated in test tubes containing liquid minimal salts medium + glucose (1.0 g/l), pH 7.0 amended with all vitamins, no vitamins, or lacking one of the aforementioned. Nitrate and ammonia utilization, as well as nitrogen fixation were analyzed both aerobically and anaerobically. For aerobic growth, test tubes containing liquid minimal salts medium + 1.0 g/l each of glucose, fructose, and sucrose, pH 7.0, minus NH_4Cl were inoculated. Each nitrogen source was added at a

concentration of 0.3 g/l. Nitrate reduction was visualized using nitrate test strips to detect a decrease in nitrate levels along with the appearance of nitrite. Degassed balch tubes containing liquid minimal salts medium (no NH_4Cl) + glucose (1.0 g/l) and 0.003 g/l each of cysteine and methionine, pH 7.0 were used for anaerobic growth. Nitrogen sources were added and reduction was observed as described above. Utilization of sulfur sources, including $MgSO_4$, $Na_2S_2O_4$, $Na_2S_2O_3$, cysteine and methionine, was tested in test tubes containing liquid minimal salts medium + glucose (1.0 g/l), pH 7.0 without $MgSO_4$ with 0.5 g/l of one of the above sulfur sources.

Autotrophy was determined by inoculating each strain in liquid minimal salts medium, pH 7.0 with $NaHCO_3$ (0.5 g/l). Strains were observed for their ability to ferment carbohydrates in test tubes containing liquid minimal salts medium, pH 7.0 with one of glucose, fructose or sucrose added at 1.0 g/l with durham vials to check for gas production. Bromocresol purple was added as a pH indicator to visually determine fermentative acid production.

The presence of amylase was evaluated on modified RO plates (0.05 g/l yeast extract with 0.4% starch), pH 7.0 (Gerhardt *et al*., 1981). Lipase activity was assessed using RO, pH 7.0 plates amended with Tween 60 to detect formation of a white precipitate surrounding the colonies (Gerhardt *et al*., 1981). For gelatinase, test tubes containing RO medium + 12.0% gelatin, pH 7.0 were used (Gerhardt *et al*., 1981). Catalase activity was determined by immediate and sustained bubbling upon the addition of a 3.0% H_2O_2 solution to biomass.

Kovacs reagent was used to assay for cyt oxidase presence after 2 days growth (Gerhardt *et al*., 1981).

Fatty acid (FA) analysis was performed using gas chromatography (GC). Cells were dried in an oven for at least 4 h and 20mg dry weight of cells was suspended in 1.0 ml 15% methanol in H_2SO_4 and 1.0 ml chloroform. Samples were boiled for 5 h and 1.0 ml distilled H_2O was added. Organic layer was collected and sent to Dennis Labossiere in the Department of Human and Nutritional Sciences, University of Manitoba for analysis by GC.

2.3.5. Resistance and Reduction of Metal(loid) Oxides

Isolates were evaluated for heavy metal(loid) oxide resistance and reduction. Liquid RO medium, pH 7.0 containing one of K_2TeO_4, K_2TeO_3, Na_2SeO_4, Na_2SeO_3, Na_3VO_4 or $NaVO_3$ at concentrations of 0, 50, 100, 500 or 1000 µg/ml were inoculated and grown for 7 days at 28^{o}C. Resistance was monitored spectrophotometrically for growth with A950 readings for Te oxides (Maltman and Yurkov, 2014) and A600 for Se and V oxides (Yurkov and Csotonyi, 2003). Reduction was observed by a change in colour of the culture: black for Te, red for Se and blue-green for V (Yurkov and Csotonyi, 2003).

2.3.6. 16S rRNA Gene Sequencing

Genomic DNA was isolated as described by Chen *et al*. (2006). Cells were suspended by vigorous pipetting in 200µl lysis buffer containing 40mM Tris, 20mM sodium acetate, 1mM EDTA and 1% SDS. 66µl of 5M NaCl was added, mixed well and the mixture was centrifuged at 12000 rpm for 10 min at 4°C. The clear supernatant was collected and mixed with an equal amount of chloroform. The tube was inverted at minimum 50 times to completely form a clear milky solution. This was then centrifuged again at 12000 rpm for 3 min at 4°C. The clear supernatant was collected and the DNA was precipitated with 100% ethanol and pelleted through centrifugation. That pellet was washed twice with 70% ethanol and dissolved in 50µl TE buffer containing 10mM Tris and 1mM EDTA and adjusted to pH 8.0. DNA was sent to Genome Quebec for PCR and full 16S rRNA gene sequencing using primers 27F, 515F and 968F. Sequences were assembled using the program DNA baser (DNA Sequence Assembler v4, 2013) and closest relatives were found by BLASTn search in NCBI GenBank. The program MEGA 6.0 (molecular evolutionary genetics analysis) was used to align sequences and build phylogenetic trees by the maximum likelihood method. 16S rRNA gene sequences were deposited to GenBank and the accession numbers are: C4, KX148515; C9, KX148516; C11, KX148517; NM4.16, KX148518; NM4.18, KX148519.

Chapter 3.

Results

3.1. Photosynthetic Complexes

3.1.1. *Roseicyclus mahoneyensis*

3.1.1.1. Wildtype Strain ML6 and its Spontaneous Mutants

Wildtype strain ML6 grown on N1 medium pH 7.8 forms small colonies, approximately 2-3 mm in size, that are pink-purple in colour. It absorbs spectrophotometrically due to BChl *a* bound to protein complexes at 871 nm (representing the LH1 complex), 806 nm, which is characteristic of the unusual monomodal LH2 and 750 nm, indicative of BPheo bound to the typical RC (Fig. 7A). ML6 spontaneously mutates to form novel stable lines, three of which were found to be photosynthetically interesting for further investigation. The first, ML6(B), appears as light brown colonies on spread plates among pink-purple wild type. Spectrophotometric analysis reveals a sole absorption peak at 805 nm, representing the LH2, whereas the LH1-RC is missing (Fig. 7B). The second, ML6(DB) emerges from ML6(B) at a frequency of 2.97% of colonies, when grown under optimal condition, or 2.1% at room temperature in the dark. This number can, however, climb to as high as 9.1% of colonies under a light/dark regimen at room temperature. It is a darker brown colour and, while it has the same BChl *a* absorption peak as ML6(B), it also has a small shoulder at 755 nm, due to BPheo in what could possibly be an incomplete RC (Fig. 7C). Finally, the third spontaneous mutant studied is ML6(BN9O). It is derived much less frequently than the other two mutants, as light brown colonies on spread plates of ML6(N9O), a morphological mutant of ML6 wildtype which has a slightly orange colour to the cells. This mutation arises in only 0.05% of colonies under optimal growth condition and that number ascends only as high as 0.26% at room temperature, or 0.2% of colonies when a light/dark cycle is applied. ML6(BN9O) is of a light brown colour, similar to that of ML6(B), but

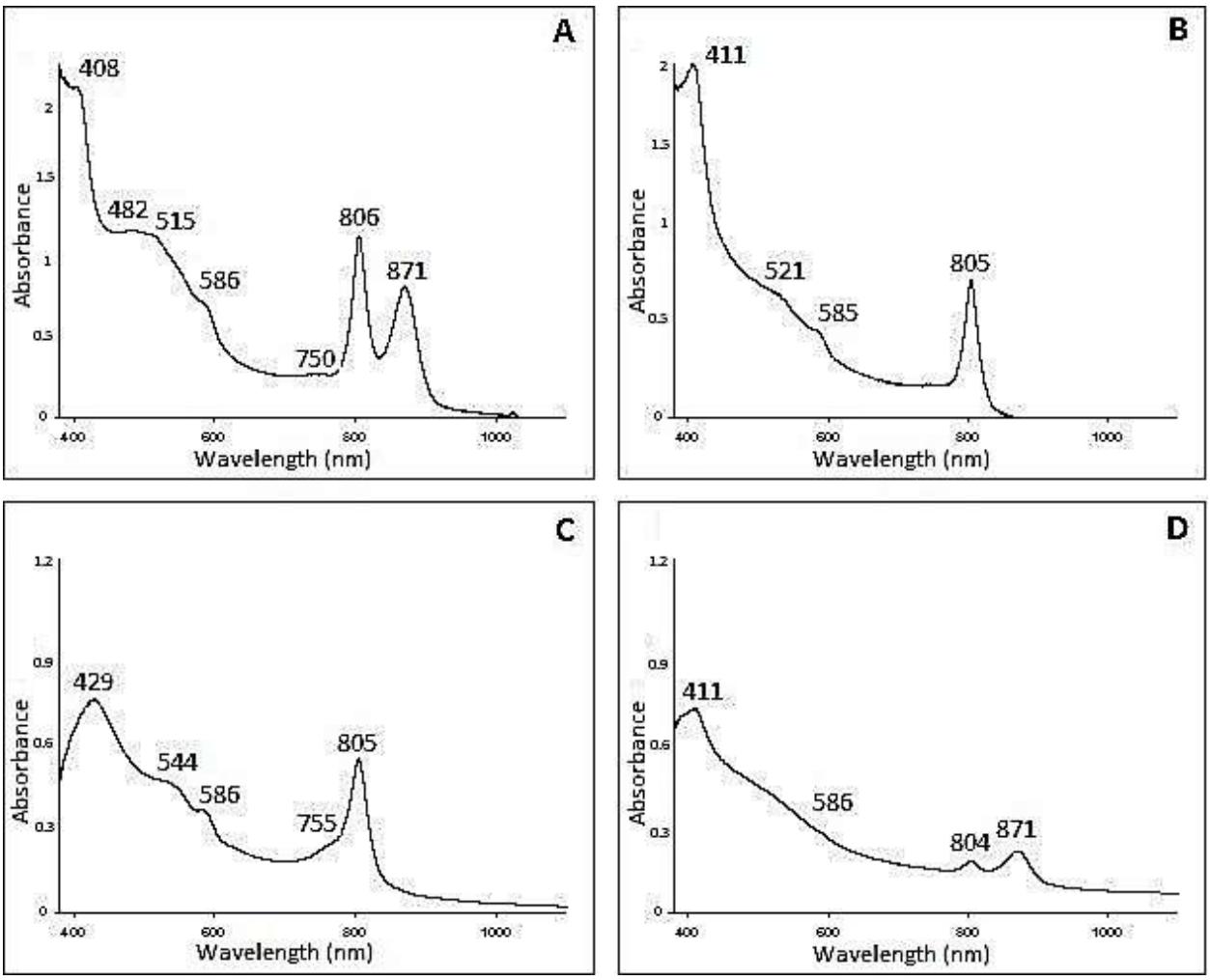

Fig. 7. Full wavelength absorption spectrum of whole actively growing cells of *Roseicyclus mahoneyensis* strains: (A) ML6; (B) ML6(B); (C) ML6(DB); (D) ML6(BN9O).

with absorption peaks at 871 and 806 nm (Fig. 7D). When subjected to conditions of changed pH (either pH 7.0 or pH 10.0), or changes in sulfate concentrations, all strains lost pigmentation, suggesting they produce BChl *a* and crt exclusively at optimal pH and sulfate levels. All of these spontaneous mutants are stable, as they can be sub-cultured in the dark indefinitely on N1 medium at 28°C without changes and no reversion to the wildtype, or to the strain the mutant was derived from.

3.1.1.2. Isolation of Membranes, Soluble Fractions and Pure Complexes

Full wavelength scans of ML6 membranes confirmed photosynthetic pigment-protein complexes with absorption peaks at approximately 870, and 805 nm as well as bound cyt*c* with peaks at 408 – 420 nm, depending on their oxidation state. Purified ML6(B) membranes showed only the LH2 peak at 805 nm, while ML6(DB) membranes had a small shoulder at 755 nm in addition to the same peak as is observed in ML6(B). Finally, ML6(BN9O) membranes had only the LH1-RC complexes with peaks at 871 and 806 nm. All results are consistent with what was seen in whole cells, confirming that protein complexes were not denatured during membrane purification. Soluble fractions of ML6, ML6(B), ML6(DB) and ML6(BN9O) showed the presence of a soluble cyt*c* absorbing at 409 nm (Fig. 8A).

Sucrose density gradients were successful showing 5-7 bands in ML6 separations (Fig. 9), up to 5 in ML6(B), 5 in ML6(DB) and 4 in ML6(BN9O). All bands were isolated and those containing photosynthetic complexes were further purified by column chromatography. The RC

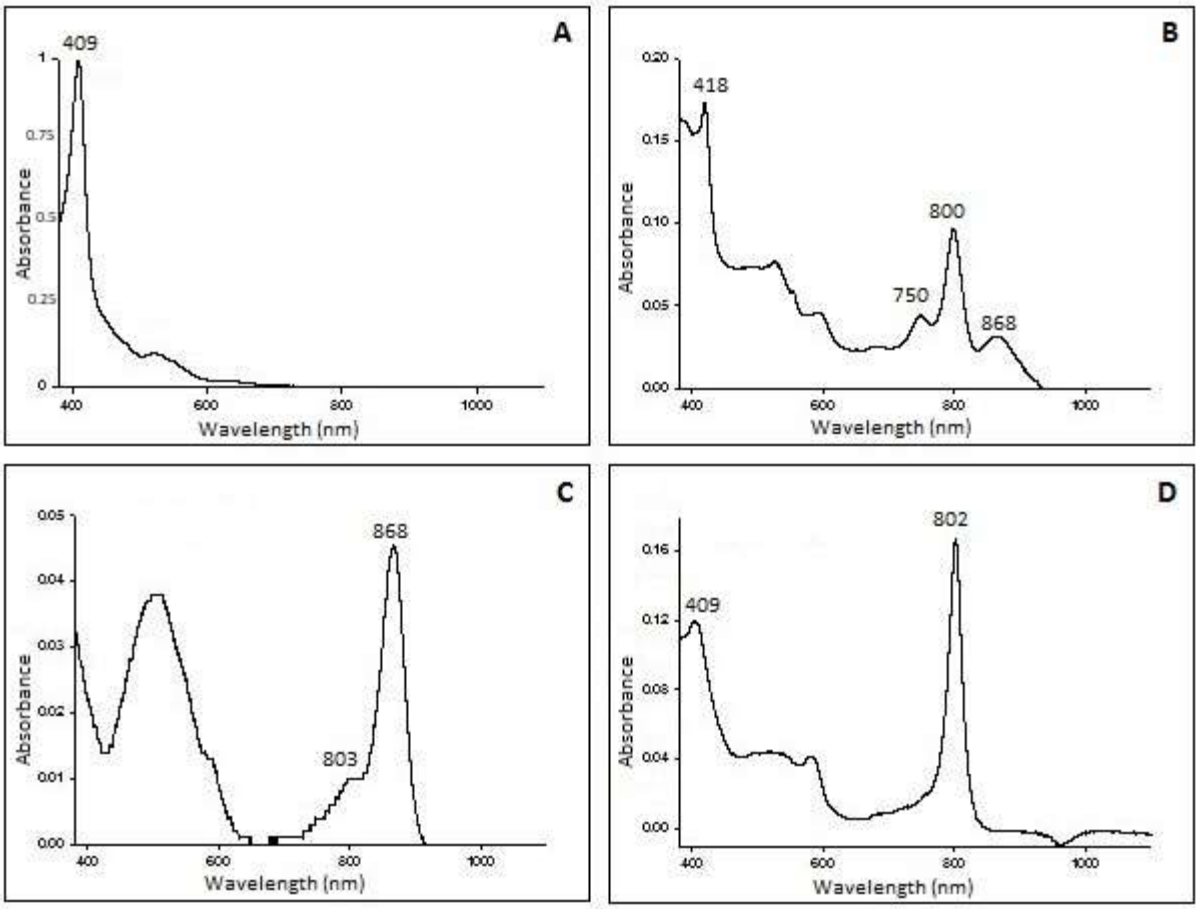

Fig. 8. Absorption spectrum of: (A) ML6 soluble fraction; (B) ML6 purified RC; (C) ML6 purified LH1-RC; (D) ML6(B) purified LH2.

Fig. 9. Sucrose density gradients of ice cold ML6 membranes treated with 8% Triton X-100 for 30 min.

from ML6 and ML6(BN9O) has BChl *a* peaks at 868 and 800 nm and BPheo peak at 750 nm (Fig. 8B). SDS-PAGE showed primary RC protein subunits measuring approximately 28, 31 and 33 KDa (Fig. 10A) and LH1 subunits at 8 and 10 KDa (Fig. 10B). The LH1-RC from ML6 shows absorption peaks at 868 nm and 803 due to BChl *a* (Fig. 8C). The LH2 complexes from ML6, ML6(B) and ML6(DB) have a single BChl *a* peak at 803 nm (Fig. 8D). SDS-PAGE bands at approximately 7 and 8 KDa are characteristic of LH2 subunits (Fig. 10C). In all strains, additional peaks between 430 nm and 600 nm are indicative of crt associated with the photosynthetic complexes and the peaks between 408-420 nm belong to cyt*c*, which is bound to the RC in addition to a soluble form.

3.1.1.3. Biophysical Analysis

Flash induced difference spectra were carried out in order to determine levels and kinetic rate of photoinduced e^- transfer. ML6 showed strong cyt*c* and P^+ signals in whole cells (Fig. 11A), membranes (Fig. 11B), purified RC, and LH1-RC complexes under aerobic and microaerophilic conditions. As can be seen in Fig. 11A, in whole cells fully reduced before the flash due to addition of dithionite, there is initially, 5ms after the actinic flash, a very strong oxidized cyt*c* signal (troughs at 420 and 552 nm), which as time progresses at 30 and 60ms after the flash, gradually decreases in size. The same can also be observed in purified membranes under ambient, oxidized conditions as a decrease in P^+ signal (peak at 420 nm and trough at 605 nm; Fig. 11B). In purified LH1-RC and RC, cyt*c* troughs similar to those in whole cells were observed, though re-reductions were slower in the isolated complexes.

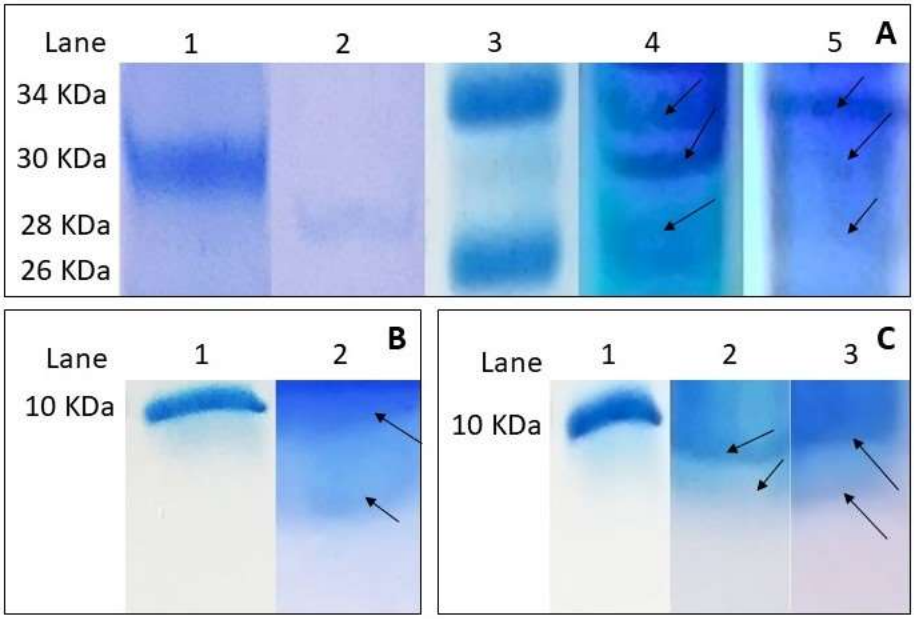

Fig. 10. SDS-PAGE gels of (A) Lanes 1, 2 and 3, standard protein ladder; Lane 2, ML6 RC complex; Lane 3, ML6(BN9O) RC complex; (B) Lane 1, standard protein ladder; Lane 2, ML6 LH1 complex; (C) Lane 1, standard protein standard; Lane 2, ML6(B) LH2 complex; Lane 3, ML6(DB) LH2 subunits. Size of bands in standard protein ladders indicated, protein bands of subunits indicated with arrows.

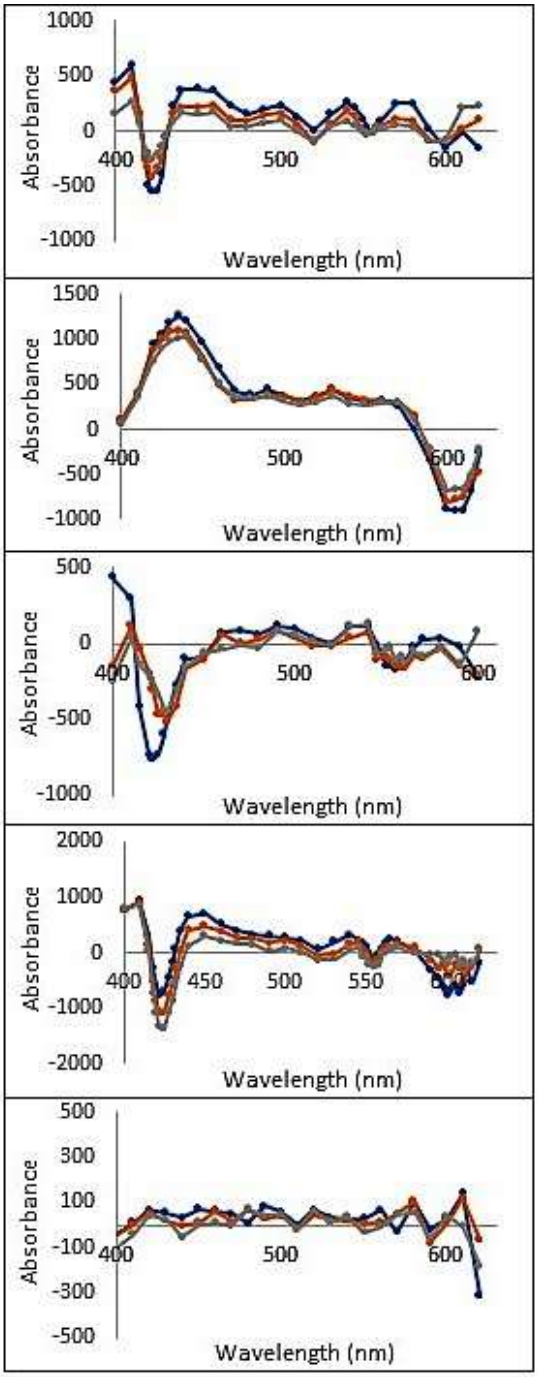

Fig. 11. Flash induced difference spectra of *Roseicyclus mahoneyensis*: (A) ML6 whole cells; (B) ML6 membranes; (C) ML6(BN9O) whole cells; (D) ML6(BN9O) purified RC; and (E) ML6(DB) whole cells. Blue: 5 ms after the actinic flash; orange: 30 ms after the actinic flash; grey: 60 ms after the actinic flash.

ML6(BN9O) exhibited similar results with cyt*c* and P^+ signals, though they were weaker in whole cells and membranes, forming smaller troughs and peaks (Fig. 11C) than observed in their wildtype counterparts. Despite the weaker signals, we can note that the rate of e^- transport in ML6(BN9O) remains rapid, particularly in purified RC, where we see the cyt*c* signals at 420 and 552 nm shrinking, while the P^+ signal at 605 nm increases in size (Fig. 11D), confirming that photoinduced e^- transport is progressing unimpeded. It should also be noted that in Fig. 11C, as re-reduction of the cyt*c* occurs in whole cells of strain ML6(BN9O), there is a shift in the trough from 420 nm to 430 nm, which is thought to be indicative of e^- being passed to the cytbc_1 complex, which like the cyt*c* is subsequently re-reduced. As was predicted, neither ML6 or ML6(BN9O) showed any sign of light induced absorbance changes in whole cells under anaerobic conditions, confirming their nature as obligately aerobic photosynthetic bacteria and showing consistency with other previously studied AAP (Yurkov and Beatty, 1998; Rathgeber *et al.*, 2004).

Whole actively growing cells of both ML6 and ML6(BN9O) were placed in a closed cuvette in the spectrophotometer and were allowed 2h to respire all the oxygen, creating an anaerobic environment before being tested again for photosynthetic e^- transport. Flash induced difference spectra revealed the absence of cyt*c* or P^+ signals under these anoxic conditions.

ML6(B) and ML6(DB) whole cells (Fig. 11E) and membrane fractions were tested for light induced e^- transfer under aerobic, semi-aerobic and anoxic conditions. Neither mutant strain produced any cyt*c* or P^+ signal, with the figure showing essentially a flat line after the actinic

flash, indicating a lack of photosynthetic ability. Subsequent analyses were therefore not performed on either strain.

Fig. 12 shows absorption spectra (blue line) of membranes and complexes in conjunction with action spectra (orange line). Action spectra are for P^+ accumulation at 605 nm (Y-axis), when samples were excited with monochromatic wavelengths of light (X-axis). As expected, in both strains, ML6 and ML6(BN9O), BChl *a* and BPheo harvest light, as confirmed by action spectra peaks at 805 nm in ML6 (Fig. 12A) and ML6(BN9O) membranes (Fig. 12C), and 750 and 800 nm in ML6 (Fig. 12B) and ML6(BN9O) purified RC (Fig. 12D), corresponding to absorption spectra peaks at the same wavelengths. Additional BChl *a* and BPheo peaks, usually masked by crt peaks, are present at 600 and 530 nm, respectively in all action spectra. Crt peaks present in absorption spectra of membranes as well as the shape of the spectrum between 450 and 600 nm compared to that of the action spectrum reveal that most if not all crt are not actually involved in light harvesting (Fig. 12A; Fig. 12C). Even crt that absorption spectra have revealed to be closely associated with the purified RC complexes in both strains do not seem to harvest light (Fig. 12B; Fig. 12D).

Finally, flash induced redox titrations were executed to determine that the redox midpoint potentials of P^+, RC-bound cyt*c* and Q_A are consistent between ML6 and ML6(BN9O) at +430mV ± 10mV, +245mV ± 10mV and +65 mV ± 10mV, respectively (Fig. 13), which all fall into the expected range for typical AAP.

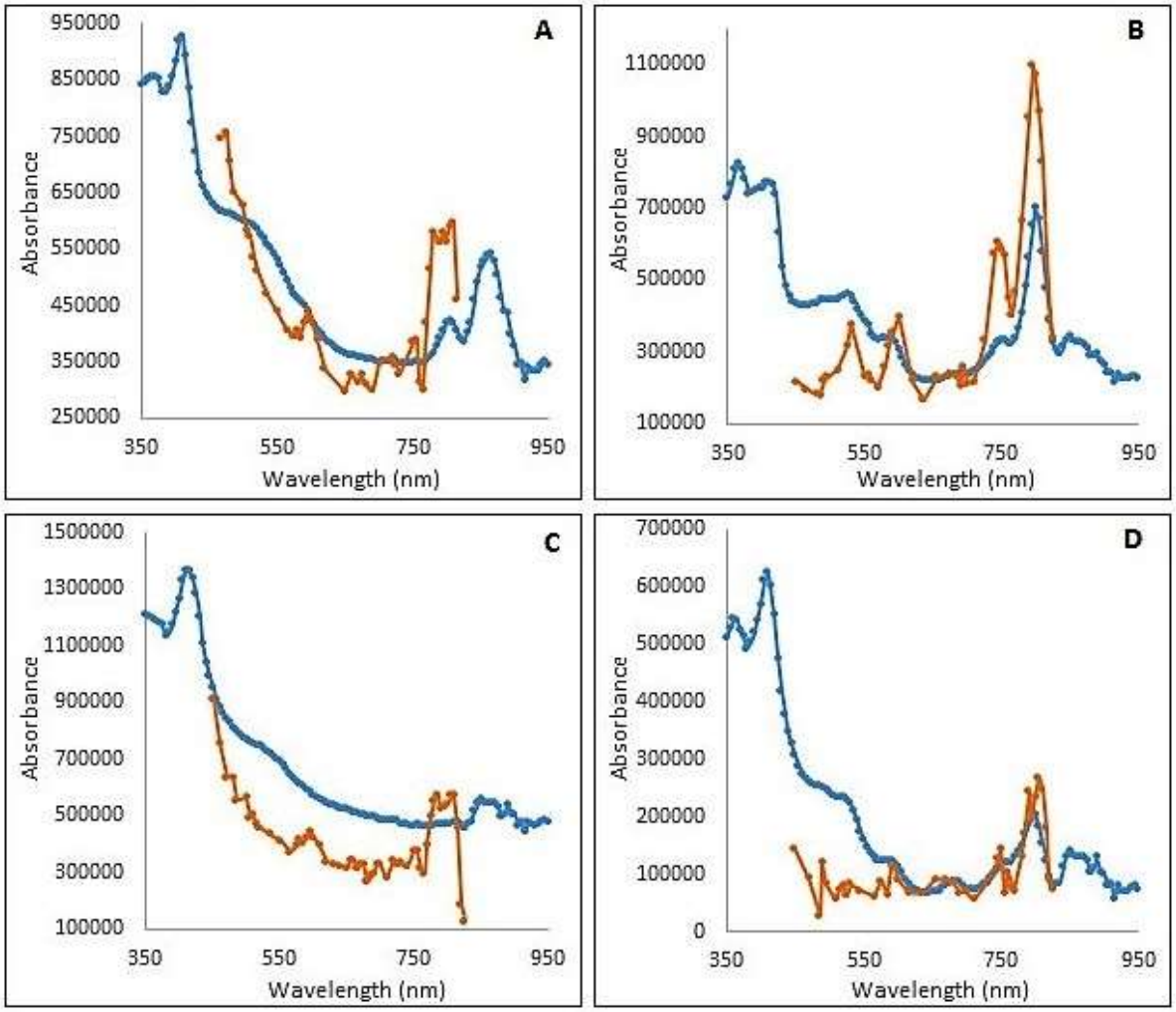

Fig. 12. Absorption spectrum (Blue) and action spectrum (Orange) where y-axis represents accumulation of P^+ measured at 605 nm and x-axis is the wavelength of light used to excite the sample of: (A) ML6 membranes; (B) ML6 purified RC; (C) ML6(BN9O) membranes; and (D) ML6(BN9O) purified RC.

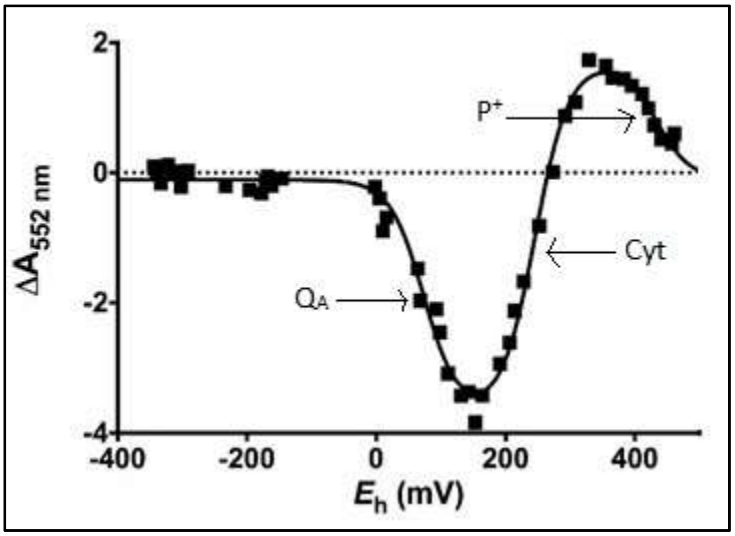

Fig. 13. Flash induced redox titrations of ML6 membranes at 552 nm. Redox midpoint potentials of Q_A, RC-bound cyt*c* and P^+ are indicated with arrows.

3.1.2. *Chromocurvus halotolerans* and *Charonomicrobium ambiphototrophicum*

3.1.2.1. Description of Cells, Membranes, Soluble Cytochromes and Purified Complexes

Strain EG19 produces small colonies that are orange/pink in colour and obligately aerobic. It is spectrophotometrically unusual with absorbance spectra of whole cells showing BChl *a* bound to an LH1 peak that is red-shifted to 879 nm, instead of the more typical 870 nm, as well as a typical RC complex with absorbance at 802 nm and a BPheo peak at 755 nm (Fig. 14A).

Aerobically grown EG17 cells are of a deep pink colour and also form small colonies. It has the same unusual LH1 as EG19 with a single peak at 879 nm and typical RC at 802 nm (Fig. 14B); however, it is also capable of anaerobic growth, giving way to darker more vibrant pink-red colonies and produces an additional LH2 at 850 nm (Fig. 14C), while retaining the same LH1-RC complexes. This is the first example of an anoxygenic phototrophic bacterium producing the same photosynthetic complexes under both oxic and anoxic conditions.

Membrane fractions of aerobically grown EG19 and EG17 as well as anaerobically grown EG17 were pelleted and full wavelength scans confirmed the same photosynthetic pigment-protein complexes as were seen in whole cells. Absorption peaks in EG19 membrane fractions were at 879, 802 and 755 nm, aerobic EG17 had peaks at 879 and 802 nm and anaerobic EG17 at 879, 850 and 802 nm. As well, absorption peaks at 420 nm in both strains under all conditions indicated membrane-bound cyt*c*. Soluble fractions were collected after membranes

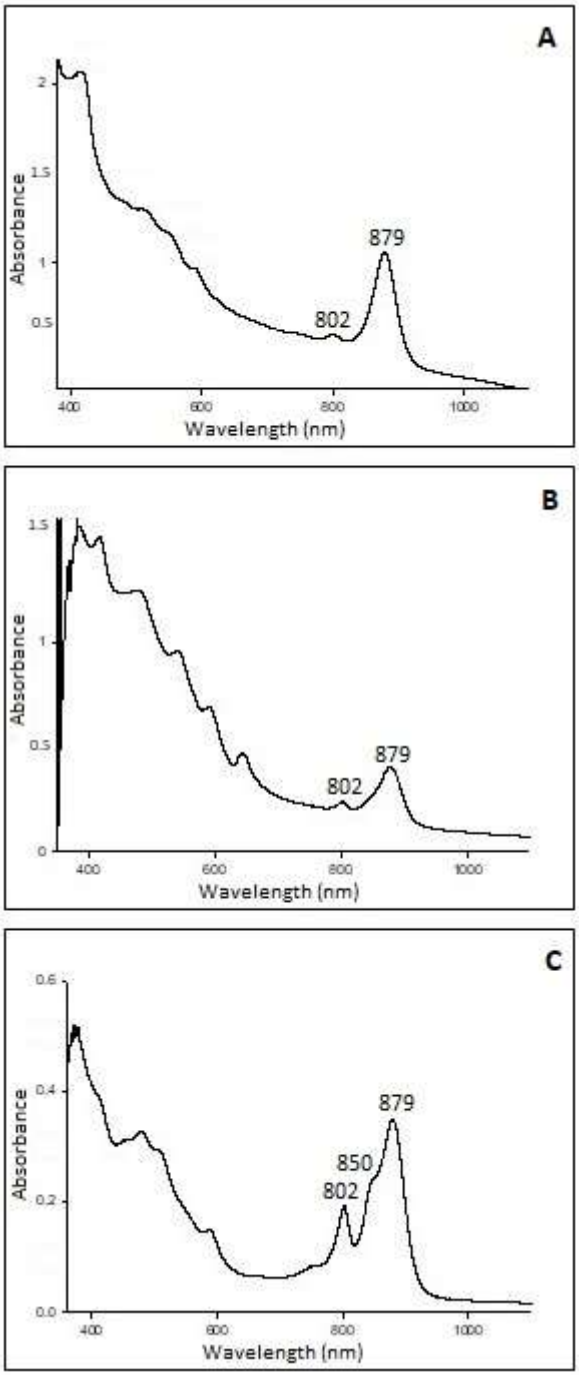

Fig. 14. Full wavelength absorption spectrum of whole actively growing cells of strains: (A) EG19; (B) aerobically grown EG17; (C) anaerobically grown EG17.

were pelleted. They showed the presence of cyt*c* absorbing at 411 nm in EG19 (Fig. 15A), though no soluble cyt were observed in EG17 samples (Fig. 15B).

Sucrose density gradients of EG19 had 5-6 bands and aerobically grown EG17 membranes had 5 bands after treatment. Bands were all carefully removed and tested spectrophotometrically for the presence of photosynthetic complexes. Those containing RC and LH1-RC complexes were isolated and further purified by column chromatography. In EG19 the RC showed peaks at 801 and 867 nm, representing BChl *a* and 755 nm for BPheo (Fig. 15C). The LH1-RC complex also showed a very large additional BChl *a* peak at 879 nm (Fig. 15D). Both also revealed the presence of cyt*c* bound to the RC peak at 411 nm (Fig. 15C; Fig. 15D). In EG17, the purified RC complexes had BChl *a* peaks at 798 and 871 nm with a BPheo shoulder at 777 nm (Fig. 15E); and the LH1-RC showed an additional large peak at 879 nm (Fig. 15F). In both strains, a variety of peaks between 420 and 600 nm are indicative of crt associated with the photosynthetic complexes and the prominent peak between 408-420 nm is for the cyt*c* bound to the RC in addition to the cytoplasmic soluble form. Subunits of the RC-LH1 complexes are of a typical size with bands at approximately 26, 27 and 31 KDa for the RC, slightly smaller than in ML6; and 8 and 11 KDa for the LH1 (Fig. 16) which is slightly larger than normal.

3.1.2.2. Biophysical Analysis

Ability to perform photosynthesis and rate at which it occurs were determined using flash induced difference spectra. EG19 whole cells showed strong cyt*c* signals immediately after

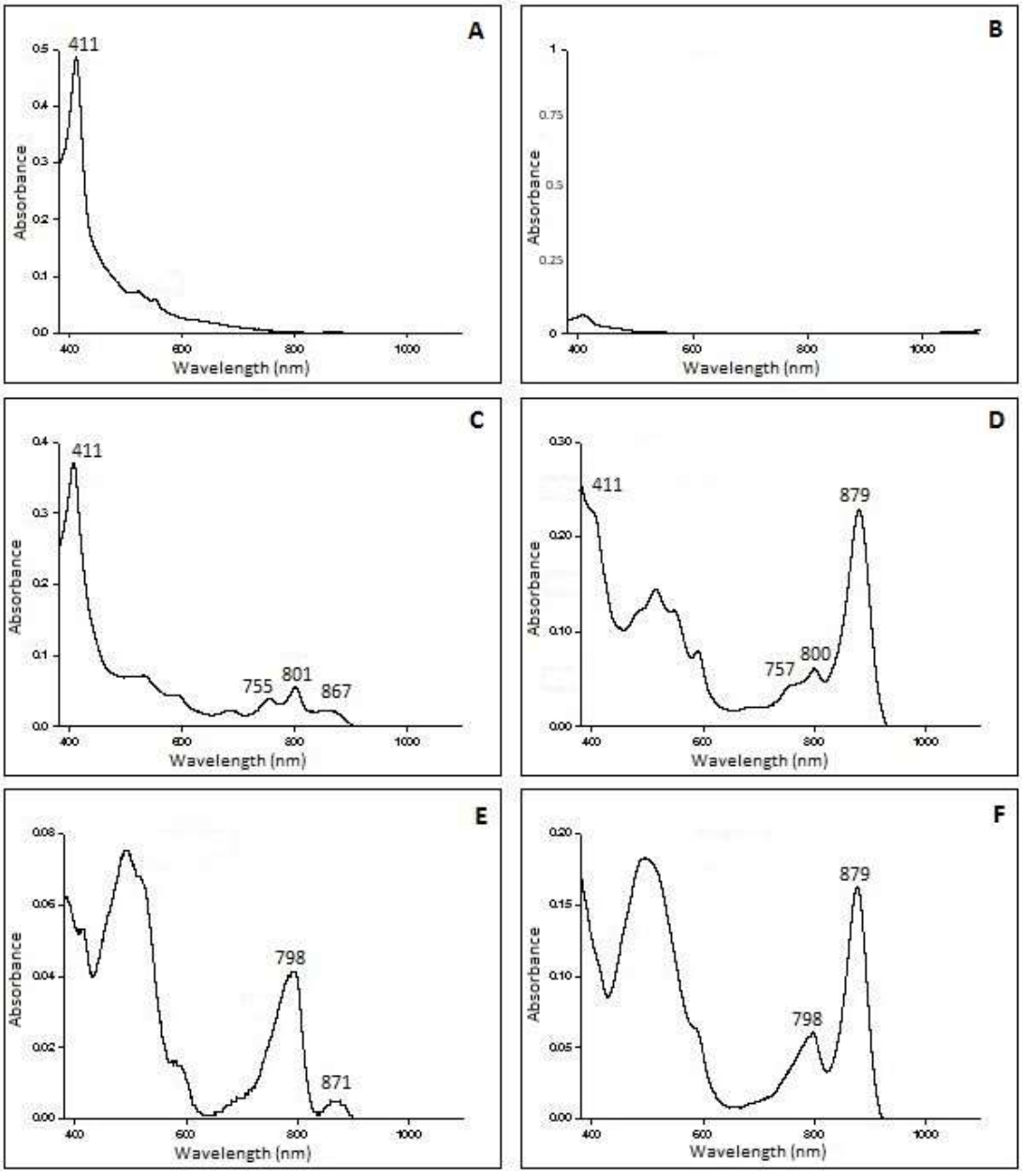

Fig. 15. Absorption spectrum of: (A) EG19 soluble fraction; (B) EG17 soluble fraction; (C) EG19 purified RC; (D) EG19 purified LH1-RC; (E) EG17 purified RC; (F) EG17 purified LH1-RC.

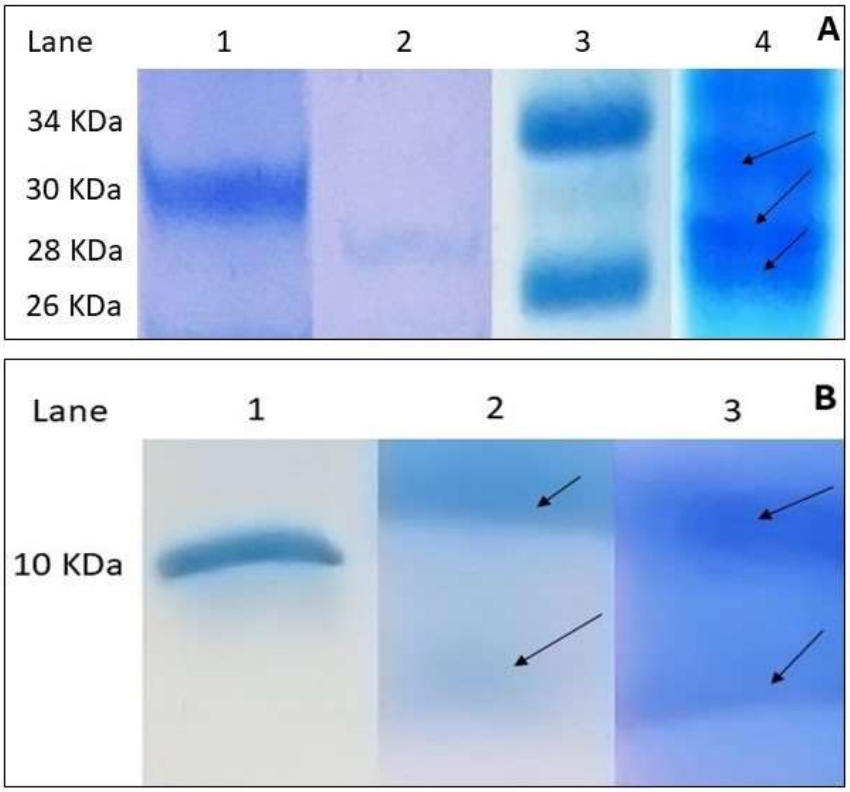

Fig. 16. SDS-PAGE gel of (A) Lanes 1, 2 and 3, standard protein ladder; Lane 2, EG17 RC complex; (B) Lane 1, standard protein ladder; Lane 2, EG17 LH1 complex; Lane 3, EG19 LH1 complex. Size of bands in standard protein ladders indicated, protein bands of subunits indicated with arrows.

photoexcitation (troughs at 420 and 550 nm) and rapid re-reduction as seen by the shrinking of the trough as the signal approaches zero, indicating active photosynthetic e^- transport (Fig. 17A). In membranes (Fig. 17B) and purified RC and RC-LH1 complexes (Fig. 17C) a strong P^+ signal was observed (peak from 430-440 nm) and e^- were rapidly passed to cyt*c* as seen by the decrease of the size of the P^+ peak and the appearance of a cyt*c* trough at 420 nm (Fig. 17C).

Aerobically grown whole cells of EG17 displayed similar results as EG19 cells with cyt*c* signals at 420 and 550 nm under ambient oxidized conditions (Fig. 18A). Decrease in size of the cyt*c* trough indicates fast re-reduction, demonstrating active photosynthetic ability. In membranes, the same strong signals are observed, although re-reduction is slower. In purified complexes a strong P^+ signal is seen, which is quickly converted to a cyt signal illustrating, once again, fast photosynthetic e^- transport (Fig. 18C). Membranes isolated from anaerobically grown EG17 cells were also tested for photosynthetic ability. They were found to have a strong P^+ signal under ambient oxidized conditions and a cyt signal when dithionite was used to fully reduce complexes before the flash, similar to that seen in aerobically grown cell membranes. However, re-reduction was very slow, taking more than 10s implying that, while necessary membrane-bound e^- carriers are present, active e^- transport is not occurring.

Actively growing EG19 and aerobic EG17 cells were loaded into a closed cuvette in the spectrophotometer and allowed to deplete all of the oxygen over a period of 2h, and were tested once again for photosynthetic ability in this newly created anoxic environment for

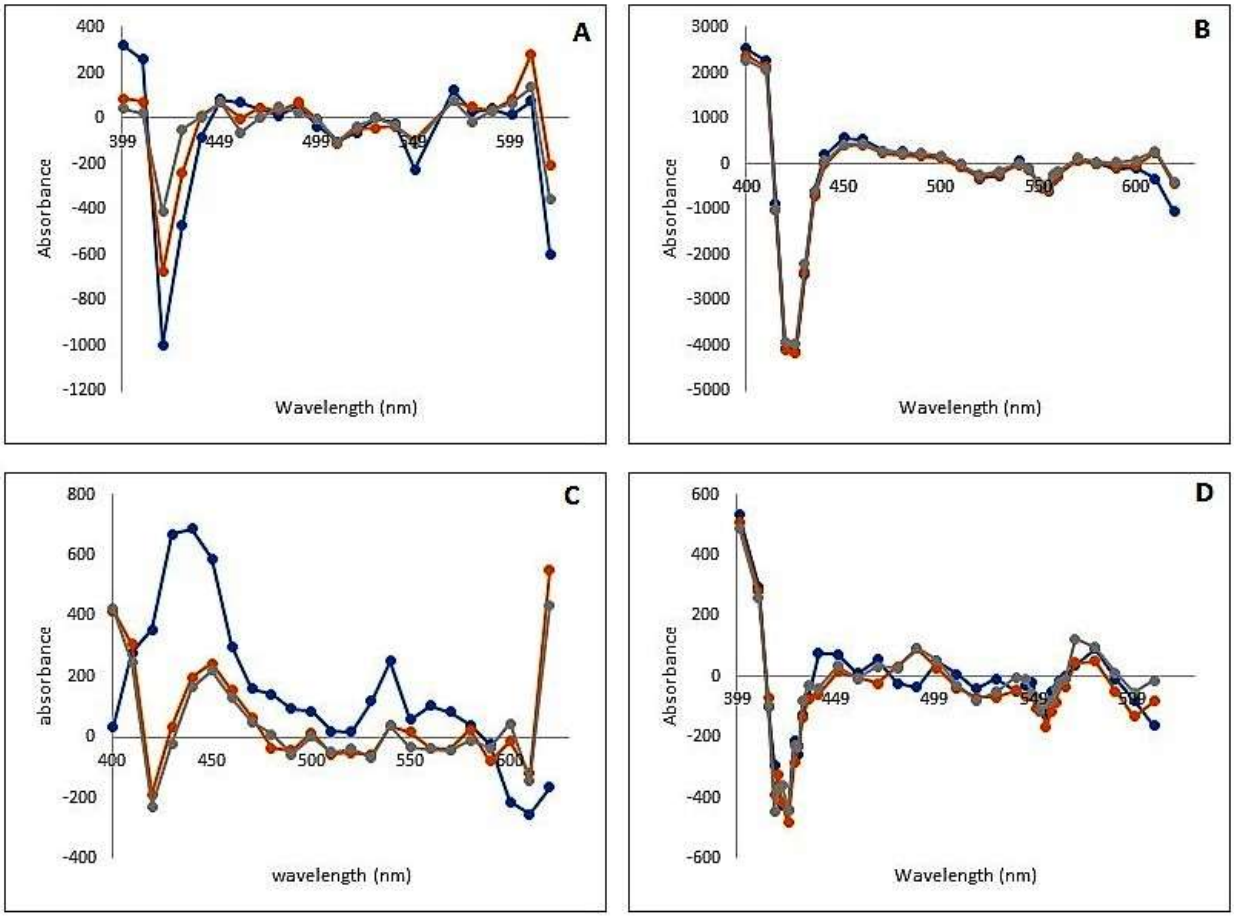

Fig. 17. Flash induced difference spectra of: (A) EG19 whole cells in the presence of oxygen; (B) EG19 membranes; (C) EG19 purified LH1-RC complexes; and (D) EG19 whole cells in an oxygen depleted environment. Blue: 5ms after the actinic flash; Orange: 30ms after the actinic flash; Grey: 60ms after the actinic flash.

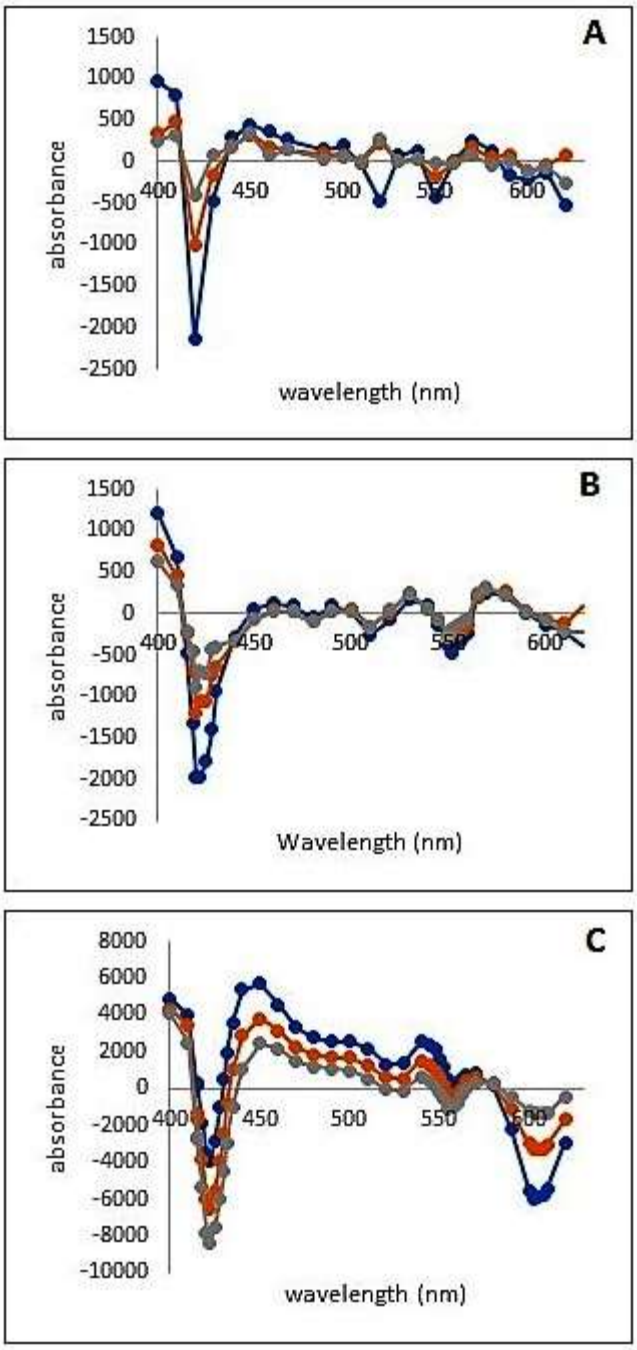

Fig. 18. Flash induced difference spectra of: (A) EG17 aerobically grown whole cells in the presence of oxygen; (B) EG17 aerobically grown whole cells in an oxygen depleted environment; and (C) EG17 purified LH1-RC complex. Blue: 5ms after the actinic flash; Orange: 30ms after the actinic flash; Grey: 60ms after the actinic flash.

anaerobic photosynthesis. EG19 showed a weak cyt*c* signal and slow re-reduction (Fig. 17D), hinting at some photosynthetic e^- transfer. EG17, in these anaerobic conditions, showed photosynthetic ability very similar to what was observed under fully aerobic conditions, with the same cyt*c* signals and fast re-reduction at the same rate as seen aerobically (Fig. 18B).

Action spectra were collected to determine what wavelengths of light are harvested for photosynthesis. In both strains, BChl *a* and BPheo harvest light, as confirmed with peaks at 805 nm in EG19 membranes (Fig. 19A), 754 and 805 nm in EG17 membranes (Fig. 19C), 750 and 800 nm in EG19 purified RC complexes (Fig. 19B) and 750 and 805 nm in EG17 purified LH1-RC complexes (Fig. 19D), corresponding to the absorption peaks at the same wavelengths (Fig. 19). Additional BChl *a* and BPheo peaks, usually masked by high levels of crt, were present at approximately 535 and 600 nm in all action spectra. Finally, purified LH1-RC complexes from EG17 showed an extra peak at 685 nm, attributed to free BChl *a*, present due to the denaturation of some of the protein complexes (Fig. 19D). Crt peaks in absorption spectra compared to action spectra revealed that the crt are not involved in light harvesting. Even when crt are associated with the RC they do not seem to actively collect photons to funnel into photosynthesis.

Finally, flash induced redox titrations were executed to determine that in EG19 the redox midpoint potential of P^+ is around +415±10mV (Fig. 20B), RC-bound cyt*c*, +260±10mV (Fig. 20A; Fig. 20B) and Q_A, +85±10mV (Fig. 20A). EG17 has the redox midpoint potentials of P^+

around +400±10mV, RC-bound cyt*c*, +310±10mV (Fig. 20C; Fig. 20D) and Q_A, +5±10mV (Fig. 20C).

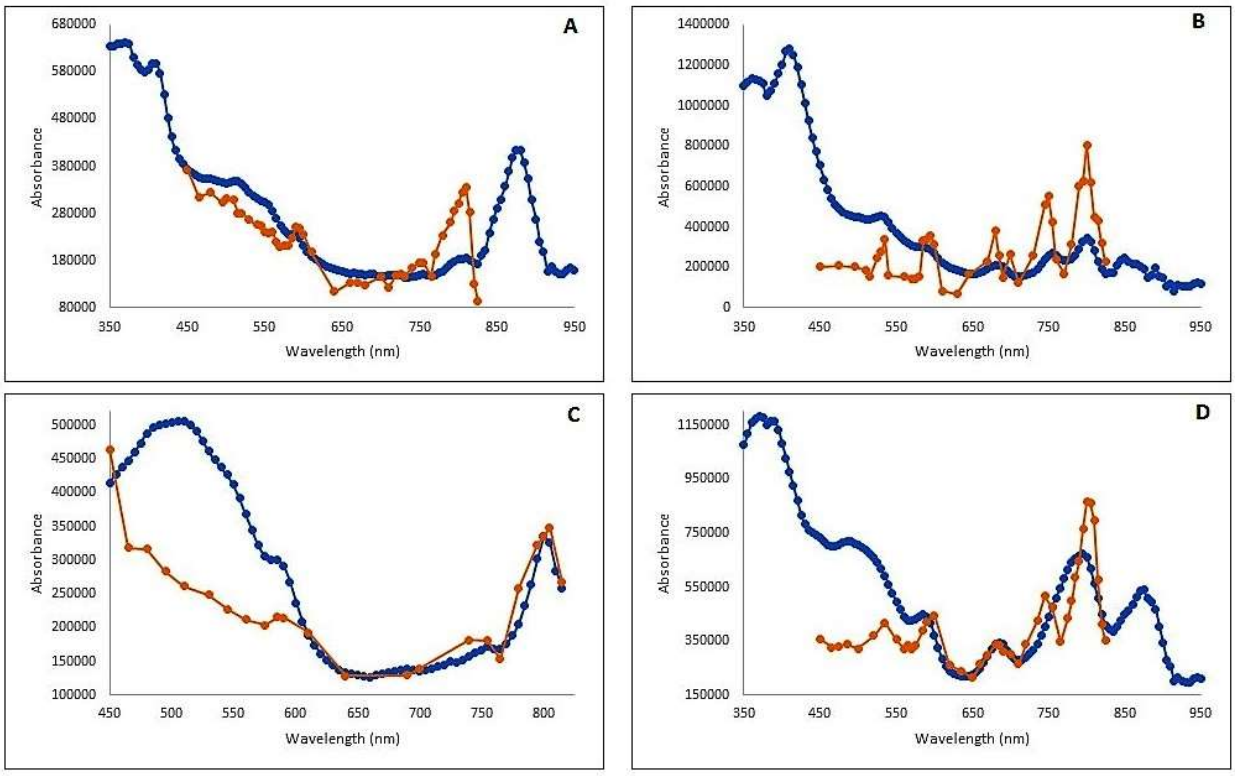

Fig. 19. Absorption spectrum (blue) and action spectrum (orange), where y-axis represents accumulation of P^+ measured at 605 nm: (A) EG19 membranes; (B) EG19 purified RC; (C) EG17 membranes; and (D) EG17 purified LH1-RC complexes.

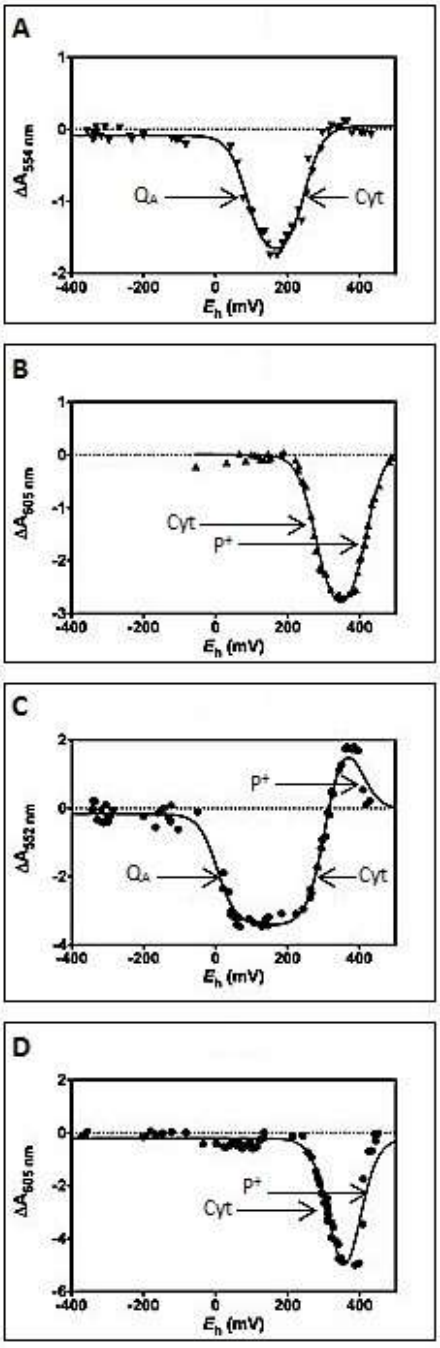

Fig. 20. Flash induced redox titrations of: (A) EG19 membranes at 554 nm; (B) EG19 membranes at 605 nm; (C) aerobically grown EG17 membranes at 552 nm; and (D) aerobically grown EG17 membranes at 605 nm. Redox midpoint potentials of Q_A, RC-bound cyt*c* and P^+ are indicated with arrows.

3.2. Extracellular Compound Produced by *Chromocurvus halotolerans*

3.2.1 Physiological Properties

C. halotolerans, EG19 was known to produce a brown-orange pigmented compound, which is excreted from the cells into the growth medium (Fig. 21A) (Csotonyi *et al.*, 2011a). This compound proved difficult to isolate and purify, nevertheless every unsuccessful attempt led to discover something new. First, it was demonstrated to be quite small, as it passed through filters with a 5000 Da molecular weight cut off and dialysis tubing with a 1500 Da pore size. Tubing with a molecular cut off of 800-1000 Da was found to be effective at trapping some of the desired product, though some still leaked through due to its tiny size. Second, extraction from the growth medium using either ether, petroleum ether or chloroform proved to be impossible as the compound is hydrophilic in nature. This experiment was then repeated, but methanol was added to the medium to change the polarity of the molecule in the hopes that it could then be removed by one of the aforementioned solvents. Unfortunately, this also did not yield positive results.

3.2.2. Spectrophotometry and Identification as a Siderophore

Strain EG19 grown on CAS plates changed the colour of the medium from blue to yellow (Fig. 22), speaking to the presence of an iron-chelating molecule (Schwyn and Neilands, 1987).

Spectrophotometry of the medium showed the pigmented compound to absorb in the UV region with peaks at 212 and 264 nm (Fig. 23B), suggesting this is a catechol type siderophore.20

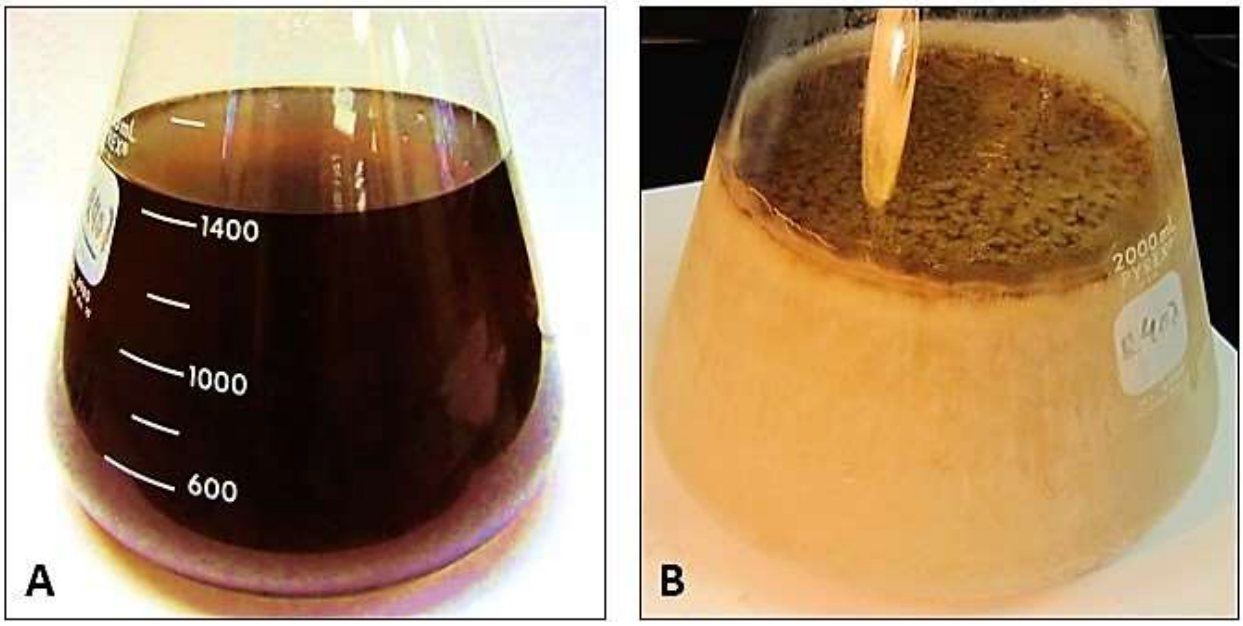

Fig. 21. Brown-orange pigmented compound secreted by strain EG19 into the growth medium. (A) Medium is dark orange-brown in colour after cells have been removed; (B) Freezing medium in a flask concentrates the molecule of interest in the top layer of ice.

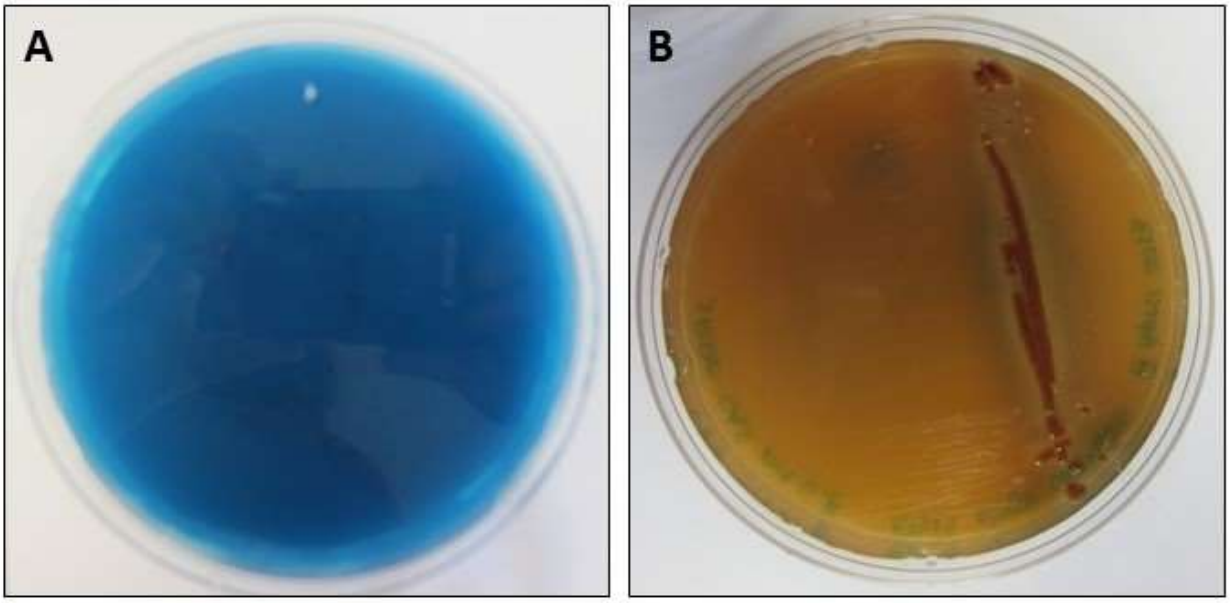

Fig. 22. Chromeazurol S (CAS) assay. (A) Blue agar plate before inoculation, indicating iron bound to CAS dye; (B) Agar plate with EG19 after 7 day growth (yellow colour indicates siderophore has removed iron from CAS dye).

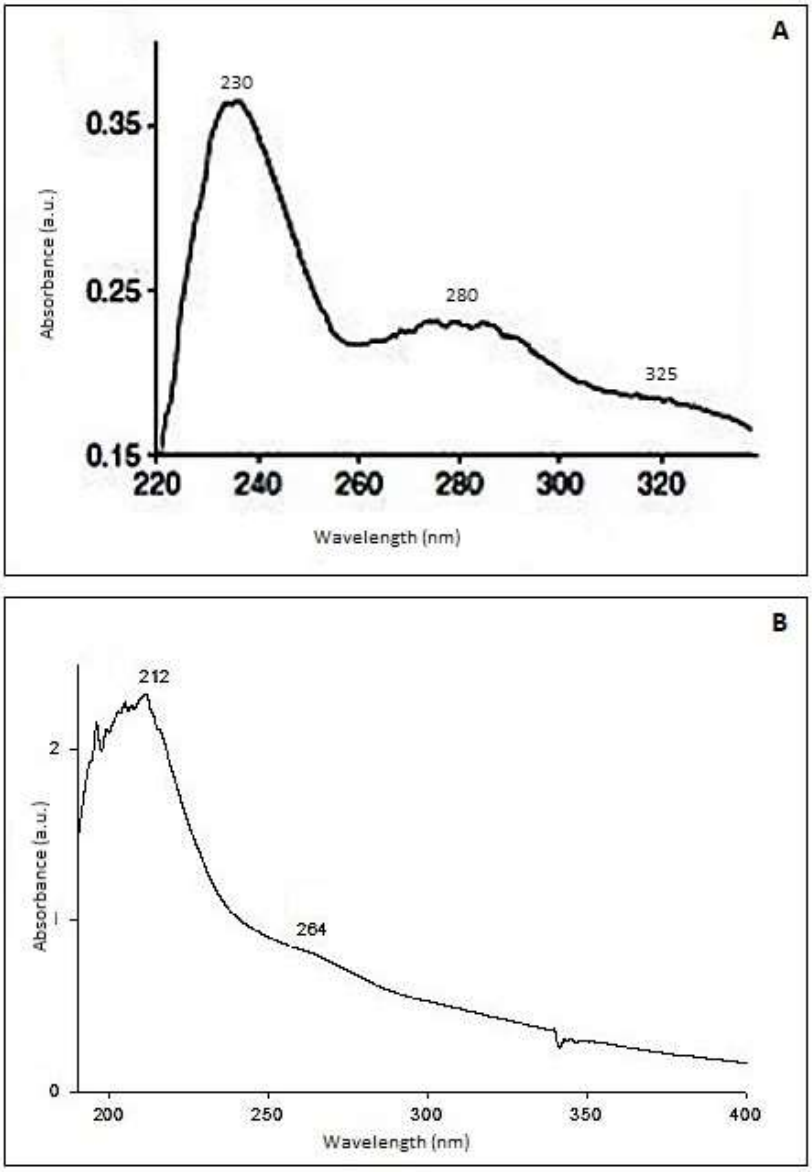

Fig. 23. (A) UV absorption spectrum of culture medium after removal of EG19 cells, as reported by Csotonyi *et al.* (2011a); (B) UV absorption spectrum of the purified siderophore excreted by EG19 into the growth medium.

We then wanted to identify whether this was a protein type siderophore or a pigment. To that end, a native gel was run using the growth medium containing the siderophore as the sample. As the siderophore is brown in colour, it was visible in the gel before staining, allowing us to see that it was present in the band after staining for protein and that it was approximately 800 Da in size (Fig. 24).

3.2.3. Isolation, Purification and Structural Analysis

Freezing was used to concentrate the siderophore at the top of a flask (Fig. 21B), this layer was then scraped off and allowed to thaw. From there a XAD7-HP resin was used in a batch method to bind the siderophore. Once eluted from the resin, the siderophore was sent for NMR analysis. Unfortunately, iron bound to a molecule interferes with NMR as well as MS. However, though we could not ascertain structure based on NMR, it did reveal signals that suggested the protein is approximately 12 amino acids in length.

The lack of positive results from NMR prompted a quest to remove iron from the isolated siderophore. This was no easy task as the role of siderophores is to specifically and tightly bind iron. A number of approaches were attempted on the sample. One method used methanol and hydroxyquiniline mixed with the sample for 3 days, followed by drying the sample and extracting in chloroforms 5 times and repeating the full siderophore purification process (Budde and Leong, 1989). Another involved a similar method but using EDTA to bind the iron instead of hydroxyquiniline as EDTA binds metals very strongly. Unfortunately, none were successful.

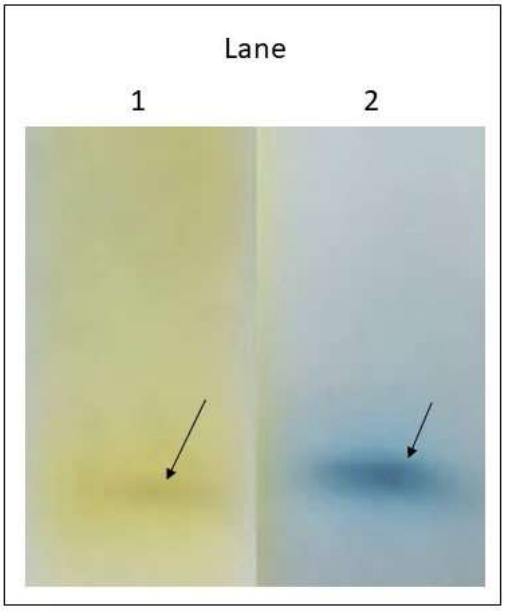

Fig. 24. SDS-PAGE of medium containing siderophore: Lane 1, before staining, band at the bottom of the gel is brown indicating this is the siderophore band; Lane 2, after staining with Coomassie blue, brown band turned blue, indicating it is a protein. Bands indicated with arrows.

3.2.4. Iron Removal and Siderophore Purification

When other methods failed to remove iron from the siderophore after binding, it was decided that the best technique would be to use an MA growth medium devoid of iron. Chelex resin was added in a batch method to de-ferrate the medium before autoclaving. EG19 was grown for 5 days, producing very little biomass, though the medium turned a darker colour than had previously been observed, suggesting a higher concentration of siderophore was produced. From there, the same freezing and XAD 7HP purification as explained above was performed to purify the siderophore.

3.2.5. Inductively Coupled Plasma Mass Spectroscopy, Amino Acid Analysis and Electrospray Mass Spectroscopy

ICP identified a number of elements present in the sample, including boron, barium, calcium, copper, potassium, lanthanum, magnesium, manganese, sodium, phosphorous, praseodymium, strontium, uranium and zinc. Notably, iron is absent from this list confirming our success at removing it from the siderophore sample.

Amino acid analysis revealed the presence of a number of amino acids, confirming the identification of the siderophore as, at least partly, a protein. Amino acids included primarily proline, valine, aspartic acid, and glutamate (Fig. 25). The large glycine peak in the Fig. 25B is due to the amino acid presence in the SDS-PAGE running buffer during protein isolation. Additionally, there were peaks that did not correspond to any known amino acids (could be a contamination from Tris, SDS, and other products used throughout siderophore purification).

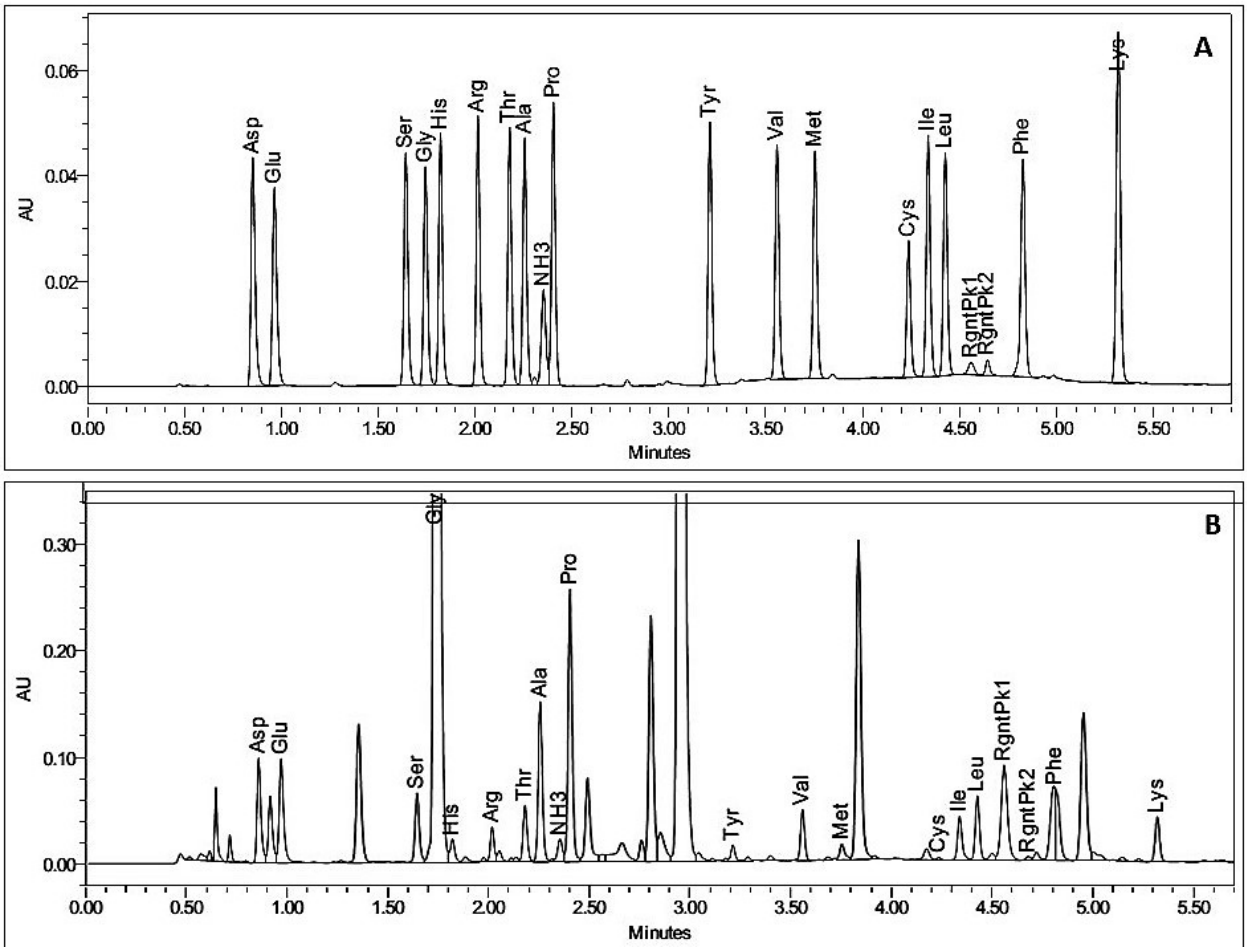

Fig. 25. Amino acid analysis of: (A) Amino acid standard where each is at a concentration of 50.0 pmoles; and (B) Siderophore sample.

Alternatively, these might be signals of the altered amino acids, as it has been shown that some siderophores contain derivatives of standard amino acids (Challis, 2005).

ES-MS was carried out to no avail. Masking the signals from the sample was a repeating pattern that suggested the presence of a polymer. This proved to be contamination from the XAD 7HP resin. This therefore had to be removed from the sample. SDS-PAGE helped to separate the siderophore from the polymer and the protein band was extracted from the gel. ES-MS was repeated. All signals were singly charged, suggesting the sample deteriorated inside the machine during the procedure. However, signal lengths that could be accurately determined coincided with some results from the amino acid analysis. Signals with mass of 99 are indicative of valine, 115 is aspartic acid, 83 (while not a true amino acid) could be 2-butenoic acid and 189 (also not an amino acid) may be N-acetyl-L-glutamic acid (Fig. 26).

3.2.6. Distribution of Siderophores Amongst AAP

Of the 101 AAP strains tested on CAS plates for presence of siderophores, 16 (C4, C9, NM4.16, NM4.18, EG17, E4(1), RB3, RB 16-17, 15-SB, SS63, SS335, Se-1-2-red, ER-Te-40B, ER-Te-65, CB-10, Se-6-2-red) were tested positive, all isolated from the Nopiming Provincial Park samples or from various aquatic environments.

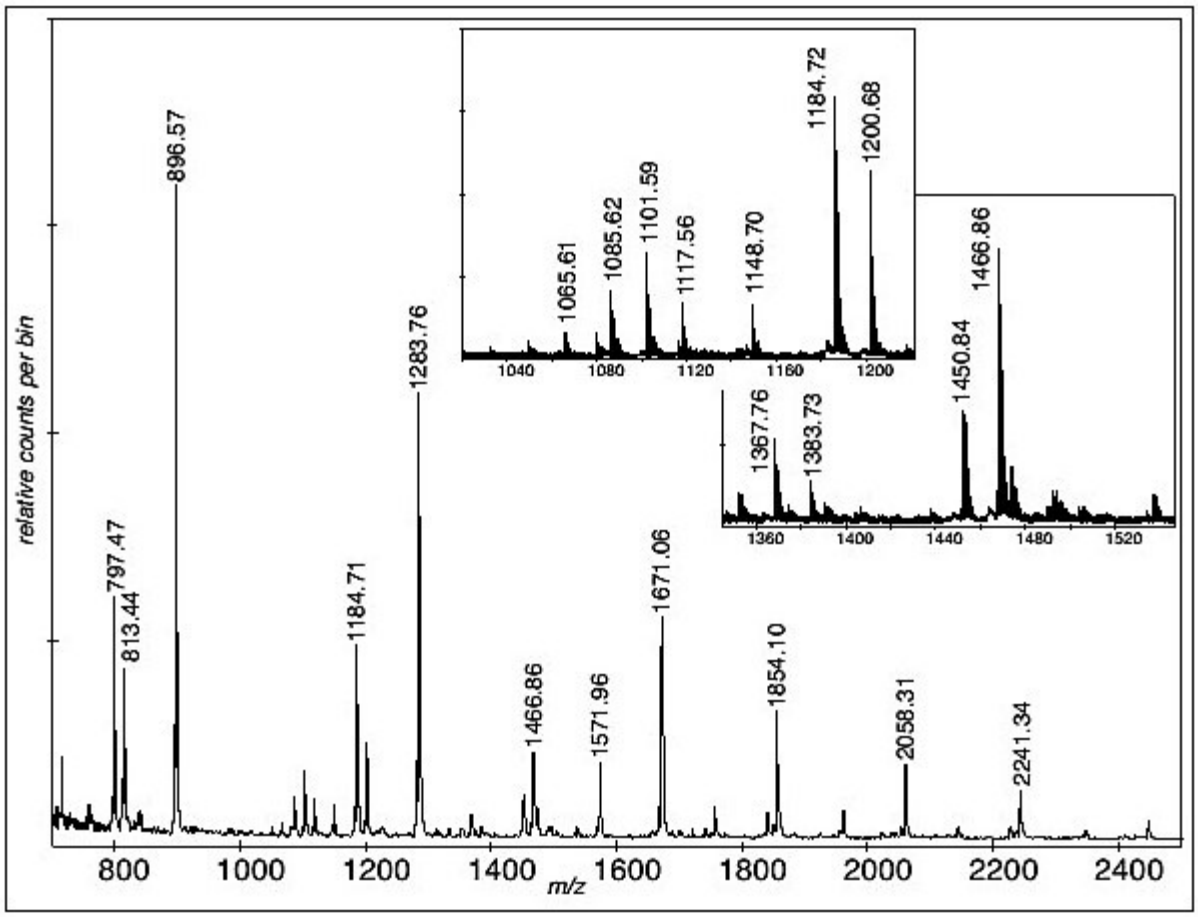

Fig. 26. Nanoelectrospray mass spectroscopy spectrum of purified siderophore, with insets showing smaller fragments.

3.3. Nopiming Provincial Park Study

3.3.1. Site Description and Enumeration

All four sites sampled at the Central Gold Mine, Nopiming Provincial Park, Canada (Fig. 27A) were desiccated due to a very long period of drought in the summer of 2011. The sediment at Site 1, Blue Pond, was yellow with grey-blue patches and pH 4.1 (Fig. 27B). Site 2, an area of tailing drainage, had pH 3.9, a dark yellow surface and a noticeable sulfide smell (Fig. 27C). Site 3 was also yellow, but with green patches, pH 7.0 and displayed a water run-off pattern (Fig. 27D). Site 4, so-called Green Pond, had a sandy color and pH 6.8. This was the only location with any visible vegetation (bull rushes), as well as some water beneath the surface (Fig. 27E).

Results obtained on the media used showed the largest abundance of microbes at Site 4 (8.80×10^5 CFU/+g soil on RO medium, pH 9.0) and the least at Site 1 (3.88×10^4 CFU/g soil on RO, pH 7.0) (Table 2). A large percentage of colonies on all plates were pigmented (3.7%, 75.8%, 28.7% and 22.8% from Sites 1, 2, 3 and 4, respectively) with a significant portion of the colonies from Sites 2, 3 and 4 producing BChl *a* (31.2%, 27.2% and 31.4%, respectively). No AAP were found at Site 1 (Table 2).

The majority of isolates were rod shaped, averaging 2.0µm in length and under 1.0µm in width, though strain NM4.16 formed long filamentous cells of approximately 15.0 x 1.0µm (Fig. 28). All were brightly coloured, either pink (strain C9), orange (C4, NM4.16) or yellow (C11, NM4.18), and formed circular, entire, mucoid colonies. Strains were proven to be AAP as they

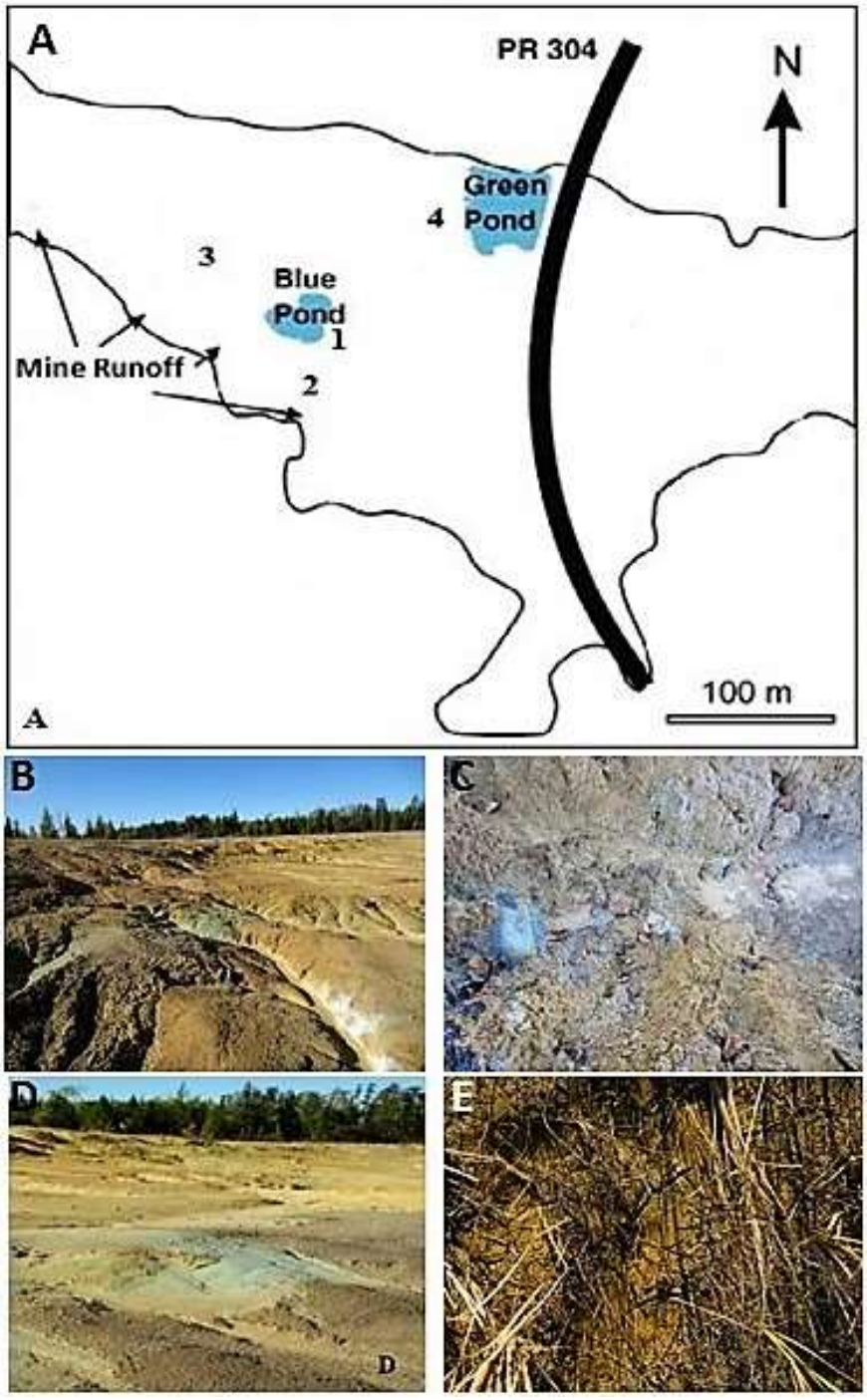

Fig. 27. Map of Nopiming Provincial Park Mine tailings. (A) Site 1 (Blue Pond); (B) Site 2 (main runoff location); (C) Site 3 (secondary runoff); and (D) Site 4 (Green Pond).

Table 2. Enumeration of the cultivable microorganisms from the Central Gold Mine in Nopiming Provincial Park on various media. AAP are presented as percentage of pigmented bacteria.

Site	RO pH 7.0	RO pH 9.0	RO + Na_2SO_4 pH 5.0	RO + Na_2SO_4 pH 7.0	% Pigmented	% AAP
1	$3.88x10^4$	-	$4.5x10^2$	$5.77x10^4$	3.7	0
2	$7.5x10^4$	-	-	$8.0x10^4$	75.8	31.2
3	$5.2x10^4$	-	-	$1.4x10^5$	28.7	27.2
4	-	$8.8x10^5$	-	-	22.8	31.4

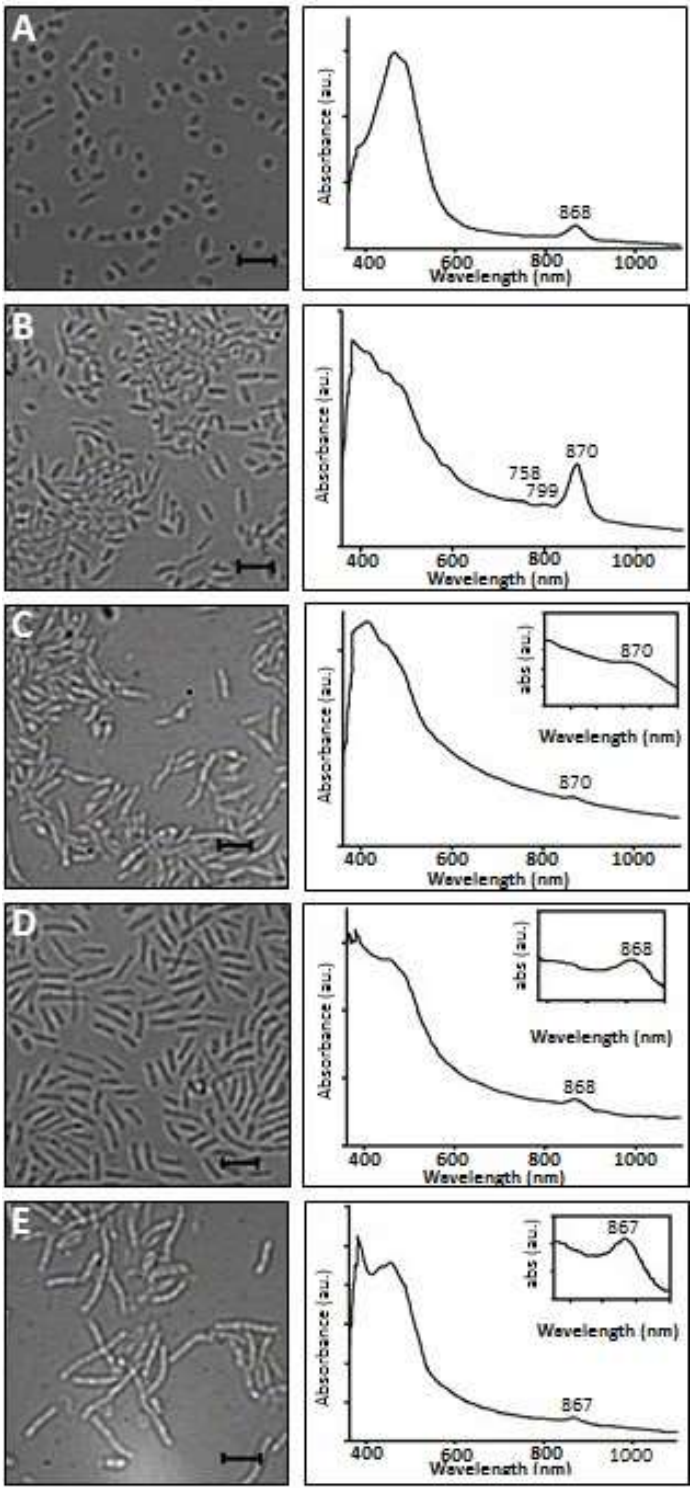

Fig. 28. *In vivo* absorption spectra (wavelength noted above BChl *a* peaks) and phase contrast micrographs (scale bars = 5µm length) of strains: (A) C4; (B) C9; (C) C11; (D) NM4.16; and (E) NM4.18.

are all Gram negative, unable to grow anaerobically, synthesize Bchl *a* (Fig. 28), which is revealed spectrophotometrically as absorption peaks representing the LH complexes at approximately 870 nm, and were incapable of photoautotrophy (Yurkov and Csotonyi, 2009). Isolates were grouped based on phenotype and spectrophotometry, and one representative from each of five groups was chosen for further analyses: NM4.16 (representing NM4.30, NM4.39, NM4.41, NM4.48 and NM4.52; Fig. 28D), NM4.18 (Fig. 28E), C4 (representing C3, C5, C6, and C13; Fig. 28A), C9 (Fig. 28B), and C11 (Fig. 28C).

3.3.2. Taxonomy of Five Representative Strains

Strains grew optimally on complex carbon sources such as yeast extract and bactopeptone, and showed weak growth on casamino acids, glucose, sucrose, glutamate and butyrate. Succinate was also of limited use to C11 (Table 3). Isolates grew at as low pH as 6.0; NM4.16 and C4 had a wide range of pH from 6.0 to 10.0 supporting growth, with an optimal performance at around pH 7.0. C9 and C11 preferentially grew at pH 8.0; however, C11 was able to thrive up to pH 10.5, and C9 was inhibited above pH 9.5. NM4.18 showed the broadest tolerance, growing from pH 6.0 to 11.0, but favoured pH 8.0 (Table 3). Growth was observed from 2 to 37^{o}C, with the exception of strain NM4.16, which could grow up to 45^{o}C. The optimal temperature was 28^{o}C for all isolates (Table 3). NaCl reduced growth of all strains except NM4.18, which grew best at 0.5% and was tolerant to the widest range (0-5%), whereas others were significantly hindered above 0.5 (NM4.16), 1.0 (C4 and C9), and 2.0% (C11) salinity (Table 3). All isolated AAP were sensitive to chloramphenicol, kanamycin, polymixin B and imipenem;

Table 3. Comparative physiological properties of AAP isolated from mine tailings at Nopiming Provincial Park, Canada.

Strain	NM4.16	NM4.18	C4	C9	C11
Utilization of[a]					
Acetate	-	-	-	-	-
Butyrate	+	+	-	+	++
Citrate	-	-	+	-	-
Formate	-	-	-	-	-
Glutamate	+	+	+	+	+
Glycolate	-	-	-	-	-
Lactate	-	-	-	-	-
Malate	-	-	-	-	+
Propionate	-	+	+	-	-
Pyruvate	-	+	-	-	-
Succinate	-	-	-	-	+
Fructose	-	-	-	-	-
Glucose	+	+	+	+	+
Sucrose	+	+	+	+	+
Ethanol	-	-	-	-	-
Methanol	-	-	-	-	-
Glycerol	-	-	-	-	-
Casamino Acids	+	+	+	+	+
Bactopeptone	+	+	+	++	+
Yeast Extract	++	++	++	++	++
RO	+++	+++	+++	+++	+++
pH range; Optimal	6.0 - 10.0; 7.0	6.0 - 11.0; 8.0	6.0 - 10.0; 7.0	6.0 - 9.5; 8.0	6.0 - 10.5; 8.0
Temperature range; Optimal (°C)	2 – 45; 28	2 – 37; 28	2 – 37; 28	2 – 37; 28	2 – 37; 28
Tolerance to NaCl range; Optimal (%)	0 - 0.5; 0	0 – 5; 0.5	0 - 0.5; 0	0 – 1; 0	0 – 2; 0
Production of[b]:					
Amylase	-	-	-	-	-
Gelatinase	+	-	+	-	-
Lipase	+	+	-	-	-
Oxidase	+	+	+	+	+
Catalase	+	+	-	-	+
Resistance to[c]:					
Chloramphenicol (30 µg)	S	S	S	S	S
Penicillin (10 IU)	S	S	R	R	R
Nalidixic acid (30 µg)	S	R	R	R	R
Kanamycin (30 µg)	S	S	S	S	S
Polymixin B (300 IU)	S	S	S	S	S
Ampicillin (2 µg)	S	S	R	R	R
Streptomycin (10 µg)	R	R	S	S	S
Imipenem (10 µg)	S	S	S	S	S
Primary Fatty Acid (%)	C18:1 (64.4)	C16:0 (51.7)	C18:1 (43.1)	C16:0 (36.3)	C16:0 (47.4)
Secondary Fatty Acid (%)	C16:0 (26.3)	C18:0 (23.1)	C16:0 (38.8)	C18:1 (20.9)	C18:1 (18.9)
Tertiary Fatty Acid (%)	C14:0 (4.1)	C14:0 (7.8)	C16:1 (7.5)	C14:0 (7.4)	C16:1 (8.9)

[a] (-) no growth; (+) minimal growth; (++) good growth; (+++) maximum growth; [b] (-) no enzyme activity; (+) enzyme produced; [c] (S) sensitive; (R) resistant

however, some strains had a natural resistance to penicillin (C4, C9 and C11), nalidixic acid (all, except for NM4.16), ampicillin (C4, C9, C11) and streptomycin (NM4.16 and NM4.18) (Table 3).

All strains were Gram negative, a defining trait of AAP, non-motile, did not require vitamins for growth and were unable to ferment sugars or reduce nitrate. They were all able to use sulfate, thiosulfate, cysteine and methionine as sulfur sources, though none could utilize H_2S. They did not fix nitrogen gas, but were able to utilize ammonia. None were able to grow photoautotrophically. Variation among tested enzyme activities was found. NM4.16 and C4 were the only strains that possessed gelatinase, while NM4.16 and NM4.18 were positive for lipase. Most strains demonstrated catalase activity, with the exceptions of C4 and C9. All strains were cyt oxidase positive, and could not degrade starch indicating an absence of amylase (Table 3).

FA analysis revealed that even numbered FA make up the majority of the membranes in all five strains. C9, C11 and NM4.18 all have C16:0 as their primary FA and either C18:0 or C18:1 as the secondary. C4 and NM4.16 are the opposite with C18:1 as the primary and C16:0 as the secondary FA (Table 3).

3.3.3. Resistance to and Reduction of Metal(loid) oxides

All tested strains were capable of high level resistance to Te, Se and V oxides. All tolerated up to 1500 µg/ml K_2TeO_4. Strain C11 was the most resistant to K_2TeO_3 at as high as 1500 µg/ml, whereas NM4.16 was least resistant and could not grow at higher than 250 µg/ml.

C9, C11 and NM4.18 were capable of growth at higher concentrations (5000 μg/ml) of Na_2SeO_4 than C4 and NM4.16 (1000 μg/ml). Na_2SeO_3 was toxic to strains NM4.16 and NM4.18 at any concentration, but was tolerated by C9, C4 and C11 at concentrations up to 1000 μg/ml, 750 μg/ml, and 1000 μg/ml, respectively. C11 and NM4.18 were highly resistant to Na_3VO_4 at a concentration of 5000 μg/ml, with C9 being least tolerant at only 500 μg/ml. Finally, $NaVO_3$ had variable toxicity, with C9 and NM4.16 not tolerating it at all and C11 and NM4.18 growing at concentrations up to 5000 μg/ml (Table 4).

Tellurite reduction to elemental Te was evident for all strains, appearing as a blackening of colonies. Selenite reduction to elemental Se causes reddening of colonies, which is complicated to assess in naturally red pigmented bacteria. Finally, reduction of metavanadate, which would cause colonies to gain a blue-green hue (Rathgeber *et al*., 2002), was not observed. However, as with selenite reduction, strong pigmentation may interfere with observation of low levels of reduction.

3.3.4. 16S rRNA Gene Sequencing

Strains C4 and NM4.16 are most closely related to the AAP *Porphyrobacter colymbid*, with 99.4% and 99.7% sequence similarity, respectively (Fig. 29). C9 and C11 have 99.1% sequence similarity to *Brevundimonas variabilis* and 98.6% sequence similarity to *Brevundimonas bacteroides*, respectively, which are both non-phototrophic organisms (Fig. 29). Finally, NM4.18 is related to the AAP *Erythromonas ursincola*, strain KR99 with 98.5% sequence similarity (Fig. 29).

Table 4. Maximum concentration of metal(loid) oxide (μg/ml), where growth and therefore resistance were observed.

Metalloid oxide	**Strains**				
	NM4.16	**NM4.18**	**C4**	**C9**	**C11**
TeO_4	≥1500	≥1500	≥1500	≥1500	≥1500
TeO_3	1000	250	750	1000	≥1500
SeO_4	1000	≥5000	1000	≥5000	≥5000
SeO_3	0	0	750	1000	1000
VO_4	1000	≥5000	2000	500	≥5000
VO_3	0	≥5000	3000	0	≥5000

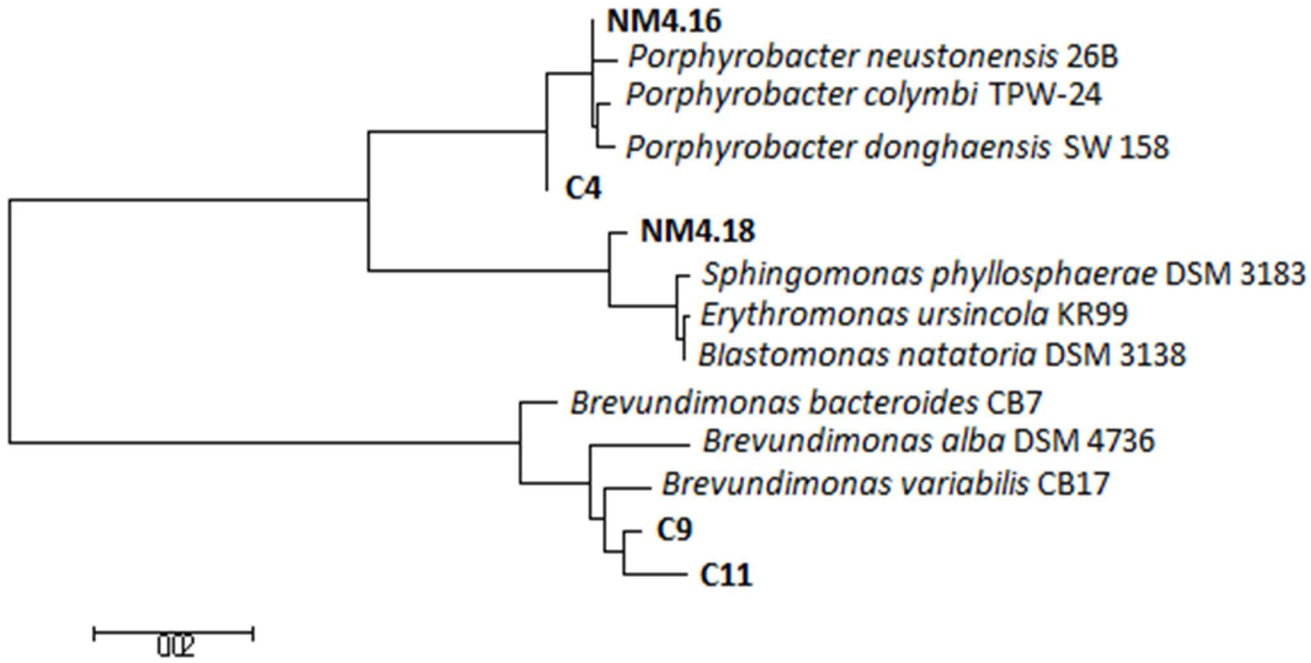

Fig. 29. Maximum likelihood phylogenetic tree of isolated strains and their three closest relatives. Bold lettering denotes strains from this study.

Chapter 4.

Discussion

4.1. Analysis of Photosynthetic Pigment-Protein Complexes

4.1.1. *Roseicyclus mahoneyensis*, Strain ML6 and its Spontaneous Mutants

4.1.1.1. Comparison of Wildtype and Mutant Complexes

While ML6 wildtype produces the RC and LH1 complexes very typical to other AAP, it also has a monomodal LH2 (Fig. 7A), which is of a rare type, having been observed in only two other genera: *Rubrimonas* (Suzuki, 1999) and *Roseobacter* (Shiba, 1991). The mutant ML6(B) is odd in that it appears to have lost the core RC-LH1 complexes, keeping only the accessory LH2 complex (Fig. 7B). This is a very interesting feature, as it is expected that without a RC, photophosphorylation will not function. Therefore, it would be unreasonable to synthesize the LH2 proteins and the light harvesting pigment BChl *a* without expecting functionality. ML6(DB) is similar as it also does not contain the LH1. However, in addition to the LH2 peak, a small shoulder at 755 nm hints at BPheo usually bound to the RC or membranes (Fig. 7C). However, the cells still lack the BChl *a* peaks typical of the RC. Possibly, ML6(DB) is able to produce an incomplete RC in an attempt to regain photosynthetic function. In AAP, some genes for RC synthesis are located within the *puf* operon and others independently in the *puh* operon region (Zheng *et al*., 2011; Yurkov and Hughes, 2013). Likely, only one operon has been lost in a mutation and the other is simply downregulated in ML6(B), but has been upregulated in ML6(DB), causing partial RC synthesis. SDS-PAGE revealed bands at about 7 and 8 KDa matching what is expected for subunits of the LH2 complex, and these bands are identical in ML6(B) and ML6(DB) (Fig. 10C). Of note, the wildtype ML6 and mutant ML6(BN9O) have RC bands at 28, 31 and 33 KDa in size (Fig. 10A). ML6(B) has the same bands at 28 and 33 KDa and ML6(DB) has those at 28 and 31 KDa, hence the RC is only partially formed in these mutants and is not

completely eliminated. This would result in the non-functional RC, which is unable to bind BChl *a* and therefore cannot be detected spectrophotometrically in the 800-900 nm range.

In ML6(BN9O) the LH2 complex is absent, but the RC-LH1 complexes are produced, though in lower numbers compared to the wildtype ML6 (Fig. 7D). This also may impede photosynthesis, though not to the same extent that the loss of the LH1-RC could. It is expected, that with lower concentrations of RC and the loss of the additional light harvesting capacity of the LH2, ML6(BN9O) will not benefit as much from photosynthesis as the wild type. In nature, such mutation would not lead to a progressive evolution.

Sub-optimal growth conditions may encourage pigment production in AAP as photosynthesis can be used for supplementary energy generation when required (Yurkov and Beatty, 1998). It was therefore hypothesized that altering the medium or incubation conditions could cause further mutations or reversion of the spontaneous mutants to the wildtype as a means of optimization or regaining of photosynthesis. However, variations in pH, temperature, light, and salinity showed no reversion of any of the mutants to the wildtype or, in the case of ML6(DB) and ML6(BN9O), to the mutant they were derived from, regardless of the conditional pressure exerted on the cells. Obviously, true irreversible mutations have occurred and not simply a change in gene expression or regulation. Future DNA analysis of the PGC will help to confirm this hypothesis. In ML6(B) and ML6(N9O), some differences in growth parameters did cause changes in the frequency of mutation to ML6(DB) and ML6(BN9O), respectively. For instance, the exposure of ML6(B) to a light/dark cycle imitating daylight transitions, induced the

appearance of ML6(DB) colonies at a much higher rate compared to when grown continually in the dark. It has been previously shown that the light/dark regimens in AAP cause them to replace up to 25% of oxidative phosphorylation with photophosphorylation (Hauruseu and Koblizek, 2012). Studies of *E. hydrolyticum* revealed that growth in complete darkness or light resulted in a lower amount of biomass. In the dark, this is due to the lack of photoexcitation of the light harvesting pigments and in continuous light, BChl *a* synthesis is inhibited. However, when the microbe was subjected to a light/dark regimen, biomass increased, indicating the use of photosynthesis with BChl *a* being produced in periods of dark (Yurkov and van Germeden, 1993). This means that mutant strain ML6(B) may be trying to upregulate RC production under these conditions causing partial synthesis of the RC as is seen in ML6(DB). The frequency of ML6(BN9O) appearance is consistently very low, with the highest occurrence being only 0.26% of colonies when grown at room temperature. The mutation to lose the LH2 obviously does not improve the efficiency of photosynthesis and is likely not energetically favourable, therefore it makes sense that it would not occur frequently.

4.1.1.2. Purified Membrane and Soluble Fractions

There are two types of photosynthetic ETC described in AAP. The first is reported for *E. ursincola, S. sibiricus, R. thiosulfatophilus* and *R. denitrificans* and it uses a RC-bound tetraheme cyt*c*. The second involves a soluble cyt*c*, which is free floating in the periplasmic space, and is not bound directly to the RC. This type has been observed in *E. ramosum, E. hydroliticum, E. ezovicum, E. litoralis* and *E. longus* (Yurkov and Beatty, 1998; Yurkov and Hughes, 2013). The presence of soluble cyt*c* in ML6 and each of its spontaneous mutants classifies them into the

second group (Fig. 8A). Membrane fractions also showed the presence of cyt*c*, indicating that in addition to the soluble cyt*c*, ML6 utilizes an RC-bound cyt*c*. Additionally, RC and LH1 complexes are present and unaltered in ML6 and ML6(BN9O) and LH2 complexes in ML6, ML6(B) and ML6(DB) after membrane isolation and purification as compared to what is observed in whole cells.

Isolation and purification of photosynthetic complexes was challenging as the LH2 complex, in particular, proved to be quite delicate, breaking down easily once removed from the membrane. This forced us to use a milder detergent Triton X-100 for membrane treatment and very slow mixing at ice cold temperatures for 30 min. Using the stronger LDAO detergent, higher concentrations of Triton X-100, warmer temperatures or vigorous mixing caused denaturation of the proteins as was also reported in previous unsuccessful studies (Rathgeber *et al*., 2012). Ultimately, purification of stable intact RC and LH1 from ML6 and ML6(BN9O) and LH2 complexes from ML6, ML6(B) and ML6(DB) was successfully accomplished. Purification of membrane-bound proteins is notoriously difficult, as they either lose functionality or denature easily upon removal from the FA. Absorption peaks of each photosynthetic pigment-protein complex were the same as was recorded in whole cells, indicating that our techniques were appropriate, and the proteins remained unaltered upon solubilization of membranes (Fig. 8).

4.1.1.3. Photosynthetic Ability of ML6 and its Mutants

Flash induced difference spectra of whole cells, membranes and purified complexes have confirmed a fully functional photosynthetic ETC in ML6 and ML6(BN9O). In ML6 whole

cells, when dithionite was used to create reduced conditions, large troughs were present immediately after excitation by the actinic flash, that diminished quickly in size over time (Fig. 11A). This is due to e^- being passed along the ETC, causing re-reduction of the cyt*c*. Under ambient oxidized conditions in membranes, we instead see a P^+ signal (peaks), which indicates the excitation of BChl *a* molecules bound to the RC (Fig. 11B). The peaks decrease at a slower rate than what was measured in cyt*c* troughs, which may be explained by partial oxidation of the membrane-bound cyt*c* has already occurred, causing obstruction of the ETC. Additionally, ML6 uses a soluble cyt*c* together with the RC-bound one. The soluble e^- carrier is missing in purified membranes, hence, while still capable of transferring energy through the entirety of the ETC, it will be slower, because the soluble cyt is responsible for shuttling e^- to the bound cyt*c* increasing the rate of the process. For similar reasons, slower e^- transfer was also observed in purified complexes (Fig. 11). The detection of cyt*c* and P^+ signals as well as re-reduction of the proteins indicates that photosynthesis is progressing in ML6 cells as expected, and corroborates with results published previously (Rathgeber *et al*., 2012).

ML6(BN9O) showed similar cyt*c* signals as ML6 wildtype, though with photosynthetic e^- transport reactions of much slower rate. This was expected, as concentrations of RC-LH1 complexes are lower in ML6(BN9O), as was obvious from the absorption readings (Fig. 7; Fig. 11). Additionally, ML6 has a LH2 complex, which allows for more efficient light harvesting and, therefore, faster flowing photosynthesis. This LH2 complex is absent in ML6(BN9O), causing the cells to lose some level of photophosphorylation. Of note, re-reduction of cyt*c* in the purified RC of ML6(BN9O) progressed at the same rate as in whole cells, suggesting that the soluble e^-

carriers may not be as crucial to photosynthesis as in the wildtype. This is interesting, as we expected identical results in both strains. It could, on the other hand, be that the membrane and complex samples of ML6(BN9O) were simply purified at a different (more appropriate) redox poise than those of the wildtype strain and are, therefore more capable of fast e^- cycling.

After live cells had depleted oxygen in the closed spectrophotometer cuvette, tests were repeated. Under anaerobic conditions, ML6 and ML6(BN9O) were incapable of photosynthetic e^- transfer, confirming that oxygen is required. This is expected as the strains are obligately AAP and it verifies previous studies (Rathgeber *et al.*, 2012).

Flash induced difference spectra of ML6(B) and ML6(DB) produced theoretically predicted results (Fig. 11E). Both strains were incapable of photosynthesis under all tested conditions due to the lack of a complete RC. Without a RC, there is no chance for energy production to take place relying on light harvested by BChl *a* or auxiliary light harvesting pigments. This raises the question: Why would the cells spend large amounts of energy to produce BChl *a* and the photosynthetic LH2, when it cannot be used for photosynthesis which is their primary purpose? There are four likely explanations: First, the complexes or pigments may play a yet undiscovered role, that only future research can reveal. Second, perhaps the cells are evolving to no longer require photosynthesis in the provided laboratory conditions and are, therefore, losing their PGC fragment by fragment. In this case, the *puf* and *puh* operons, responsible for RC and LH1 complexes production (Zheng *et al*., 2011), would be gone, but the *puc* operon, responsible for LH2 production (Zheng *et al*., 2011), and *bch* genes for BChl *a*

production (Zheng *et al*., 2011) have not yet been lost. Also, many genes encoding for the production of cyt, crt and quinones are not always found in the PGC (Zheng *et al*., 2011), making them unlikely to be lost alongside the genes for RC and LH1 synthesis. Third, although we saw no reversion to the wildtype when pressuring/stimulating the strains by various growth conditions, it is possible that the loss of RC-LH1 is simply a change in gene expression, and all the genes remain fully intact but silent, meaning that functional photosynthesis could be regained. In this instance, we possibly did not stress the cells correctly or did not apply necessary conditions to induce expression of the gene operons. Finally, instead of a change in the genes responsible for RC-LH1 production, there could be a mutation in a gene responsible for a control mechanism in the PGC, causing only partial repression or partial expression of the cluster of operons. The best way to determine for sure what is occurring in the cells of ML6(B) and ML6(DB) during the photosynthetic complex production is through full genome sequencing and comparison of the PGC in the wildtype to that in its spontaneous mutants.

4.1.1.4. Role of Carotenoids

Action spectra were carried out on membranes and purified complexes of ML6 and ML6(BN9O) to define what wavelengths of light are harvested for photosynthesis. This allows us to see what, if any, crt are involved in a photoexcitation of the ETC. The lack of peaks in the action spectrum correlated to crt in the absorption spectrum shows that the majority of crt are not associated with light harvesting in ML6 and ML6(BN9O) (Fig. 12). The lack of light harvesting by crt has been observed previously in AAP such as *E. ramosum* and *R. thiosulfatophilus* (Yurkov *et al.*, 1994), and in the case of *E. longus*, more than 70% of crt did not participate in light

collection (Noguchi *et al.*, 1992). As further confirmation, we note the much higher crt peaks in membrane fractions compared to peaks in pure complexes (Fig. 12), indicating that many crt are not tightly associated with the RC and LH complexes, and are instead spread out elsewhere in the cells. All of this implies, they may play an alternative role, such as in photoprotection. Crt have been shown to quench oxidative radicals, protecting the cells from oxidative stress, which is very important in AAP. The process of synthesizing BChl *a* in the presence of light and O_2 results in the production of singlet oxygen and triplet BChl, which both exert oxidative stress on the cells. This is one of the prominent speculations to explain why AAP tend to have a very high ratio of crt to BChl *a* in their membranes, compared to the much lower ratio observed in their PNSB counterparts (Yurkov and Beatty, 1998; Yurkov and Csotonyi, 2009; Yurkov and Hughes, 2013).

4.1.1.5. Redox Potentials of the Q_A, RC-bound Cytochrome and P^+

The range of redox potentials observed for P^+, RC-bound cyt*c* and Q_A of both ML6 and ML6(BN9O) are about +430mV, +245mV, and +65mV, respectively (Fig. 13), are very typical of AAP (Yurkov, Schoepp and Verméglio, 1995; Yurkov and Beatty, 1998) and corroborate previous studies by Rathgeber *et al.* (2012), suggesting that Q_A redox midpoint potential may contribute to the inability of ML6 and ML6(BN9O) to perform anaerobic photosynthetic e^- transfer. However, other AAP, such as *P. meromictius* and *R. denitrificans* have been reported to have Q_A potentials of -25mV and -50mV, respectively (Schwarze *et al.*, 2000; Rathgeber *et al.*, 2012), suggesting the positive Q_A redox potential may not be the sole reason for the AAP lack of anaerobic photosynthesis. In the two given examples, the Q_A redox potentials are closer to

what is expected in PNSB, which are negative (Prince and Dutton, 1978), yet still remain incapable of anaerobic photophosphorylation. It is therefore likely, that other causes exist, such as the lack of an alternative quinol oxidase pathway to re-oxidize the Q_A, inducing it to remain over-reduced, so it can no longer accept e^- (Yurkov and Csotonyi, 2009; Yurkov and Hughes, 2013). For example, PNSB may use the autotrophic Calvin Cycle to keep their photosynthetic e^- carriers at the correct redox poise. NADH is required for CO_2 fixation, hence NAD^+ can take excess e^- from the reduced Q_A to become NADH, oxidizing the Q_A in the process.

4.1.2. *Chromocurvus halotolerans* and *Charonomicrobium ambiphototrophicum*

4.1.2.1. Isolation of Photosynthetic Complexes

Although the photosynthetic complexes of strains EG19 and EG17 show some similarities, such as the red-shifted LH1 complex absorbing at 879 nm and the typical RC complex (Fig. 14), there are some key differences. First, EG19 has a soluble cyt*c* as an e^- carrier as well as a RC-bound cyt*c*; however, EG17 shows only a RC-bound cyt*c* (Fig. 15). This could mean that either strain EG17 exclusively uses RC-bound cyt*c* or it additionally operates with a different carrier, that is not a cyt, does not absorb in the visible light spectrum, and was therefore not detected in our experiments. One example would be a high potential iron-sulfur protein (HiPiP) (Schoepp *et al*., 1995). Second, EG17 is capable, under anoxic conditions, of producing a LH2 complex (Fig. 14C), which has never been observed in the strictly aerobic EG19. Possibly, as aerobic BChl synthesis exerts oxidative stress on the cells, a coping mechanism used by EG17 is to downregulate the genes for LH2 production. This would require the cells to make less BChl *a* than they do under anaerobic conditions, saving them from some oxidative damage.

Finally, while isolating photosynthetic complexes it was found that those in EG17 were much more fragile than in EG19. This is due to different protein arrangements and composition. Ice cold EG17 membranes had to be treated with the same detergent as ML6 membranes, Triton X-100 for a short amount of time with a moderate mixing to prevent protein denaturation upon removal of complexes from the membranes. EG19 membranes were processed at room temperature with the harsher detergent (1.2% LDAO) for a longer period of time with fast mixing to solubilize the membranes without any adverse effects on the proteins. LDAO is a more commonly used detergent than Triton X-100 for photosynthetic complex purification, as reported for *E. litoralis, E. ursincola* and *S. sibiricus* (Yurkov *et al.*, 1998). Eventually, membranes and complexes were all successfully isolated and purified and had the same absorption peaks as measured in whole cells, proving that they were not degraded or changed throughout the processes (Fig. 14). SDS-PAGE revealed that LH1 polypeptides are slightly larger (8-11 KDa) than the norm (Fig. 16B), which is generally around 7-10 KDa. This slight difference in size could contribute to the red-shifting of the LH1 absorption peak. The sizes of the RC subunits were 26, 27 and 31 KDa, which is typical of RC in PNSB and AAP.

4.1.2.2. Photosynthetic Ability of Strains EG19 and EG17

Flash induced difference spectra of aerobically grown whole cells, membranes and purified complexes of EG19 and EG17 confirmed fully functional photosynthetic ETC (Fig. 17; Fig. 18). This was predicted, as both strains contain a typical AAP RC. Transfer of e^- was demonstrated in all samples by strong cyt*c* and P^+ signals, which quickly decreased in size, approaching zero. Once aerobically grown cells were allowed to deplete the oxygen in the

closed cuvette of the spectrophotometer, EG17 complexes continued to function normally (Fig. 18B), while EG19 complexes were capable of only very slow e^- transfer (Fig. 17D). This suggests that EG17 has strategies potentially similar to those of the PNSB, to keep the appropriate redox potential of its Q_A, RC-bound cyt*c* and P^+ to support e^- transfer under the reduced conditions of an anoxic environment. Conversely, EG19 is more similar to typical AAP in that its e^- carriers have either the inappropriate redox midpoint potentials for quick oxidation/reduction cycles under reduced conditions, or the cells lack an alternative quinol oxidase pathway, used by many PNSB to force the e^- carriers back to the correct redox state (Yurkov and Csotonyi, 2009; Yurkov and Hughes, 2013).

Membranes from anaerobically grown cells of EG17 were also tested for photosynthetic activity, and while cyt*c* and P^+ signals were observed, meaning that the e^- carriers were present and functional, re-reduction was too slow to indicate a truly effective photosynthesis. This was not expected, as previous studies (Csotonyi *et al.*, 2011b) and our own physiological growth experiments indicated that photosynthesis does take place anaerobically. There are a number of likely reasons to explain these results. First, it could be that an additional soluble e^- carrier other than a cyt is required anaerobically. For example, a HiPiP (Schoepp *et al.*, 1995) could have been lost during membrane purification. Second, under our experimental conditions the redox poise of the membrane-bound e^- carriers may be causing the Q_A to be over-reduced, halting efficient e^- transfer. Third, possibly the cells have an alternative quinol oxidase pathway, helping the Q_A to remain at the right potential. Some crucial element of the pathway could be lost during membrane isolation and therefore the Q_A cannot be oxidized. Additional

experimentation is needed to understand the true reason for the lack of photosynthesis in the cuvette.

One very interesting feature of the EG19 and EG17 photosynthetic complexes is that they have a red-shifted LH1 with an absorption peak at around 879 nm. It seems that the shift has not caused any difference in the activity of the light dependent ETC as compared to other tested AAP. However, the shift implies that there might be a difference in the protein environment for binding BChl *a* or in the structural composition of the BChl *a* molecule. For example, in the genus *Acidiphilium*, BChl *a* contains zinc as the core metal instead of magnesium. This delivers a slight blue-shift of BChl *a* in the spectrum (Cogdell, *et al*., 2002). The shift in EG19 and EG17 may be due to the physical difference in the sizes of the alpha or beta subunits as was mentioned in Section 4.1.2.1. or variation in amino acid sequence of the BChl *a* binding sites. Further research is required to resolve the speculations.

4.1.2.3. Carotenoids in Photosynthesis

Action spectra were carried out on membranes and purified complexes of EG19 and EG17 to determine the wavelengths of light used for photosynthesis (Fig. 19). This allows us to see what, if any, crt are involved in the passing of light energy to the ETC. The lack of any peaks correlated to crt in the action spectrum compared to peaks in the absorption spectrum shows that crt are not associated with light harvesting in either EG19 or EG17, implying they may play an alternative role in photoprotection as was discussed in Section 4.1.1.4.

4.1.2.4. Analysis of the Q_A, RC-bound Cytochrome and P^+

In EG19, the range of redox potentials are very typical of AAP (Fig. 20A; Fig. 20B). The high redox midpoint potential of the Q_A (+85mV) may contribute to strain's inability to efficiently perform anaerobic photosynthetic e^- transfer, as the Q_A would be over-reduced under anoxic conditions. However, other reasons may also contribute (see section 4.1.1.5.).

In EG17, the redox potentials of the P^+ and RC-bound cyt*c* are typical of AAP (approximately +400mV and +310mV, respectively) (Fig. 20C; Fig. 20D). However, the potential of Q_A, at +5mV is lower compared to what is commonly reported in AAP (Fig. 20C). Most AAP studied to date have Q_A potentials ranging from +5mV to +150mV, with a couple of exceptions (see Section 4.1.1.5.) (Yurkov and Hughes, 2013). PNSB tend to have Q_A potentials in the negative range (Prince and Dutton, 1978), putting that of EG17 right between what is expected of AAP and PNSB. This intermediately poised Q_A potential may allow the strain to function photosynthetically, both aerobically and anaerobically. Likely, the Q_A does not become over reduced under anoxic conditions, and therefore, photosynthetic reactions can flow without interruption.

4.2. Siderophores

4.2.1. Physical Properties of the Brown Component

The compound of interest excreted by strain EG19 into the growth medium is very small in size (less than 1000 Da), falling into the expected size range for siderophores, which can be as high as 2000 Da, but are more commonly under 1000 Da (Reid *et al*., 1993; Wandersman and

Delepelaire, 2004; Challis, 2005; Schalk, Hannauer and Braud, 2011; Grobelak and Hiller, 2017). Additionally, it is highly hydrophilic, and cannot be extracted with organic solvents from the water phase.

4.2.2. Spectrophotometric Analysis and Identification

A wavelength scan in the UV spectrum can be used to determine protein with peaks at 280 nm. In this case, the peak was not observed, though it could still be present, but masked under much larger peaks. As well, the shape of the curve is different from previous findings (Fig. 23) (Csotonyi *et al*., 2011a). In the 2011 study, it was observed that the brown-orange compound was only excreted into the growth medium when cells were grown in the presence of yeast extract. Therefore, a spectrum was collected from the medium containing yeast extract and compared to that from a defined medium. It was then assumed that the difference observed in the spectrum was absorption by the brown-orange compound. However, this may not be the case as many differences in protein and metabolite production can occur based on what organic compounds are available for metabolism. Therefore, the spectrum achieved by us from the pure siderophore is more accurate. The peaks that were detected resembled those of a siderophore (pyochelin), which has absorption peaks at 310, 250, and 210 nm (Sokol *et al.*, 1992). Not only did this allow us to hypothesize that this molecule is a siderophore, but it indicated the catechol type, based on its absorbance in the UV spectrum. Contrarily, if it were a hydroxamate type siderophore, it would have absorbed in the 400-500 nm range.

As CAS medium changed colour (Fig. 22), we can conclude that EG19 is producing a molecule that chelates iron from the surrounding environment (Schwyn and Neilands, 1987). This is a standard test that has been widely accepted to confirm the presence of a siderophore. Additionally, the molecule acts as would be expected of a protein. It could pass through a polyacrylamide gel and was then stained by Coomassie blue (Fig. 24), indicating that this molecule is a protein.

4.2.3. Iron Removal and Siderophore Purification

Removal of iron from the siderophore after binding was extremely challenging. The siderophore binds iron very strongly, making it a powerful tool for EG19 under iron deplete conditions. Why the strain would require this however, is unclear, as the East German Creek System, where the strain was isolated has very high natural concentrations of iron, as evidenced by the bright orange colour of the sediments in the springs. Although unlikely, perhaps the cells have evolved to use iron containing molecules in many more metabolic processes compared to other bacteria and, therefore need higher amounts of iron than most. Conversely, perhaps instead of using the iron for its physiology, in the habitats where concentrations are toxic to the cells, EG19 is using siderophores to remove excess iron from the environment as a detoxification strategy to create a micro-niche of lower iron concentrations. Additional functions of siderophores have also been reported. They can be used for chelation of other metals that may be in growth limiting quantities. If metals are elevated to toxic levels, which might be detected in such an extreme place as the East German Creek System, the siderophore could be binding them to lower the toxicity in direct contact with the cells (Schalk,

Hannauer and Braud, 2011). The molecules could also have antibacterial properties (Adler *et al*., 2012), that aid EG19 in community competition. Either way, our speculations on the role of siderophores in EG19 requires more time for confirmation as our discovery of the first siderophore in AAP is just the beginning of a large project to be developed in the laboratory.

Nevertheless, the iron had to be removed, as it would interfere with MS and NMR, and it was achieved by eliminating it in the growth medium instead of knocking it out of the siderophores. If there is no iron to bind in the first place, there will be no iron bound to the siderophore. Inoculation of EG19 into the iron free medium resulted in very slow weak growth, but the concentration of siderophores, observed visually by colour change in the medium, was higher than observed in media containing iron. This additionally confirms the identity of the molecule as a siderophore. When the cells were in iron deficient conditions, they produced high levels of siderophores to collect as much iron as possible to support growth.

4.2.4. Structural Analysis of Siderophores

There are several reasons why MS (Fig. 26) has not been conclusive in determining structure of the siderophore. First, there could be unusual or altered amino acids in the structure, which are difficult to identify. For instance, there may be acetylated glutamate and possibly 2-amino butanoic acid. Both are very similar to amino acids but have some small differences. Second, the molecule could be a short polypeptide backbone with a larger non-protein fragment attached to it. This would allow the siderophore to travel through a polyacrylamide gel and be coomassie stained, but not be a truly conventional protein. Third,

the molecule may be degrading in the mass spectrometer, which could account for the lack of a true pattern in the peaks. Fourth, there may be a metal ion integral to the molecule. This could interfere with the mass spectrophotometer readings – like iron does.

To begin eliminating possibilities, ICP was performed to see what metal ions are present in the sample, and therefore determine which may be important to the structure of the molecule, and particularly to check that iron had truly been eliminated. As EG19 can only produce the siderophores when complex carbon sources are provided, it is likely that there is a component not included in defined media compositions, that may be crucial to siderophore synthesis. There were many elements present in the sample, notably barium, lanthanum, praseodymium, strontium and uranium. Other elements detected, such as magnesium and zinc, were added to the growth medium in trace amounts as essential components for growth. These are almost impossible to remove once they are present, and are expected to be in all samples. Sodium was also reported in very high concentrations, as it is an important part of glass. Hence, when samples are stored in glass vials (as ours were), sodium can leach into the contents in appreciable amounts (Fearn *et al*., 2006).

Finally, amino acid analysis was performed to identify some components of the sample. This confirmed the MS signals corresponding to valine and aspartic acid. Proline is however reported in high amounts but there is no MS signal correlating to this amino acid, suggesting it may be a component that has become fragmented in the machine. Finally, signals that do not

match to known amino acids in the analysis may indicate altered molecules such as acetylated glutamate and possibly 2-amino butanoic acid, as mentioned above (Fig. 25).

4.2.5. Distribution of Siderophores Amongst AAP

Of the strains that produce siderophores, all were isolated from marine habitats, hot springs, or mine tailings at Nopiming Provincial Park (Hughes *et al*., 2017), and only two from the East German Creek System with none from meromictic Blue Lake or Mahoney Lake. This suggests that environment may play an important role in the evolutionary development of siderophore production. Their presence in mine tailings suggest they may play a role other than iron acquisition in AAP, as Fe is in high enough concentration that it is likely not a limiting nutrient in the habitat (Sherriff *et al*., 2007). Their absence from lakes is also of note as iron may be limiting for growth. Future study could test our collections of AAP from the Banff hot springs and Lake Winnipeg to see if they are produced in only some hot springs and lakes and not others. It also suggests that siderophore presence is not a prominent feature of AAP as they are yielded in only 16% of tested strains. The hope of this experiment was that siderophores would be present in all tested AAP providing a novel taxonomic marker for this group of bacteria. Unfortunately, it did not work this way and we must continue identification of AAP based on the production of BChl *a*, bright pigments and their inability to grow anaerobically.

4.3. Nopiming Provincial Park

4.3.1. AAP in the Environment

A high abundance of microbes was observed at Site 4 in the mine tailings at Nopiming Provincial Park, likely due to the presence of some water allowing for a more actively developing community, as compared to Site 1, which was very dry, and consequently had the lowest number of CFU. Not surprisingly, a large percentage of the organisms found were AAP, as they have been detected in abundance in many extreme environments all over the world (Table 2) (Yurkov and Hughes, 2017). Having such a large presence in this toxic human created ecosystem implies that AAP may play an important ecological role at the gold mine tailings.

4.3.2. Taxonomy of Isolated Strains

The preferential use of complex organics (Table 3) is a typical feature of most known AAP (Yurkov and Hughes, 2013), as these sources provide a wide range of nutrients for heterotrophic growth, which is essential in this group. Another common trait amongst AAP, which was also observed here is the variable tolerance to antibiotics (Table 3). This is of note, as the appearance of antibiotic resistance genes in microbes from pristine environments (where antibiotics have not been added by humans), suggests that it is a natural feature (Martínez, 2008). Microorganisms can naturally produce antibacterial compounds to gain a competitive advantage over other bacteria in the same community.

The wide range of pH tolerance among isolates is expected (Table 3) for proliferation in such extreme habitats with seasonably fluctuating conditions, because summer desiccation can

concentrate the compounds present in the water or soil reducing the pH, and high levels of precipitation dilute the solutes, raising the pH. It was interesting, that although Sites 1 and 2 had very low pH (4.1 and 3.9, respectively), no isolates from those locales were capable of growth below pH 5.0. Possibly, bacteria persisted in a dormant state awaiting better conditions (Roszak and Colwell, 1987). Also, bacteria in nature can control their own cytoplasmic pH at optimum, despite the acidity of the environment. One suggested mechanism could be the neutralization of the immediate area around the cells through production of base molecules from acidic molecules similar to what is seen in *Clostridium acetobutylicum*, which uses butyrate to produce butanol and *Klebsiella aerogenes*, which makes butanediol from acetate (Booth, 1985). *Helicobacter pylori* causes peptic ulcers, but first it must be able to colonize the stomach despite the acidity of the environment. To do so it imports urea and hydrolyzes it to ammonia, which neutralizes the periplasmic space and interior of the cells allowing for growth at its preferred neutral pH (Fong *et al*., 2011). Another potential mechanism could be the active transport of protons out of the cell (Booth 1985). A similar trend is expected for NaCl tolerance, as desiccation concentrates salts in the habitat and precipitation dilutes them. The wide temperature range was also predicted. The strains would have to survive extreme Manitoba weather conditions: very hot in summer (over 30°C) and extremely cold in winter (below -40°C). In the laboratory, all isolates however, behave as typical mesophiles with 28°C being the optimum (Table 3).

No strains grow photoautotrophically, similar to all other known AAP, which lack the Calvin cycle key RUBISCO (Yurkov and Hughes 2013). All strains were cyt oxidase positive, which

is expected for AAP (bacteria that use oxygen as a terminal e^- acceptor in respiration). The variations in enzyme activity in our isolates are also well established in the group (Table 3) (Yukov and Beatty, 1998); for instance, of 33 strains studied from Mahoney Lake, 24 hydrolyzed Tween 60, 20 had gelatinase activity and only 14 could break down starch (Yurkova *et al*., 2002). FA were also as expected for bacteria, with the majority being even numbered with few un-saturations (Table 3). FA analysis became a required taxonomical test only 10-15 years ago, for the classification of novel photosynthetic bacteria. However, with the exception of extremophiles, that exhibit changes in FA to maintain fluidity in their membranes, this information does not seem to be particularly illuminating. Perhaps FA analysis should therefore not be required.

4.3.3. Closest Relatives and Potential Novel Species and Genera

Like the majority of known AAP, all organisms in this study belong to the α-*Proteobacteria* (Yurkov and Beatty, 1998; Yurkov and Hughes, 2013). Strains C4 and NM4.16 are potentially novel species within the genus *Porphyrobacter*, though DNA-DNA hybridization will resolve how closely related they truly are, as is standard practice, and what taxon they represent. While C9 and C11 have very high 16S rRNA sequence similarity to species in the genus *Brevundimonas*, their ability to photosynthesize sets them apart, suggesting a possibility to recognize them taxonomically as a novel genus. Finally, for NM4.18, DNA-DNA hybridization is required to determine its relationship to *E. ursincola*, strain KR99 (Fig. 29).

4.3.4. Potential for Bioremediation and Biometallurgy

Vanadate and selenite are both found naturally in minute quantities in nature (Yurkov and Csotonyi, 2003). Biologically, selenium is an essential part of the 21st amino acid, selenocysteine (Böck *et al*., 1991), making it an interesting and important element for study. In contrast, tellurite is usually less abundant than other metal(loid) oxides, but is found at higher concentrations in the presence of gold (Yurkov and Csotonyi, 2003). We therefore expected it to be a significant component in gold mine tailings, contributing to their toxicity. While all of these oxides are toxic to most microorganisms at concentrations as low as 1.0 µg/ml, high resistance to them is a known trend among AAP (Yurkov and Csotonyi, 2003). It is speculated that through evolution and horizontal gene transfer, they have acquired metal resistance in order to thrive in extreme locations (Yurkov and Csotonyi, 2003).

In addition to being extremely resistant (Table 4), all isolates were able to reduce tellurite to elemental Te and accumulate Te crystals inside cells. This could potentially be applied in the future for bioremediation of pollutants as well as for biometallurgy of the very rare yet industrially important metalloid (Yurkov and Csotonyi, 2003). Future research can determine the mechanism and cellular localization of reduction, which may resemble a reduction physiology published in *E. hydrolyticum*, requiring a whole cell and *de novo* protein synthesis for function (Maltman and Yurkov, 2015). Alternatively, there is a chance for a reduction strategy reported in *E. ezovicum, E. ramosum, E. ursincola, S. sibiricus* and *R. thiosulfatophilus,* which all employ a constitutively produced membrane associated enzyme

(Maltman and Yurkov, 2015). Additionally, a novel strategy different from those previously described could be found.

Chapter 5.

Conclusions and Future Prospects

5.1. Major Thesis Discoveries

The first part of this project was to research the unusual AAP, *R. mahoneyensis*, as it mutates rapidly to form the photosynthetically modified strains ML6(B), ML6(DB) and ML6(BN9O). They appear as brown pigmented colonies on plates of either pink wildtype strain ML6 or other spontaneous mutants. Upon pressuring the cells with changes in growth conditions, it was found that none of the mutants showed reversion to the wildtype, indicating that true mutations are taking place and mutant phenotypes are not due to a simple change in gene expression. The mutated strains were compared and contrasted to the wildtype for the quality of photosynthetic pigment-protein complexes, light induced e^- transport, role of crt, and redox midpoint potentials of e^- carriers.

Strain ML6(BN9O), while lacking the LH2 complex, behaved very similarly to ML6. Both were capable of active photosynthetic e^- cycling under aerobic conditions and could not perform photosynthesis anaerobically. Both also employed a soluble and an RC-bound cyt*c* and did not utilize crt for light harvesting. The redox midpoint potentials of the primary e^- carrier Q_A, P^+ and RC-bound cyt*c* were all typical of AAP, and may contribute to their inability to photosynthesize anaerobically. The strains ML6(B) and ML6(DB) lack the RC and LH1 complexes and therefore, as it was hypothesized, did not show any signs of photosynthetic ability. Why they would therefore continue to produce BChl *a* and LH2 complexes remains a question for future research. RC and LH complex subunits in ML6 and its mutants were all found to be of a very typical AAP size. This makes it unlikely that the size of the complexes contributes to the preference of ML6 to photosynthesize under microaerophilic conditions.

Photosynthetic units in *C. halotolerans*, strain EG19 were examined next, as it has an unusual red-shifted LH1 complex. In this case, the light-induced ETC was found to be active under aerobic conditions and remained somewhat functional, though slow, anoxically. The strain employs both soluble and RC-bound cyt*c*, does not utilize crt for light harvesting and has very typical redox midpoint potentials of its e^- carriers. It appears that the red-shift in LH1 did not cause any difference in the expected results for photosynthetic function. We can therefore conclude that it is likely a simple structural modification in the protein arrangements, which does not affect functionality.

C. ambiphototrophicum, strain EG17 was the final bacterium chosen for study and is the most photosynthetically interesting. It has the same red-shifted LH1 as EG19, but unlike any other AAP known to date, produces its photosynthetic complexes under both aerobic and anaerobic conditions. Aerobically grown cells, membranes and purified complexes showed active photosynthetic e^- transport in the presence and absence of oxygen, with little difference between the two conditions, indicating that oxygen concentration is not an obligate requirement for this strain. Crt were not used for light harvesting and an RC-bound cyt*c* was used for e^- transfers. While the P^+ and RC-bound cyt*c* had redox midpoint potentials typical of AAP, that of the Q_A was quite low at only +5mV, putting it exactly between what we would expect of the AAP and the PNSB. This feature potentially contributes to the microbe's ability to carry out photosynthesis equally under both anoxic and oxic conditions.

Unexpectedly, flash induced difference spectra of anaerobically grown membranes of EG17 did not show active photosynthesis. However, previous study of liquid cultures clearly confirmed that anaerobically grown cells do retain the ability to grow photosynthetically. It is likely that a crucial e^- carrier was lost during membrane purification, therefore further experimentation is required to establish the reason.

EG17 additionally has a red-shifted LH1 similar to that of EG19. While both strains possessed very typically sized RC subunits, the LH1 polypeptides were slightly larger than expected. This supports the speculation mentioned above that the proteins are structurally modified in a way that does not affect photosynthetic function.

The second part of this thesis deals with the purification and characterization of the orange-brown pigmented product excreted by strain EG19 into the growth medium. It was defined as a small protein, hydrophilic in nature, which binds iron very strongly. It was then confirmed to be a catechol type siderophore, the first isolated from and identified in AAP. While amino acid analysis and MS did allow speculations into the structure of the protein, we have not yet been able to definitively determine the full complex.

Finally, the third section of this research was the enumeration, isolation and taxonomic identification of novel AAP strains from the Central Gold Mine tailings at Nopiming Provincial Park, Canada. As AAP were found in very high proportions in this habitat, we can assume that they play an influential role in the ecosystem. While none have any unexpected characteristics

and their photosynthetic complexes are very typical, it should be noted that very high tolerance to the toxic heavy metal(loid) oxides tellurite, tellurate, selenate, selenite, metavanadate and orthovanadate, were observed in all strains, as was hoped for based on their habitat of isolation. The ability to reduce tellurate and tellurite to tellurium, rendering it less toxic, was also detected. This may, in the future, be of use in bioremediation and biometallurgy.

5.2. Future Prospects

There are many remaining questions related to the photosynthetic complexes of AAP, particularly to the unusual ones studied in this project. In the future, the entire DNA sequencing of ML6 and its mutants will reveal whether true mutations and which kind are in fact occurring. Specifically, in strains ML6(B) and ML6(DB) that produce the LH2 complex despite a lack of RC and LH1 and therefore photosynthetic function. Sequencing of the PGC in DNA of EG19 and EG17 as well as x-ray crystallography could also provide insight into what changes have occurred to produce the red-shifted LH1 complex.

Much work is also required to understand the true difference between anoxygenic photosynthesis in PNSB and AAP. Why does it occur anaerobically in one and aerobically in the other? These answers could begin to come to light with more study of EG17, as it is the only organism known to function under both conditions. To start, it must be confirmed that EG17 can photosynthesize anaerobically. This can be done by performing flash induced difference spectra on whole anaerobically grown cells of EG17. The soluble fraction from anaerobically grown cells can also be added back into membrane fractions to determine if photosynthesis is

restored. This would confirm the presence of a crucial soluble e^- carrier such as HiPiP (Schoepp *et al.*, 1995). Next, DNA sequencing of the PGC could reveal what genes are present in multiple forms, or missing, or added to the genome as compared to what is typical in related AAP and PNSB. Finally, more research into all metabolic pathways present in the organism may show if there are alternative quinol oxidase pathways that could keep the Q_A in the appropriate redox state to accept e^- in a reduced environment.

The role of high levels of crt in AAP is also unclear at this time. They are hypothesized to primarily aid in photoprotection of the cells (Yurkov and Beatty, 1998; Klassen, 2009; Zheng *et al.*, 2011), though this has not yet been proven. They could also contribute greatly to the ability of so many AAP to resist high levels of toxic metalloid oxides, which affect the cells primarily through oxidative stress (Yurkov and Csotonyi, 2003). It would be interesting to study the affect of crt in these cases. Finally, some of them can contribute to light harvesting, but it is unclear if there are specific crt that are always used in photosynthesis or if it varies based on the strain. Only performing action spectra, as done in this project, or fluorescence emission spectra on a wider range of AAP can provide us with a large enough database to come to any solid conclusions.

The study of siderophores among AAP is in its infancy, having been discovered for the first time in this project. There are therefore many directions the scientific community can undertake. First, more AAP need to be screened for the presence of siderophores using a simple CAS assay (Schwyn and Neilands, 1987) to determine their prevalence. This will

hopefully establish an environmental pattern to reveal what growth conditions induce AAP to produce siderophores. It is also possible that only certain phylogenetic groups of AAP have this ability. Next, we would need to see if there is any continuity to what type of siderophores are made by AAP. Are they primarily protein or not, and are they catechol type as found in EG19, or are they of any other types? Are they structurally similar to each other or is there a range of different forms? A start to answering these would be to determine the structure of the novel siderophore from EG19 through further MS, NMR and possibly N-terminal sequencing. Finally, there are a wide range of possible purposes for siderophores, and their function in AAP which must yet be determined. This may be partially answered if a pattern is found for the type of environment in which siderophores are being synthesized. For instance, in oligotrophic habitats, they may be used for their primary function of collecting iron. However, strains from mine tailings, which should be rich in iron, showed siderophore activity. In this instance, they may be used to sequester other metals (Schalk, Hannauer and Braud, 2011), allowing the bacteria to thrive in this toxic niche. Purified siderophores from AAP can also be tested for antimicrobial effects, which may be used by their producers to limit community competition in nature (Adler *et al.*, 2012).

Lastly, while some answers are coming to light in terms of the AAP ecological significance in aquatic environments, very little has been investigated in other ecosystems including soils, and extreme habitats such as mine tailings. Clearly, AAP are important as they are enumerated in very high proportions in all environment tested. In addition to what we know already about their contribution to carbon cycling based on their ability to grow quickly to

a large size and then be preferentially grazed upon, they may also play an important role in detoxification of polluted habitats. AAP are commonly highly tolerant to toxic metal(loid) oxides and can reduce them to their less harmful elemental forms (Yurkov and Csotonyi, 2003). This capability could be crucial to the initial establishment of microbial communities and, later, to the appearance of higher organisms as the sites are slowly being microbially remediated. This could potentially be harnessed at the industrial level in the future to clean up toxic waste after industrial processes. Clearly, for that to happen more research needs to be done to understand how they manage to tolerate and detoxify their habitats. While the identification of tellurite and selenite reductase enzymes in some AAP has been recently published (Maltman, Donald and Yurkov, 2017), it may only be one piece of the puzzle. Others could be the use of crt to prevent oxidative stress or siderophores to sequester the metal(loid) oxides, or there could be additional processes we have not yet found.

Obviously, AAP are of great interest for a plethora of reasons and future research following the parameters laid out above could yield some important discoveries in AAP photosynthesis, the role of siderophores, significance in natural ecosystems and potential bioremediation applications.

References

Adler, C., Corbalán, N., Seyedsayamdost, M., Pomares, MF., de Cristóbal, R., Clardy, J., Kolter, R., and Vincent, P. (2012) Catecholate siderophores protect bacteria from pyochelin toxicity. PLOS ONE. 7(10): e46754.

Barker, R., Boden, N., Cayley, G., Charlton, S., Henson, R., Holmes, M., Kelly, I., and Knowles, P. (1979) Properties of cupric ions in benzylamine oxidase from pig plasma as studied by magnetic-resonance and kinetic methods. Biochemical Journal. 177: 289-302.

Beatty, J. T. (2005) On the natural selection and evolution of the aerobic phototrophic bacteria. *In* "Discoveries in Photosynthesis"*,* (Govindjee, J. T. Beatty, H. Gest and J.F. Allen, eds.). 1099–1104. Springer.

Biebl, H., Tindall, B. J., Pukall, R., Lünsdorf, H., Allgaier, M., and Wagner-Döbler, I. (2006) *Hoeflea phototrophica* sp. nov., a novel alphaproteobacterium that forms bacteriochlorophyll *a*. International Journal of Systematic and Evolutionary Microbiology. 56: 821-826.

Bill, N., Tomasch, J., Riemer, A., Muller, K., Kleist, S., Schmidt-Hohagen, K., Wagner-Döbler, I., and Schomburg, D. (2017) Fixation of CO2 using the ethylmalonyl-CoA pathway in the photoheterotrophic marine bacterium *Dinoroseobacter shibae*. Environmental Microbiology. 19(7): 2645-2660.

Bilyj, M., Lepitzki, D., Hughes, E., Swiderski, J., Stackebrandt, E., Pacas, C., and Yurkov, V. (2014) Abundance and diversity of the phototrophic microbial mat communities of Sulphur Mountain Banff Springs and their significance to the endangered snail, *Physella johnsoni*. Open Journal of Ecology. 4: 488-516.

Bock, A., Forchhammer, K., Heider, J., Leinfelder, W., Sawers, G., Veprek, B., and Zinoni, F. (1991) Selenocysteine: the 21st amino acid. Molecular Microbiology. 5(3): 515‐520.

Boeuf, D., Cottrell, MT., Kirchman, DL., Lebaron, P., Jeanthon, C. (2013) Summer community structure of aerobic anoxygenic phototrophic bacteria in the Western Arctic Ocean. FEMS Microbiology Ecology. 85(3): 417-32.

Boldareva-Nuianzina, EN., Bláhová, Z., Sobotka, R., and Koblížek, M. (2013) Distribution and origin of oxygen-dependent and oxygen-independent forms of Mg-protoporphyrin monomethylester cyclase among phototrophic proteobacteria. Applied and Environmental Microbiology. 79(8): 2596-2604.

Booth, I. (1985) Regulation of cytoplasmic pH in bacteria. Microbiological Reviews. 49(4): 359‐378.

Budde, AD., and Leong, SA. (1989) Characterization of siderophores from *Ustilago maydis*. Mycopathologia. 108:125-133.

Cepáková, Z., Hrouzek, P., Žišková, E., Nuyanzina-Boldareva, E., Salka, I., Grossart, H-P., and Koblížek, M. (2016) High turnover rates of aerobic anoxygenic phototrophs in European freshwater lakes. Environmental Microbiology. 18(12): 5063-5071.

Challis, G. (2005) A widely distributed bacterial pathway for siderophore biosynthesis independent of nonribosomal peptide synthesis. ChemBioChem. 6: 601-611.

Chen, WP., and Kuo, TT. (2006) A simple and rapid method for the preparation of Gram negative bacterial genomic DNA. Nucleic Acids Research. 21(9): 2260.

Cogdell, RJ., Howard, TD., Isaacs, NW., McLuskey, K., and Gardiner, AT. (2002) Structural factors which control the position of the Qy absorption band of bacteriochlorophyll *a* in purple bacterial antenna complexes. Photosynthesis Research. 74: 135–141.

Cottrell, MT., Ras, J., and Kirchman, D. (2010) Bacteriochlorophyll and community structure of aerobic anoxygenic phototrophic bacteria in a particle-rich estuary. International Society of Microbial Ecology Journal: Multidisciplinary Journal of Microbial Ecology. 4: 945-954.

Crosa, J., and Walsh, C. (2002) Genetics and assembly line enzymology of siderophore biosynthesis in bacteria. Microbiology and Molecular Biology Reviews. 66(2): 223-249.

Csotonyi, J., Swiderski, J., Stackebrandt, E., and Yurkov, V. (2008) Novel halophilic aerobic anoxygenic phototrophs from a Canadian hypersaline spring system. Extremophiles. 12: 529-539.

Csotonyi, JT., Swiderski, J., Stackebrandt, E., and Yurkov, V. (2010). A new environment for aerobic anoxygenic phototrophic bacteria: biological soil crusts. Environmental Microbiology Reports. 2(5): 651–656.

Csotonyi, J., Stackebrandt, E., Swiderski, J., Schumann, P., and Yurkov, V. (2011a). *Chromocurvus halotolerans* gen. nov., sp. nov., a gammaproteobacterial obligately aerobic anoxygenic phototroph, isolated from a Canadian hypersaline spring. Archives of Microbiology. 193(8): 573-582.

Csotonyi, JT., Stackebrandt, E., Swiderski, J., Schumann, P., and Yurkov, V. (2011b) An alphaproteobacterium capable of both aerobic and anaerobic anoxygenic photosynthesis but incapable of photoautotrophy: *Charonomicrobium ambiphototrophicum*, gen. nov., sp. nov. Photosynthesis Research. 107: 257–268.

Csotonyi, JT., Maltman, C., and Yurkov, V. (2014) Influence of tellurite on synthesis of bacteriochlorophyll and carotenoids in aerobic anoxygenic phototrophic bacteria. Trends in Photochemistry and Photobiology. 16: 1-17.

Csotonyi, JT., Maltman, C., Swiderski, J., Stackebrandt, E., and Yurkov, V. (2015) Extremely 'vanadiphilic' multiple metal-resistant and halophilic aerobic anoxygenic phototrophs, strains EG13 and EG8, from hypersaline springs in Canada. Extremophiles. 19: 127-134.

Cuadrat, R., Ferrera, I., Grossart, H-P., and Dávila, A. (2016) Picoplankton bloom in global south? A high fraction of aerobic anoxygenic phototrophic bacteria in metagenomics from a coastal bay (Arraial do Cabo-Brazil). OMICS A Journal of Integrative Biology. 20(2): 76-87.

Cŭperová, Z., Holzer, E., Salka, I., Sommaruga, R., and Koblížek, M. (2013) Temporal changes and altitudinal distribution of aerobic anoxygenic phototrophs in mountain lakes. Applied and Environmental Microbiology. 79(20): 6439-6446.

Denner, E., Vybiral, D., Koblížek, M., Busse, H. J., and Velimirov, B. (2002) *Erythrobacter citreus* sp. nov., a yellow pigmented bacterium that lacks bacteriochlorophyll *a*, isolated from the western Mediterranean Sea. International Journal of Systematic and Evolutionary Microbiology. 52: 1655-1661.

DNA Sequence Assembler v4 (2013), Heracle BioSoft, www.DnaBaser.com

D'Onofrio, A., Crawford, J., Stewart, E., Witt, K., Gavrish, E., Epstein, S., Clardy, J., and Lewis, K. (2010) Siderophores from neighbouring organisms promote the growth of uncultured bacteria. Chemistry and Biology. 17: 254-264.

Eiler, A., Beier, S., Säwström, C., Karlsson, J., and Bertilsson, S. (2009) High ratio of bacteriochlorophyll biosynthesis genes to chlorophyll biosynthesis genes in bacteria of humic lakes. Applied and Environmental Microbiology. 75(22): 7221-7228.

Faraldo-Gómez, J., and Sansom, M. (2003) Acquisition of siderophores in Gram-negative bacteria. Nature Reviews: Molecular Cell Biology. 4: 105-116.

Fauteux, L., Cottrell, M., Kirchman, DL., Borrego, CM., Garcia-Chaves, MC., and del Giorgio, PA. (2015) Patterns in abundance, cell size and pigment content of aerobic anoxygenic phototrophic bacteria along environmental gradients in northern lakes. PLOS ONE. 10(4): e0124035.

Fearn, S., McPhail, DS., Morris, RJH., and Dowsett, MG. (2006) Sodium and hydrogen analysis of room temperature glass corrosion using low energy Cs SIMS. Applied Surface Science. 252: 7070–7073.

Feng, Y., Lin, X., Mao, T., and Zhu, J. (2011). Diversity of aerobic anoxygenic phototrophic bacteria in paddy soil and their response to elevated atmospheric CO_2. Microbial Biotechnology. 4(1): 74–81.

Ferrera, I., Gasol, J., Sebastián, M., Hojerová, E., and Koblížek, M. (2011) Comparison of growth rates of aerobic anoxygenic phototrophic bacteria and other bacterioplankton groups in coastal Mediterranean waters. Applied and Environments Microbiology. 77(21): 7451-7458.

Ferrera, I., Sarmento, H., Priscu, J., Chiuchiolo, A., González, J., and Grossart, H-P. (2017) Diversity and distribution of freshwater aerobic anoxygenic phototrophic bacteria across a wide latitudinal gradient. Frontiers in Microbiology. Doi: 10.3389/fmicb.2017.00175.

Fong, YH., Wong, HC., Chuck, CP., Chen, YW., Sun, H., and Wong, KB. (2011) Assembly of preactivation complex for urease maturation in *Helicobacter pylori* crystal structure of UreF-UreH protein complex. Journal of Biological Chemistry. 286: 43241-43249.

Garcia-Chaves, MC., Cottrell, DL., Derry, AM., Bogard, MJ., and del Giorgio, PA. (2015) Major contribution of both zooplankton and protists to the top-down regulation of freshwater aerobic anoxygenic phototrophic bacteria. Aquatic Microbial Ecology. 76: 71-83.

Garcia-Chaves, M., Cottrell, M., Kirchman, D., Ruiz-González, C., and del Giorgio, P. (2016) Single-cell activity of freshwater aerobic anoxygenic phototrophic bacteria and their contribution to biomass production. ISME Journal. 10: 1579-1588.

Gerhardt, P., Murray, RGE., Costilow, RN., Nester, EW., Wood, WA., Krieg, NR., and Phillips, GB. (1981) Manual of methods for general bacteriology. American Society for Microbiology, Washington, D.C.

Granger, J., and Price, N. (1999) The importance of siderophores in iron nutrition of heterotrophic marine bacteria. Limnology and Oceanography. 44(3): 541-555.

Grobelak, A., and Hiller, J. (2017) Bacterial siderophores promote plant growth: screening of catechol and hydroxamate siderophores. International Journal of Phytoremediation. DOI: 10.1080/15226514.2017.1290581

Hall, K.J., and Northcote, T.G. (1986) Conductivity-temperature standardization and dissolved solids estimation in a meromictic saline lake. Canadian Journal of Fisheries and Aquatic Sciences. 43: 2450-2454.

Hauruseu, D., and Koblížek, M. (2012) Influence of light on carbon utilization in aerobic anoxygenic phototrophs. Applied and Environmental Microbiology. 78(20): 7414-7419.

Hebermehl, M., and Klug, G. (1998) Effect of oxygen on translation and posttranslational steps in expression of photosynthesis genes in *Rhodobacter capsulatus*. Journal of Bacteriology. 180(15): 3983-3987.

Hibbing, M., Fuqua, C., Parsek, M., and Peterson, SB. (2010) Bacterial competition: surviving and thriving in the microbial jungle. Nature Reviews: Microbiology. 8: 15-25.

Hughes, E., Head, B., Maltman, C., Piercey-Normore, M., and Yurkov, V. (2017) Aerobic anoxygenic phototrophs in gold mine tailings in Nopiming Provincial Park, Manitoba, Canada. Canadian Journal of Microbiology. 63: 212–218.

Ivanova, EP., Bowmanc, JP., Lysenkod, AM., Zhukovae, NV., Gorshkovab, NM., Kuznetsovab, TA., Kalinovskayab, NI., Shevchenkob, LS., and Mikhailovb, VV. (2005) *Erythrobacter vulgaris* sp. nov., a novel organism isolated from the marine invertebrates. Systematic and Applied Microbiology. 28: 123-130.

Jiang, H., Dong, H., Yu, B., Lv, G., Deng, S., Wu, Y., Dai, M., and Jiao, N. (2009) Abundance and diversity of aerobic anoxygenic phototrophic bacteria in saline lakes on the Tibetan plateau. FEMS Microbiology Ecology. 67: 268–278.

Jiao, N., Zhang, R., and Zheng, Q. (2010) Coexistence of two different photosynthetic operons in *Citromicrobium bathyomarinum* JL354 as revealed by whole-genome sequencing. Journal of Bacteriology. 192(4): 1169-1170.

Joliot, P., Béal, D., Frilley, B. (1980) Une nouvelle méthode spectrophotométrique destinée á l'étude des reactions photosynthétiques. Journal de Chimie Physique. 77: 209–216

Jung, YT., Park, S., Oh, TK., and Yoon, JH. (2011) *Erythrobacter marinus* sp. nov., isolated from seawater of the Yellow Sea in Korea. International Journal of Systematic and Evolutionary Microbiology. 62: 2050–2055.

Kim, BC., Park, JR., Bae, JW., Rhee, SK., Kim, KH., Oh, JW., and Park, YH. (2006) *Stappia marina* sp. nov., a marine bacterium isolated from the Yellow Sea. International Journal of Systematic and Evolutionary Microbiology. 56: 75-79.

Klassen, J. (2009) Pathway evolution by horizontal transfer and positive selection is accommodated by relaxed negative selection upon upstream pathway genes in purple bacterial carotenoid biosynthesis. Journal of Bacteriology. 191(24): 7500-7508.

Koblížek, M., Mašín, M., Ras, J., Poulton, AJ., and Prášil, O. (2007) Rapid growth rates of aerobic anoxygenic phototrophs in the ocean. Environmental Microbiology. 9: 2401–2406.

Koblížek, M., Janouškovec, JJ., Oborník, M., Johnson, JH., Ferriera, S., and Falkowski, PG. (2011) Genome sequence of the marine photoheterotrophic bacterium *Erythrobacter* sp. Strain NAP1. Journal of Bacteriology. 193(20): 5881-5882.

Kolber, ZS., Plumley, FG., Lang, AS., Beatty, JT., Blankenship, RE., VanDover, CL., Vetriani, C., Koblížek, M., Rathgeber, C., and Falkowski, PG. (2001) Contribution of aerobic photoheterotrophic bacteria to the carbon cycle in the ocean. Science. 292: 2492–2495.

Lamont, I., Beare, P., Ochsner, U., Vasil, A., and Vasil, M. (2002) Siderophore-mediated signaling regulates virulence factor production in *Pseudomonas aeruginosa*. Pof the National Academy of Science. 99(10): 7072-7077.

Lee, YS., Lee, DH., Kahng, HY., Kim, EM., and Jung, JS. (2010) *Erythrobacter gangjinensis* sp. nov., a marine bacterium isolated from seawater. International Journal of Systematic and Evolutionary Microbiology, 60: 1413-1417.

Lehours, AC., Cottrell, MT., Dahan, O., Kirchman, DL., and Jeanthon, C. (2010) Summer distribution and diversity of aerobic anoxygenic phototrophic bacteria in the Mediterranean Sea in relation to environmental variables. FEMS Microbiology Ecology. 74: 397–409.

Lehours, AC., and Jeanthon, C. (2015) The Hydrological context determines the beta-diversity of aerobic anoxygenic phototrophic bacteria in European Arctic Seas but does not favor endemism. Frontiers in Microbiology. 6(638): doi: 10.3389/fmicb.2015.00638.

Lew, S., Lew, M., and Koblížek, M. (2016) Influence of selected environmental factors on the abundance of aerobic anoxygenic phototrophs in peat-bog lakes. Environmental Science and Pollution Research. 23: 13853-13863.

Li, X., Koblížek, M., Feng, F., Li, Y., Jian, J., and Zeng, Y. (2013) Whole-genome sequence of a freshwater aerobic anoxygenic phototroph, *Porphyrobacter* sp. Strain AAP82, isolated from the Huguangyan Maar Lake in Southern China. Genome Announcements. 1(2).

Liu, R., Zhang, Y., and Jiao, N. (2010) Diel variations in frequency of dividing cells and abundance of aerobic anoxygenic phototrophic bacteria in a coral reef system of the South China Sea. Aquatic Microbial Ecology. 58(3): 303-310.

Londry, K., and Sherriff, B. (2007) Comparison of microbial biomass, biodiversity, and biogeochemistry in three contrasting gold mine tailing deposits. Geomicrobiology Journal. 22: 237-247.

Maltman, C., and Yurkov, V. (2014) The impact of tellurite on highly resistant marine bacteria and strategies for its reduction. International Journal Environmental Engineering and Natural Resources. 1(3): 109-119.

Maltman, C., Piercey-Normore, M., and Yurkov, V. (2015) Tellurite-, tellurate-, and selenite-based respiration by strain CM-3 isolated from gold mine tailings. Extremophiles. 19(5):1013-1019.

Maltman, C., and Yurkov, V. (2015) The effect of tellurite on highly resistant freshwater aerobic anoxygenic phototrophs and their strategies for reduction. Microorganisms. 3:826-838.

Maltman, C., Donald, L., and Yurkov V. (2017) Two distinct periplasmic enzymes are responsible for tellurite/tellurate and selenite reduction by strain ER-Te-48 associated with the deep sea hydrothermal vent tube worms at the Juan de Fuca Ridge black smokers. Archives of Microbiology. 199(8): 1113-1120.

Martínez, J. (2008) Antibiotics and Antibiotic Resistance Genes in Natural Environments. Science. 321(5887): 365-367.

Mašín, M., Cŭperová, Z., Hojerová, E., Salka, I., Grossart, HP., and Koblížek, M. (2012) Distribution of aerobic anoxygenic phototrophic bacteria in glacial lakes of Northern Europe. Aquatic Microbial Ecology. 66: 77-86.

Masuda, S., Berleman, J., Hasselbring, BM., and Bauer, CE. (2008) Regulation of aerobic photosystem synthesis in the purple bacterium *Rhodospirillum centenum* by CrtJ and AerR. Photochemical Photobiological Sciences. 7: 1267–1272.

Medová, H., Koblížek, M., Elster, J., and Nedbalová, L. (2016) Abundance of aerobic anoxygenic bacteria in freshwater lakes on James Ross Island, Antarctic Peninsula. Antarctic Science. 28(2): 101-102.

Najafi, MBH., and Pezeshki, P. (2013) Bacterial mutation; types, mechanisms and mutant detection methods: A review. European Science Journal. 4: 1857–7881.

Noguchi, TH., Hayashi, H., Shimada, K., Takaichi, S., and Tasumi, M. (1992) *In vivo* states and function of carotenoids in an aerobic photosynthetic bacterium, *Erythrobacter longus*. Photosynthesis Research. 31: 21–30.

Oh, HM., Giovannoni, SJ., Ferriera, S., Johnson, J., and Cho, JC. (2009) Complete genome sequence of *Erythrobacter litoralis* HTCC2594. Journal of Bacteriology. 191(7): 2419-2420.

Pfennig, N. (1978) *Rhodocyclus purpureus* gen. nov. and sp. nov., a ring-shaped vitamin B12-requiring member of the family Rhodospirillaceae. International Journal of Systematic Bacteriology. 28: 283-288.

Prince, RC., and Dutton, PL. (1978) Protonation and the reducing potential of the primary electron acceptor. *In* "The photosynthetic bacteria", (Clayton, RK., and Sistrom, WR., eds.). 439–453. Plenum Press, New York.

Rathgeber, C., Yurkova, N., Stackebrandt, E., Beatty, JT., and Yurkov, V. (2002) Isolation of tellurite- and selenite-reducing bacteria from hydrothermal vents of the Juan de Fuca Ridge in the Pacific Ocean. Applied and Environmental Microbiology. 68: 4613-4622.

Rathgeber, C., Beatty, JT., and Yurkov, V. (2004) Aerobic phototrophic bacteria: new evidence for the diversity, ecological importance and applied potential of this previously overlooked group. Photosynthesis research. 81: 113-128.

Rathgeber, C., Yurkova, N., Stackebrandt, E., Schumann, P., Beatty, JT., and Yurkov, V. (2005) *Roseicyclus mahoneyensis* gen nov., sp. nov., an aerobic phototrophic bacterium isolated from a meromictic lake. International Journal of Systematic and Evolutionary Microbiology. 55: 1597–1603.

Rathgeber, C., Yurkova, N., Stackebrandt, E., Schumann, P., Humphrey, E., Beatty, JT., and Yurkov, V. (2007) *Porphyrobacter meromictius* sp. nov., an appendaged bacterium, that produces bacteriochlorophyll *a*. Current Microbiology. 55: 356–361.

Rathgeber, C., Alric, J., Hughes, E., Vermeglio, A., and Yurkov, V. (2012) The photosynthetic apparatus and photoinduced electron transfer in the aerobic phototrophic bacteria *Roseicyclus mahoneyensis* and *Porphyrobacter meromictius*. Photosynthesis Research. 110(3): 193-203.

Raymond, J., and Blankenship, RE. (2004) Biosynthetic pathways, gene replacement and the antiquity of life. Geobiology. 22: 199-203.

Reid, R., Live, D., Faulkner, DJ., and Butler, A. (1993) A siderophore from a marine bacterium with an exceptional ferric ion affinity constant. Nature. 366: 455-458.

Ritchie, AE., and Johnson, ZI. (2012) Abundance and genetic diversity of aerobic anoxygenic phototrophic bacteria of coastal regions of the Pacific Ocean. Applied and Environmental Microbiology. 78(8): 2858-2866.

Roszak, DB., and Colwell, RR. (1987) Survival strategies of bacteria in the natural environment. Microbiological Reviews. 51(3): 365-379.

Salka, I., Cuperova, Z., Masin, M., Koblížek, M., and Grossart, HP. (2011) *Rhodoferax*-related *pufM g*ene cluster dominates the aerobic anoxygenic phototrophic communities in German freshwater lakes. Environmental Microbiology. 13(11): 2865-2875.

Salka, I., Srivastava, A., Allgaier, M., and Grossart, HP. (2014) The draft genome sequence of *Sphingomonas* sp. Strain FukuSWIS1, obtained from acidic Lake Grosse Fuchskuhle, indicates photoheterotrophy and a potential for humic matter degradation. Genome Announcements. 2(6).

Sato-Takabe, Y., Hamasaki, K., and Suzuki, K. (2011). Photosynthetic characteristics of marine aerobic anoxygenic bacteria *Roseobacter* and *Erythrobacter* strains. Archives of Microbiology. DOI 10.1007/s00203-011-0761-2

Sato-Takabe, Y., Hamasaki, K., and Suzuki, K. (2012) Photosynthetic characteristics of marine aerobic anoxygenic phototrophic bacteria *Roseobacter* and *Erythrobacter* strains. Archives of Microbiology. 194: 331-341.

Sato-Takabe, Y., Suzuki, S., Shishikura, R., Hamasaki, K., Tada, Y., Kataoka, T., Yokokawa, T., Yoshie, N., and Suzuki, S. (2015) Spatial distribution and cell size of aerobic anoxygenic phototrophic bacteria in the Uwa Sea, Japan. Journal of Oceanography. 71(1): 151–159.

Sato-Takabe, Y., Nakao, H., Kataoka, T., Yokokawa, T., Hamasaki, K., Ohta, K., and Suzuki, S. (2016) Abundance of common aerobic anoxygenic phototrophic bacteria in a coastal aquaculture area. Frontiers in Microbiology. doi: 10.3389/fmicb.2016.01996.

Schalk, I., Hannauer, M., and Braud, A. (2011) New roles for bacterial siderophores in metal transport and tolerance. Environmental Microbiology. 13(11): 2844-2854.

Schoepp, B., Parot, P., Menin, L., Gaillard, J., Richaud, P., and Verméglio, A. (1995) In vivo participation of a high potential iron-sulfur protein as electron donor to the photochemical reaction center of *Rubrivivax gelatinosus*. Biochemistry. 34(37): 11736-11742.

Schwarze, C., Carluccio, AV., Venturoli, G., and Labahn, A. (2000) Photo-induced cyclic electron transfer involving cytochrome *bc*1 complex and reaction center in the obligate aerobic phototroph *Roseobacter denitrificans*. European Journal of Biochemistry. 267: 422–433.

Schwyn, B., and Neilands, JB. (1987) Universal assay for the detection and determination of siderophores. Analytical Biochemistry. 160: 47-56.

Selyanin, V., Hauruseu, D., and Koblížek, M. (2016) The Variability of Light Harvesting Complexes in Aerobic Anoxygenic Phototrophs. Photosynthesis Research. Doi: 10.1007/s11120-015-0197-7.

Sherriff, B., Sidenko, N., and Salzsauler, K. (2006) Differential settling and geochemical evolution of tailings' surface water at the Central Manitoba Gold Mine. Applied Geochemistry. 22(2): 342-356.

Shiba, T., Simidu, U., and Taga, N. (1979) Distribution of aerobic bacteria which contain bacteriochlorophyll *a*. Applied and Environmental Microbiology. 38: 43–45.

Shiba, T., and Simidu, U. (1982) *Erythrobacter longus* gen. nov., sp. nov., an aerobic bacterium which contains bacteriochlorophyll *a*. International Journal of Systematic Bacteriology. 32: 211–217.

Shiba, T. (1991) *Roseobacter litoralis* gen. nov., sp. nov., and *Roseobacter denitrificans*sp. nov., aerobic pink-pigmented bacteria which contain bacteriochlorophyll *a*. Systematic and Applied Microbiology. 14(2): 140-145.

Sieracki, ME., Gilg, IC., Their, EC., Poulton, NJ., and Goericke, R. (2006) Distribution of planktonic aerobic photoheterotrophic bacteria in the northwest Atlantic. Limnology and Oceanography 51: 38–46.

Šlouf V, Fuciman M, Dulebo A, Kaftan D, Koblížek M, Frank HA and Polívka T (2013) Carotenoid Charge Transfer States and Their Role in Energy Transfer Processes in LH1-RC Complexes from Aerobic Anoxygenic Phototrophs. J Phys Chem 117:10987-10999.

Sokol, P., Lewis, C., and Dennis, J. (1992) Isolation of a novel siderophore from *Pseudomonas cepacian*. Journal of Medical Microbiology. 36: 184-189.

Spring, S., Lünsdorf, H., Fuchs, BM., and Tindall, BJ. (2009) The photosynthetic apparatus and its regulation in the aerobic gammaproteobacterium *Congregibacter litoralis* gen. nov., sp. nov. PLOS ONE. 4(3): e4866.

Stegman, MR., Cottrell, MT., and Kirchman, DL. (2014) Leucine incorporation by aerobic anoxygenic phototrophic bacteria in the Delaware Estuary. International Society of Microbial Ecology Journal. 8: 2339-2348.

Stiefel, P., Zambelli, T., and Vorholt, JA. (2013) Isolation of optically targeted single bacteria by application of fluidic force microscopy to aerobic anoxygenic phototrophs from the phyllosphere. Applied and Environmental Microbiology. 79(16): 4895-4905.

Suyama, T., Shigematsu, T., Takaichi, S., Nodasaka, Y., Fujikawa, S., Hosoya, H., Tokiwa, Y., Kanagawa, T., and Hanada, S. (1999) *Roseateles depolymerans* gen. nov., sp. nov., a new bacteriochlorophyll a-containing obligate aerobe belonging to the subclass of the Proteobacteria. International Journal of Systematic Bacteriology. 49(2): 449–457.

Suzuki, T., Muroga, Y., Takahama, M., and Nishimura, Y. (1999) *Roseivivax halodurans* gen. nov., sp. nov. and *Roseivivax halotolerans* sp. nov., aerobic bacteriochlorophyll-containing bacteria isolated from a saline lake. International Journal of Systematic Bacteriology. 49: 629–634.

Swingley, WD., Sadekar, S., Mastrian, SD., Matthies, HJ., Hao, J., Ramos, H., Acharya, CR., Conrad, AL., Taylor, HL., Dejesa, LC., Shah, MK., O'Huallachain, ME., Lince, MT., Blankenship, RE., Beatty, JT., and Touchman, JW. (2007) The complete genome sequence of *Roseobacter denitrificans* reveals a mixotrophic rather than photosynthetic metabolism. Journal of Bacteriology. 189: 683–690.

Tang, K., Zong, R., Zhang, F., Xiao, N., and Jiao, N. (2010) Characterization of the photosynthetic apparatus and proteome of *Roseobacter denitrificans*. Current Microbiology. 60: 124-133.

Tang, KH., Tang, Y., and Blankenship, RE. (2011) Carbon metabolic pathways in phototrophic bacteria and their broader evolutionary implications. Frontiers in Microbiology. 2(165), doi: 10.3389/fmicb.2011.00165.

Tycholiz, C., Ferguson, IJ., Sherriff, B., Cordeiro, M., Ranjan, R., and Pérez-Flores, M. (2016) Geophysical delineation of acidity and salinity in the Central Manitoba Gold Mine tailings pile, Manitoba, Canada. Journal of Applied Geophysics. 131: 29-40.

Wandersman, C., and Delepelaire, P. (2004) Bacterial iron sources: From siderophores to hemophores. Annual Review of Microbiology. 58: 611-647.

Woese, CR. (1987) Bacterial evolution. Microbiology Reviews. 51: 221–271.

Wu, HX., Lai, PY., Lee, OO., Zhou, XJ., Miao, L., Wang, H., and Qian, PY. (2012) *Erythrobacter pelagi* sp. nov., a member of the family *Erythrobacteraceae* isolated from the Red Sea. International Journal of Systematic and Evolutionary Microbiology. 62: 1348-1353.

Xu, M., Xin, Y., Yu, Y., Zhang, J., Zhou, Y., Liu, H., Tian, J., and Li, Y. (2010). *Erythrobacter nanhaisediminis* sp. nov., isolated from marine sediment of the South China Sea. International Journal of Systematic and Evolutionary Microbiology. 60: 2215-2220.

Yamamoto, S., Okujo, N., and Sakakibara, Y. (1994) Isolation and structure of acinetobactin, a novel siderophore from *Acinetobacter baumannii*. Archives of Microbiology. 162: 249-254.

Yildiz, FH., Gest, H., and Bauer, CE. (1991) Attenuated effect of oxygen on photopigment synthesis in *Rhodospirillum centenum*. Journal of Bacteriology. 173: 5502–5506.

Yoon, JH., Kim, H., Kim, IG., Kang, KH., and Park, YH. (2003) *Erythrobacter flavus* sp. nov., a slight halophile from the East Sea in Korea. International Journal of Systematic and Evolutionary Microbiology. 53: 1169-1174.

Yoon, JH., Kang, KH., Oh, TK., and Park, YH. (2004) *Erythrobacter aquimaris* sp. nov., isolated from sea water of a tidal flat of the Yellow Sea in Korea. International Journal of Systematic and Evolutionary Microbiology. 54: 1981–1985.

Yoon, JH., Kang, KH., Yeo, SH., and Oh, TK. (2005a) *Erythrobacter luteolus* sp. nov., isolated from a tidal flat of the Yellow Sea in Korea. International Journal of Systematic and Evolutionary Microbiology. 55: 1167-1170.

Yoon, JH., Oh, TK., and Park, YH. (2005b) *Erythrobacter seohaensis* sp. nov. and *Erythrobacter gaetbuli* sp. nov., isolated from a tidal flat of the Yellow Sea in Korea. International Journal of Systematic and Evolutionary Microbiology. 55: 71-75.

Yoon, BJ., Lee, DH., and Oh, DC. (2012) *Erythrobacter jejuensis* 1 sp. nov., isolated from seawater. International Journal of Systematic and Evolutionary Microbiology. 63(4): 1421-1426.

Yurkov, V. (1990) Ph.D. thesis. Academy of Sciences, Moscow, Russia.

Yurkov, VV., and Gorlenko, VM. (1990) *Erythrobacter sibiricus* sp. nov., a new freshwater aerobic bacterial species containing bacteriochlorophyll a. Microbiology (New York). 59(1): 120-126.

Yurkov, VV., Lysenko, AM., and Gorlenko, VM. (1991) Hybridization analysis of the classification of bacteriochlorophyll a-containing freshwater aerobic bacteria. Microbiology (New York). 60(3): 518-523.

Yurkov, VV., and Gorlenko, VM. (1992a) A new genus of freshwater aerobic bacteriochlorophyll a-containing bacteria, *Roseococcus* gen. nov. Microbiology (New York). 60(5): 902-907.

Yurkov, VV., and Gorlenko, VM. (1992b) New species of aerobic bacteria from the genus *Erythromicrobium* containing bacteriochlorophyll a. Microbiology (New York). 61(2): 248-255.

Yurkov, V., and Hughes, E. (2013) Genes associated with the peculiar phenotypes of the aerobic anoxygenic phototrophs. *In* "Genome Evolution of Photosynthetic Bacteria", (Beatty, JT., Jacquot, JP., and Gadal, P., eds.). 66: 327-358. Elsevier Ltd.

Yurkov, V., Gadon, N., and Drews, G. (1993) The major part of polar carotenoids of the aerobic bacteria *Roseococcus thiosulfatophilus*, RB3 and *Erythromicrobium ramosum*, E5 is not bound to the bacteriochlorophyll a-complexes of the photosynthetic apparatus. Archives of Microbiology. 160: 372-376.

Yurkov, VV., Gorlenko, VM., and Kompantseva, EI. (1993) A new type of freshwater aerobic orange colored bacterium *Erythromicrobium* gen. nov., containing bacteriochlorophyll a. Microbiology (New York). 61(2): 256-260.

Yurkov, V., and Van Germeden, H. (1993) Impact of light/dark regimen on growth rate, biomass formation and bacteriochlorophyll synthesis in *Erythromicrobium hydrolyticum*. Archives of Microbiology. 159: 84-89.

Yurkov, V., Angerhofer, A., Gadon, N., and Drews, G. (1994) The light-harvesting complexes of *Roseococcus thiosulfatophilus*, RB3 and *Erythromicrobium ramosum*, E5 and energy transfer from the carotenoids to reaction center. Zeitschrift fur Naturforschung (in English). 49: 579-586.

Yurkov, V., Stackebrandt, E., Holmes, A., Fuerst, JA., Hugenholtz, P., Golecki, J., Gorlenko, VM., Kompantseva, EI., and Drews, G. (1994) Phylogenetic positions of novel aerobic, bacteriochlorophyll *a*-containing bacteria and description of *Roseococcus thiosulfatophilus* gen. nov., sp. nov., *Erythromicrobium ramosum* gen nov., sp. nov., and *Erythrobacter litoralis* sp. nov. International Journal of Systematic Bacteriology. 44**:** 427–434.

Yurkov, V., Schoepp, B., and Vermeglio, A. (1995) Electron transfer carriers in obligately aerobic photosynthetic bacteria from genera *Roseococcus* and *Erythromicrobium*. *In* "Photosynthesis: from light to biosphere", (Mathis, P., ed.). 543-546. Kluwer Academic Publishing, Dordrecht/Boston/London.

Yurkov, V., Stackebrandt, E., Buss, O., Verméglio, A., Gorlenko, V., and Beatty, JT. (1997) Reorganization of the genus *Erythromicrobium*: description of "*Erythromicrobium sibiricum*" as *Sandaracinobacter sibiricus* gen. nov., sp. nov., and of "*Erythromicrobium ursincola*" as *Erythromonas ursincola* gen. nov., sp. nov. International Journal of Systematic Bacteriology. 47: 1172-1178.

Yurkov, V., and Beatty, JT. (1998) Aerobic anoxygenic phototrophic bacteria. Microbiology and Molecular Biology Reviews. 62: 695–724.

Yurkov, V., Menin, L., Schoepp, B., and Vermeglio, A. (1998) Purification and characterization of reaction centers from the obligate aerobic phototrophic bacteria *Erythrobacter litoralis*, *Erythromonas ursincola* and *Sandaracinobacter sibiricus*. Photosynthesis Research. 57: 129-138.

Yurkov, V., Krieger, S., Stackebrandt, E., and Beatty, JT. (1999) *Citromicrobium bathyomarinum*, a novel aerobic bacterium isolated from deep-sea hydrothermal vent plume waters that contains photosynthetic pigment-protein complexes. Journal of Bacteriology. 181: 4517–4525.

Yurkov, V., and Csotonyi, J. (2003) Aerobic anoxygenic phototrophs and heavy metalloid reducers from extreme environments. Recent Research Developments in Bacteriology. 1: 247-300.

Yurkov, V., and Csotonyi, J. (2009) New light on aerobic anoxygenic photosynthesis. *In* "The Purple Phototrophic Bacteria" (Hunter, CN., Daldal, F., Thurnauer, MC., and Beatty, JT., eds.). 31-55. Springer Science + Business Media B.V.

Yurkov, V., and Hughes, E. (2013) Genes associated with the peculiar phenotypes of the aerobic anoxygenic phototrophs. *In* "The genome evolution of photosynthetic bacteria", (Betty, JT., ed). 66: 327-358. Elsevier Ltd.

Yurkov, V., and Hughes, E. (2017) Aerobic anoxygenic phototrophs: Four decades of mystery. *In* "Modern Topic in the Phototrophic Prokaryotes", (Hallenbeck, PC., ed). 193-214. Springer International Publishing, Switzerland.

Yurkova, N., Rathgeber, C., Swiderski, J., Stackebrandt, E., Beatty, JT., Hall, K., and Yurkov, V. (2002) Diversity, distribution and physiology of the aerobic phototrophic bacteria in the mixolimnion of a meromictic lake. FEMS Microbiology Ecology. 40: 191-204.

Zeng, Y., Shen, W., and Jiao, N. (2009) Genetic diversity of aerobic anoxygenic photosynthetic bacteria in open ocean surface water and upper twilight zones. Marine Biology. 156: 425–437.

Zeng, Y., Feng, F., Liu, Y., Li, Y., and Koblížek, M. (2013a) Genome Sequences and Photosynthesis Gene Cluster Composition of a Freshwater Aerobic Anoxygenic Phototroph, *Sandarakinorhabdus* sp. Strain AAP62, Isolated from the Shahu Lake in Ningxia, China. Genome Announcements. 1(1).

Zeng, Y., Koblížek, M., Feng, F., Liu, Y., Wu, Z., and Jian, J. (2013b) Whole-Genome Sequencing of an Aerobic Anoxygenic Phototroph, *Blastomonas* sp. Strain AAP53, Isolated from a Freshwater Desert Lake in Inner Mongolia. Genome Announcements. 1(2).

Zeng, Y., Dong, P., Qiao, Z., and Zheng, T. (2016) Diversity of the aerobic anoxygenic phototrophy gene *pufM* in Arctic and Antarctic coastal seawaters. Acta Oceanologica Sinica. 35(6): 68-77.

Zheng, Q., Zhang, R., Koblížek, M., Boldareva, EN., Yurkov, V., Yan, S., and Jiao, N. (2011). Diverse arrangement of photosynthetic gene clusters in aerobic anoxygenic phototrophic bacteria. PLOS ONE. 6(9): e25050.

Zheng, Q., Liu, Y., Steindler, L., and Jiao, N. (2015) Pyrosequencing Analysis of Aerobic Anoxygenic Phototrophic Bacterial Community Structure in the Oligotrophic Western Pacific Ocean. FEMS Microbiology Letters. 362(8): fnv03.

Zheng, Q., Lin, W., Liu, Y., Chen, C., and Jiao, N. (2016) A comparison of 14 *Erythrobacter* genomes provides insights into the genomic divergence and scattered distribution of phototrophs. Frontiers in Microbiology. doi: 10.3389/fmicb.2016.00984.